NAVAL POSTGRADUATE SCHOOL

MONTEREY, CALIFORNIA

THESIS

INTENSITY CHANGES IN TYPHOON SINLAKU AND TYPHOON JANGMI IN RESPONSE TO VARYING OCEAN AND ATMOSPHERIC CONDITIONS

by

Charles A. DePalma

March 2011

Thesis Advisor:	Patrick Harr
Second Reader:	Russell Elsberry

Approved for public release; distribution is unlimited

THIS PAGE INTENTIONALLY LEFT BLANK

REPORT DOCUMENTATION PAGE		Form Approved OMB No. 0704-0188

1. AGENCY USE ONLY *(Leave blank)*	2. REPORT DATE	3. REPORT TYPE AND DATES COVERED
	March 2011	Master's Thesis

4. TITLE AND SUBTITLE Intensity Changes in Typhoon Sinlaku and Typhoon Jangmi in Response to Varying Ocean and Atmospheric Conditions.	5. FUNDING NUMBERS
6. AUTHOR(S) Charles A. DePalma	
7. PERFORMING ORGANIZATION NAME(S) AND ADDRESS(ES) Naval Postgraduate School Monterey, CA 93943-5000	8. PERFORMING ORGANIZATION REPORT NUMBER
9. SPONSORING /MONITORING AGENCY NAME(S) AND ADDRESS(ES) N/A	10. SPONSORING/MONITORING AGENCY REPORT NUMBER

11. SUPPLEMENTARY NOTES The views expressed in this thesis are those of the author and do not reflect the official policy or position of the Department of Defense or the U.S. Government.

12a. DISTRIBUTION / AVAILABILITY STATEMENT	12b. DISTRIBUTION CODE
Approved for public release; distribution is unlimited	

13. ABSTRACT (maximum 200 words)

Impacts of ocean heat content (OHC) and vertical wind shear on intensity changes of Typhoon Sinlaku and Typhoon Jangmi during the Tropical Cyclone Structure-2008 and THORPEX Pacific Asian Regional Campaign are investigated. Observations of ocean structure variables were obtained in the environment of each typhoon via aircraft-deployed expendable bathythermographs (AXBTs). Strong correspondence among storm intensity changes, ocean features, and vertical wind shear is identified as each tropical cyclone passed over regions of warm and cold ocean features with varying vertical wind shears. Typhoon Sinlaku passed over a cold ocean and with a consistently low vertical wind shear, the storm did not intensify for 12 hours. Sinlaku then reached maximum intensity as it passed over a warm ocean feature while vertical wind shear remained low. Sinlaku also weakened as it passed over an intense cold eddy at a time when vertical wind shear was increasing. Similar impacts are defined for TY Jangmi. Comparison of the AXBT profiles with the East Asian Sea Nowcast/Forecast System (EASNFS) analyses consistently indicated the EASNFS mixed layer depths (MLD) were too shallow, had steeper slopes in the thermocline, and a warm sea-surface temperature (SST) bias. The MLD and SST biases compensated causing OHC differences to be reduced.

14. SUBJECT TERMS	15. NUMBER OF PAGES
Tropical Cyclone Structure (TCS08), Ocean Heat Content (OHC), Mixed Layer Depth (MLD), Sea Surface Temperature (SST), Vertical Wind Shear, Tropical Cyclone Intensification	129
	16. PRICE CODE

17. SECURITY CLASSIFICATION OF REPORT	18. SECURITY CLASSIFICATION OF THIS PAGE	19. SECURITY CLASSIFICATION OF ABSTRACT	20. LIMITATION OF ABSTRACT
Unclassified	Unclassified	Unclassified	UU

NSN 7540-01-280-5500

Standard Form 298 (Rev. 2-89)
Prescribed by ANSI Std. 239-18

THIS PAGE INTENTIONALLY LEFT BLANK

Approved for public release; distribution is unlimited

INTENSITY CHANGES IN TYPHOON SINLAKU AND TYPHOON JANGMI IN RESPONSE TO VARYING OCEAN AND ATMOSPHERIC CONDITIONS

Charles A. DePalma
Lieutenant Commander, United States Navy
B.S., Mississippi State University, 2005

Submitted in partial fulfillment of the
requirements for the degree of

MASTER OF SCIENCE IN METEOROLOGY AND OCEANOGRAPHY

from the

NAVAL POSTGRADUATE SCHOOL
March 2011

Author: Charles A. DePalma

Approved by: Patrick Harr
Thesis Advisor

Russell Elsberry
Second Reader

Philip Durkee
Chair, Department of Meteorology

THIS PAGE INTENTIONALLY LEFT BLANK

ABSTRACT

Impacts of ocean heat content (OHC) and vertical wind shear on intensity changes of Typhoon Sinlaku and Typhoon Jangmi during the Tropical Cyclone Structure-2008 and THORPEX Pacific Asian Regional Campaign are investigated. Observations of ocean structure variables were obtained in the environment of each typhoon via aircraft-deployed expendable bathythermographs (AXBTs). Strong correspondence among storm intensity changes, ocean features, and vertical wind shear is identified as each tropical cyclone passed over regions of warm and cold ocean features with varying vertical wind shears. Typhoon Sinlaku passed over a cold ocean and with a consistently low vertical wind shear, the storm did not intensify for 12 hours. Sinlaku then reached maximum intensity as it passed over a warm ocean feature while vertical wind shear remained low. Sinlaku also weakened as it passed over an intense cold eddy at a time when vertical wind shear was increasing. Similar impacts are defined for TY Jangmi. Comparison of the AXBT profile with the East Asian Sea Nowcast/Forecast System (EASNFS) analyses consistently indicated the EASNFS mixed layer depths (MLD) were too shallow, had steeper slopes in the thermocline, and a warm sea-surface temperature (SST) bias. The MLD and SST biases compensated causing OHC differences to be reduced.

THIS PAGE INTENTIONALLY LEFT BLANK

TABLE OF CONTENTS

LIST OF FIGURES

THIS PAGE INTENTIONALLY LEFT BLANK

LIST OF TABLES

THIS PAGE INTENTIONALLY LEFT BLANK

LIST OF ACRONYMS AND ABBREVIATIONS

AXBT: Airborne Expendable Bathythermograph

CMISS: Cooperative Institute for Meteorological Satellite Studies

EASNFS: East Asian Seas Nowcast/Forecast System

ECMWF: European Center Medium Range Forecast Model

ENSO: El Nino – Southern Oscillation

EOL: Earth Observing Laboratory

ESRL: Earth Systems Research Laboratory

IR: Infra Red Satellite

ITOP: Impact of Typhoons on the Ocean in the Pacific

JTWC: Joint Typhoon Warning Center

MLD: Mixed Layer Depth

MTSAT: Meteorological Satellite

MW: Microwave Satellite

NOAA: National Oceanic and Atmospheric Administration

NOGAPS: Navy Operational Global Atmospheric Prediction System

NRL SSC: Naval Research Laboratory at Stennis Space Center, MS

OHC: Ocean Heat Content (based on 26^{o}C Isotherm)

OHC24: Ocean Heat Content (based on 24^{o}C Dew Point Temperature)

SHIPS: Statistical Hurricane Intensity Prediction Scheme Model

SST: Sea Surface Temperature

STY: Super Typhoon

T100: Average Temperature of the top 100 meters of the Ocean

TC: Tropical Cyclone

TCSnn: Numbered Tropical Cyclone Structure pre-Disturbance

TCS-08: Tropical Cyclone Structure-2008

TCS-10: Tropical Cyclone Structure-2010

TD: Tropical Depression

THORPEX: The Observing System Research and Predictability Experiment

T-PARC: THORPEX-Pacific Asian Regional Campaign

TS: Tropical Storm

TUTT: Tropical Upper Tropospheric Trough

TY: Typhoon

UCAR: University Corporation for Atmospheric Research

UTC: Coordinated Universal Time

WESTPAC: Western Pacific Ocean

WV: Water Vapor Satellite

Z26: Depth of the 26^{o}C Isotherm

ACKNOWLEDGMENTS

I would like to thank my thesis advisor Professor Patrick Harr for his patience, expertise, involving me in the ITOP 2010 program, the hours that he spent improving my thesis and overall reducing the stress during the whole thesis process during my stay here at NPS. I would like to thank Professor Russell Elsberry for his technical writing excellence and bringing better science into my thesis during the editing process.

I would like to thank Dr. Pete Black for his excellent ideas, expertise in everything concerning AXBTs their use and processing, and for his superior enthusiasm during ITOP 2010 while on Guam. I would also like to thank Robert E. Lee and Jeff Curling for making ITOP 2010 a much easier event for me as well.

Thank you to CDR Richard Jeffries now retired but working at CNMOC N4/7 for talking me into coming to Postgraduate School though it was not the greatest experience in my naval career it was a great experience.

To my class mates of the amazing shrinking class, George, Cynthia, Paul and Chad thank you for your support!!

Finally to my wife Yvonne and children once again you endured a lengthy time apart with me this time 2,000 miles away. You were my greatest source of inspiration to power me through the completion of this master's degree.

THIS PAGE INTENTIONALLY LEFT BLANK

I. INTRODUCTION

A. MOTIVATION AND OBJECTIVE

During December 1944, Admiral Halsey chose to have the U. S. Navy Fleet remain on station in the Philippine Sea and ride out Typhoon Cobra (Halsey's Typhoon, Figure 1) with the devastating loss of 790 sailors, three capsized destroyers, and damage to many other vessels. A second encounter by Halsey and a typhoon in June 1945 led to the loss of 6 sailors and 75 carrier aircraft with severe damage to a number of ships (Melton 2007). At the time, Halsey considered the war and the Fleet's presence in those locations to be more important than the potential risk to his Fleet by bad weather.

Figure 1. Radar image of the eye of Typhoon Cobra on 18 December 1944 from a ship located at the center of the area shown (from NOAA Library at http://www.photolib.noaa.gov/historic/nws/wea01232.htm).

Since that time, observational advances such as satellite and remote sensing and numerical weather prediction models have contributed to improvements in the forecasting

of tropical cyclones (TC) such that once a TC has formed the forecasts of the storm path are often very accurate. However, much work still needs to be done in predicting the location where a TC will form and then how quickly it will intensify into a mature TC. In addition, once a storm becomes a fully developed TC, an important forecast issue is what will be the potential maximum intensity under the influence of the atmospheric and oceanic environment, or will it succumb to vertical wind shear or dissipate over cooler water. This is the forecast challenge in an effort to provide safe navigation of ships in oceans vulnerable to TCs.

A large number of TCs occur in tropical waters along the east coast of the United States, in the Indian Ocean, and in the western North Pacific Ocean, which are all areas that U.S. Navy and other maritime shipping frequently operate. In the western North Pacific Ocean, TCs can occur in all months, as Admiral Halsey discovered in December 1944. During the fall of 2004, a major Pacific anti-submarine exercise called TASWEX 2004 was planned for early October. Typhoon Meari formed northwest of Guam and eventually passed right through the TASWEX operational area, which delayed the start of the exercise for three days. Eventually, the storm recurved near Okinawa to make landfall on Japan (Figure 2).

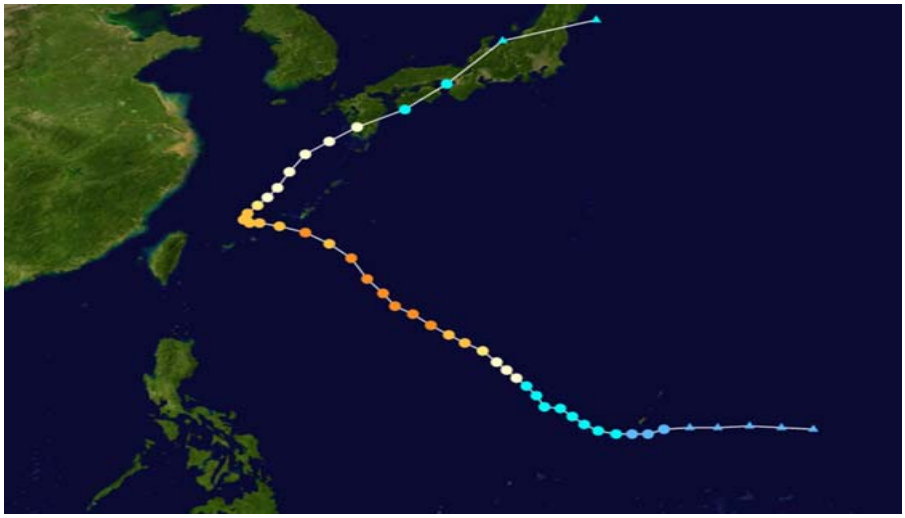

Figure 2. Joint Typhoon Warning Center track position of TY Meari (25W) each 6 h from 1800 UTC 19 September to 0000 UTC 30 September 2004.

The intensity of a TC is influenced by both atmosphere and ocean environments in which the TC exists. Therefore, the interaction among several complex physical processes contributes to the difficulty in forecasting the intensity of TCs. Atmospheric and oceanic forecast models were initially developed independently, but coupled models have recently been developed in an effort to include the entire set of forecast variables needed to accurately predict TC intensity. Often, the atmosphere tends to have the dominant role in influencing a storm. For example, the presence of vertical wind shear can prevent a storm from forming or strengthening regardless of how much heat and moisture are potentially available from the warm ocean beneath it. That is, the evaporation of warm ocean water contributes to latent heat release in deep convective clouds near the center of the storm, which is the primary physical mechanism by which heat stored in the ocean becomes the energy source for the TC.

The objective of this study is to examine the relative contributions of the atmospheric and ocean processes on the intensification of two western North Pacific typhoons (Typhoon Sinlaku and Super Typhoon Jangmi) that occurred during the combined THORPEX-Pacific Asian Regional Campaign (T-PARC) and the Tropical Cyclone Structure-2008 (TCS-08) field program.

B. BACKGROUND - FORECASTING TROPICAL CYCLONE INTENSITY

Forecasts of tropical cyclone intensity in the modern age of remote satellite sensing of the atmosphere and ocean remain marginal at best. Two key areas in cyclone development that require accurate forecasts are the transformation from an open wave to a tropical depression and then its development to a mature TC. Three major components must be understood and used effectively in a coupled manner to produce an accurate intensity change forecast (Marks and Shay 1997). The first is the structure of the upper-ocean circulations that lead to variations in the ocean mixed layer heat content (OHC). The second is the inner-core dynamics and characteristics of the storm. The third is the structure of the synoptic-scale atmospheric environment.

It is well known that a warm ocean with temperatures greater than 26^{o}C is favorable for TC formation, but a large ocean mixed layer depth also prevents cold water from being entrained into a storm from below and inhibiting intensification (Lin et al. 2005, Wu et al. 2007). Therefore, OHC, which takes into account both the sea-surface temperature (SST) and the ocean temperature structure down to 26^{o}C, is a more appropriate measure for potential cyclone intensity than SST alone (Mainelli et al. 2008). A value of 60 kJ cm^{-2} is listed in Lin et al. (2008) and Mainelli et al. (2008) as the minimum available OHC that would allow a storm to obtain category 5 intensity (135 kt sustained winds). Most warm ocean basins have OHC values less than this outside of a warm-core eddy or warm current such as the Kuroshio, Gulf Stream, or Loop Current. Without these deep warm layers, a TC can cause mixing of cooler water from below at the top of the thermocline and lower the SST below the air temperature and cut off the heat and moisture fluxes needed to sustain the TC. A cooling of 2.5^{o}C is typically the temperature drop from the initial SST that a TC will produce in a shallow, warm layer in the wake after storm passage. A deep warm layer that extends downward to 120-130 meters will still have a SST above the critical 26^{o}C temperature after a TC passes. However, the SST in a typical ocean may decrease to 21^{o}C or less if the mixed layer is deepened to the 100 meter depth. Therefore, the deeper warm layer will minimize the mixing of cooler water from below, which would normally hinder TC intensification (Lin et al. 2008).

Ocean horizontal variability is also an important factor for consideration in intensity forecasts. A region of large ocean variability exists over the northern portion of the Philippine Sea, which is referred to as the western North Pacific Ocean eddy zone (Lin et al. 2005). This region defines the boundary between the warm, deep OHC environment of the Philippine Sea from the cooler water to the north of 20^{o} N. Another highly variable ocean region that has varying depths and warm currents is the Loop Current in the Gulf of Mexico, which undulates and sometimes breaks off to form a warm ring that drifts westward toward Texas. One of these warm rings provided extra surface fluxes for Hurricanes Katrina and Rita in 2005 as both reached Category 5 intensity when they traversed the loop. Warm currents such as the Kuroshio and Gulf Stream may also

have brief, but significant effects on storms crossing them. For example, Hurricane Andrew in 1992 rapidly deepened from a Category 1 to a Category 5 storm while crossing the Gulf Stream between the Bahamas and Florida.

Lin et al. (2009) investigated the impact of the storm translation speed on its ability to couple with the ocean. A key component here is the ratio of the moisture exchange coefficient (C_E) and the drag coefficient (C_D), which is valid up to a wind speed intensity of 33 m s^{-1}. This ratio C_E vs. C_D is approximately 0.7 for a tropical storm and 0.75 for a TC (Black et al. 2007). In addition, the TC must move within a prescribed range of translation speeds over the ocean surface. If the storm moves too slowly, the ocean mixing will be large and the SST will drop below the air temperature. If the storm moves too fast, the time necessary to extract moisture and heat from the ocean is less than optimum to fully develop the storm. Lin et al. (2009) define a minimum translation speed in the zonal direction, a specific depth of the 26^{o}C isotherm layer, and a range of speeds from 2.6 m s^{-1} to 6.4 m s^{-1} that would support increasing cyclone intensity.

As mentioned above, the atmosphere, ocean and individual storm dynamics related to cyclone intensity forecasts have been individually examined with moderate success, but it is harder to define their total collective influence due to their complex interactions. However, DeMaria et al. (2005) showed that inclusion of OHC derived from satellite altimetry improved forecasts of TC intensity over the eastern North Pacific by up to 7% over 12-72 hours. Mainelli et al. (2008) showed that use of OHC rather than SST improved Atlantic intensity forecasts by up to 3.5% over 72 hours. Mainelli et al. (2008) also showed that OHC was more significant when forecasting stronger storms because a higher value of OHC is required to intensify a storm above Category 2 strength. For example, they noted that when OHC was added to the Statistical Hurricane Intensity Prediction Scheme (SHIPS) technique the intensity errors decreased by 5% for all Category 5 storms, and up to 20% for some individual storms with the most gain in the 72-96 hour period.

The focus of this thesis is the influence of the OHC value and its changes through the analysis of *in situ* observations and model analyses on Typhoons Sinlaku and Jangmi

in September 2008 as they moved over the western North Pacific Ocean and eventually interacted with the island of Taiwan. Both storms formed over the deep, warm Pacific Ocean water and moved through warm and cold eddies with varying effects of vertical wind shear along their paths.

C. TROPICAL CYCLONE AND OCEAN CONDITIONS AUG-SEPT 2008

Typhoon Sinlaku and Super Typhoon Jangmi occurred in the western North Pacific Ocean in September 2008 during the Tropical Cyclone Structure 2008 (TCS-08) project (Elsberry and Harr 2008). The U.S. Air Force Reserve reconnaissance WC-130J aircraft investigated both of these storms and obtained atmospheric data using dropwindsondes and oceanic data using Airborne Expendable Bathythermographs (AXBTs). These data sets plus satellite imagery and real-time numerical forecast models are the tools used for analyzing TCs and their interaction with the ocean environment and the atmospheric environment. Impact of Typhoons on the Ocean in the Pacific (ITOP 2010) also studied TC interaction with the ocean with AXBTs deployed in several TCs in the western North Pacific in 2010. While both projects occurred in almost the same location roughly between Guam and Taiwan in the western North Pacific Ocean, only data from TCS-08 are examined in this study.

1. Tropical Cyclone Structure 2008 (TCS-08)

The combined TCS-08/T-PARC field experiment was sponsored by the Office of Naval Research (ONR) and the National Science Foundation (NSF) to study the mechanisms and predictability of TC formation, intensification, and structure change. The objectives of TCS-08 were to obtain *in situ* observations by application of sensors, dropwindsondes, and AXBTs to increase understanding of the processes occurring during changes in intensity and storm structure in real- or near-real time over the lifecycle of one or more TCs. Additionally, *in situ* observations were obtained to validate satellite-based tropical cyclone intensity estimates against concurrent satellite overpasses. Seven aircraft operations were conducted over the life cycle of TY Sinlaku, and three aircraft operations were conducted during STY Jangmi as it passed from the deep warm ocean region to a

warm eddy and finally over a cold eddy. During the same time period, Jangmi had intensified from a Category 1 to a Category 5 super typhoon.

2. Western Pacific Ocean During September 2008

During the winter of 2007–2008, the El Nino Southern Oscillation (ENSO) event was transitioning from a warm El Nino phase to a neutral condition. During the summer of 2008, a cool La Nina condition began to develop. In the central Pacific Ocean, a cold SST anomaly existed while a warm SST anomaly existed in the western North Pacific over the Philippine Sea between Guam and Taiwan (Figure 3).

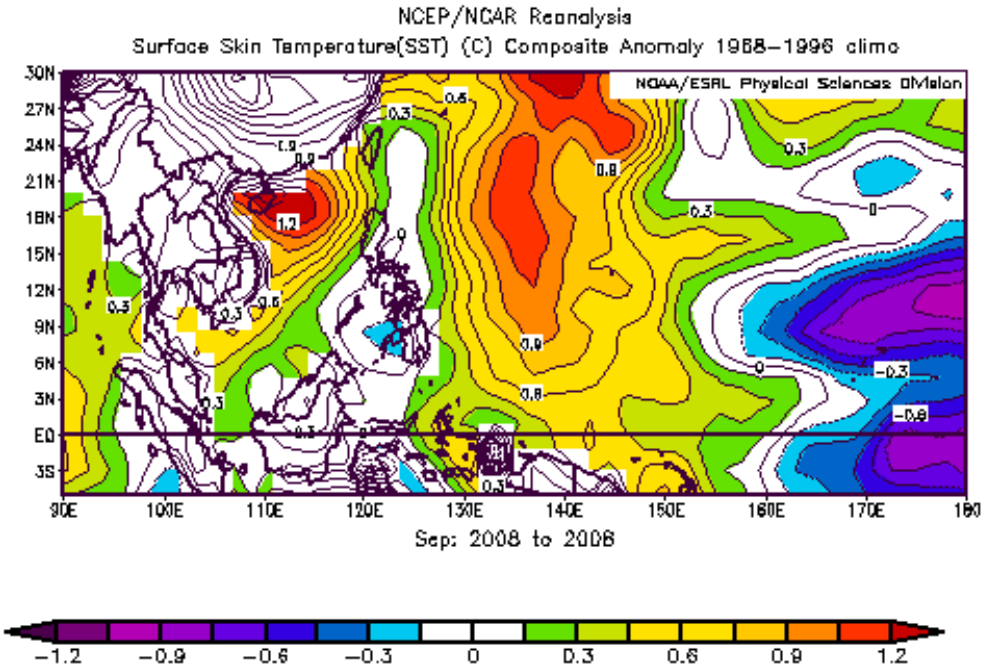

Figure 3. Analyzed SST anomaly (^{o}C) over the Philippine Sea during Sept 2008.

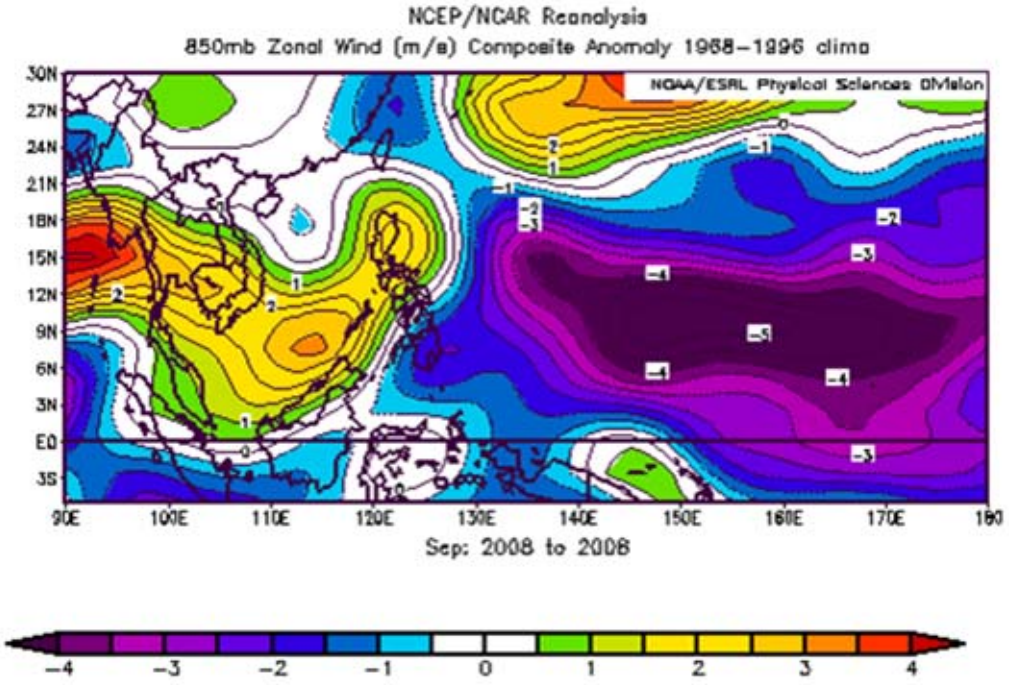

Figure 4. Zonal wind anomaly (m s^{-1}) at 850 hPa over the Philippine Sea during Sept 2008.

A large region of anomalous easterly 850 hPa zonal winds extended throughout the tropical western North Pacific Ocean during September 2008 (Figure 4), which is also an indicator of a developing La Nina condition. This pattern of anomalous low-level winds is associated with enhanced trade winds and a very weak (or non-existent) monsoon trough over the Philippine Sea. During a La Nina (Figure 5b), TC formation and track pattern are very different from during normal and El Nino years (Figure 5a). Under a La Nina condition, TC formation in the western North Pacific occurs farther west than normal and the storms have tracks more toward the South China Sea and eastern China with fewer storms recurving poleward toward Japan (Wang and Chan 2002).

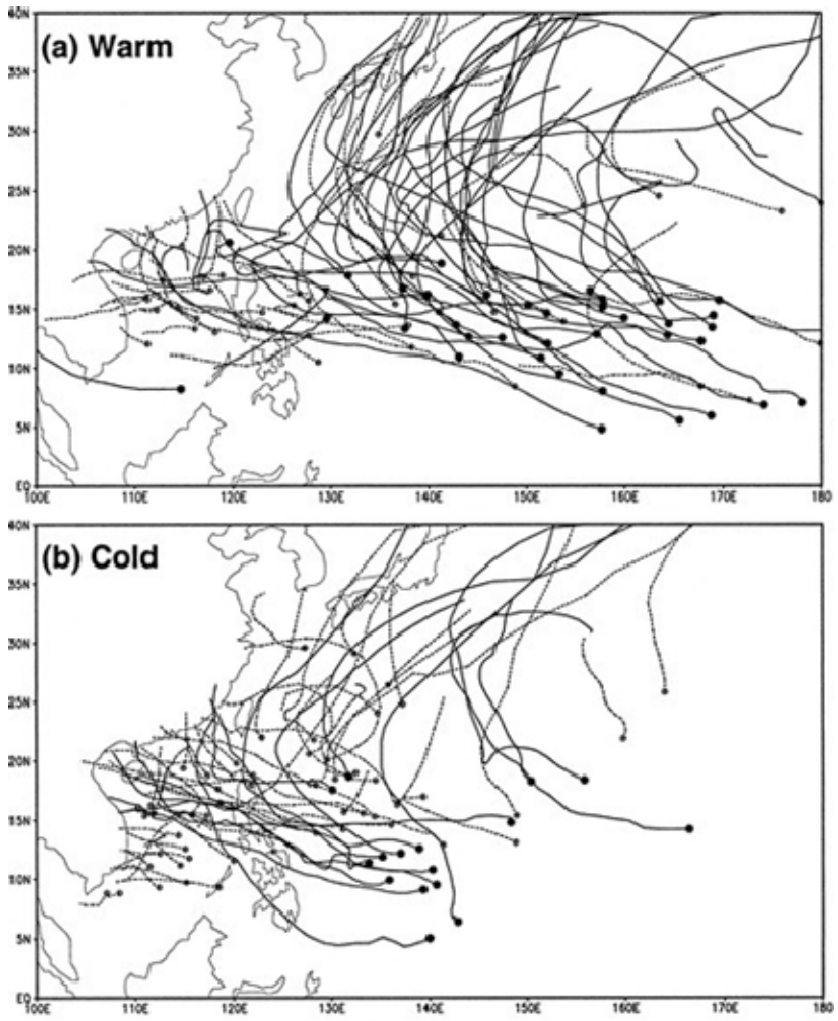

Figure 5. (a) El Nino (warm signal) and (b) La Nina (cold signal) TC formation locations (dots) and tracks for the six warmest and coldest years between 1965-1999 (Wang and Chan 2002).

Near real-time analyses of SST (Figure 6) and OHC (Figure 7) from the Naval Research Lab Stennis Space Center (NRLSSC) East Asian Seas Nowcast/Forecast System (EASNFS) for 6 September 2008 confirm the warm conditions over the Philippine Sea that existed just before the formation of Typhoon Sinlaku. During September 2008, much of the ocean between Guam and Taiwan had SSTs of 30.5^{o}C, which was 1 ^{o}C to 1.5 ^{o}C warmer than is typical during of September. Over this same region, OHC is greater than the 60 kJ cm^{-2} threshold needed to support category 5

typhoons (Lin et al. 2008 and Mainelli et al. 2008). Note that to the east of Taiwan a significant cold-core eddy exists that will actually persist throughout the month and influence Super Typhoon Jangmi when it eventually passes over this part of the ocean.

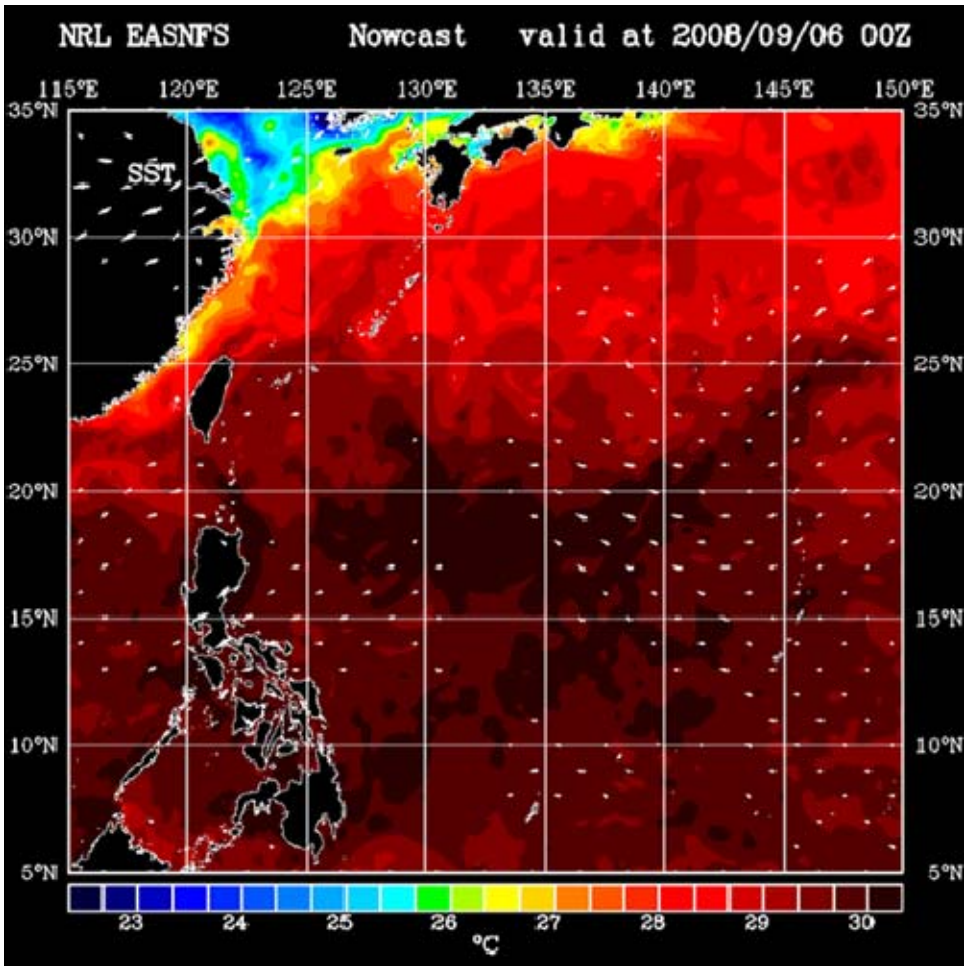

Figure 6. Analysis of SST (°C) from the EASNFS Nowcast Forecast System at 0000 UTC 6 September 2008 from the NRLSSC.

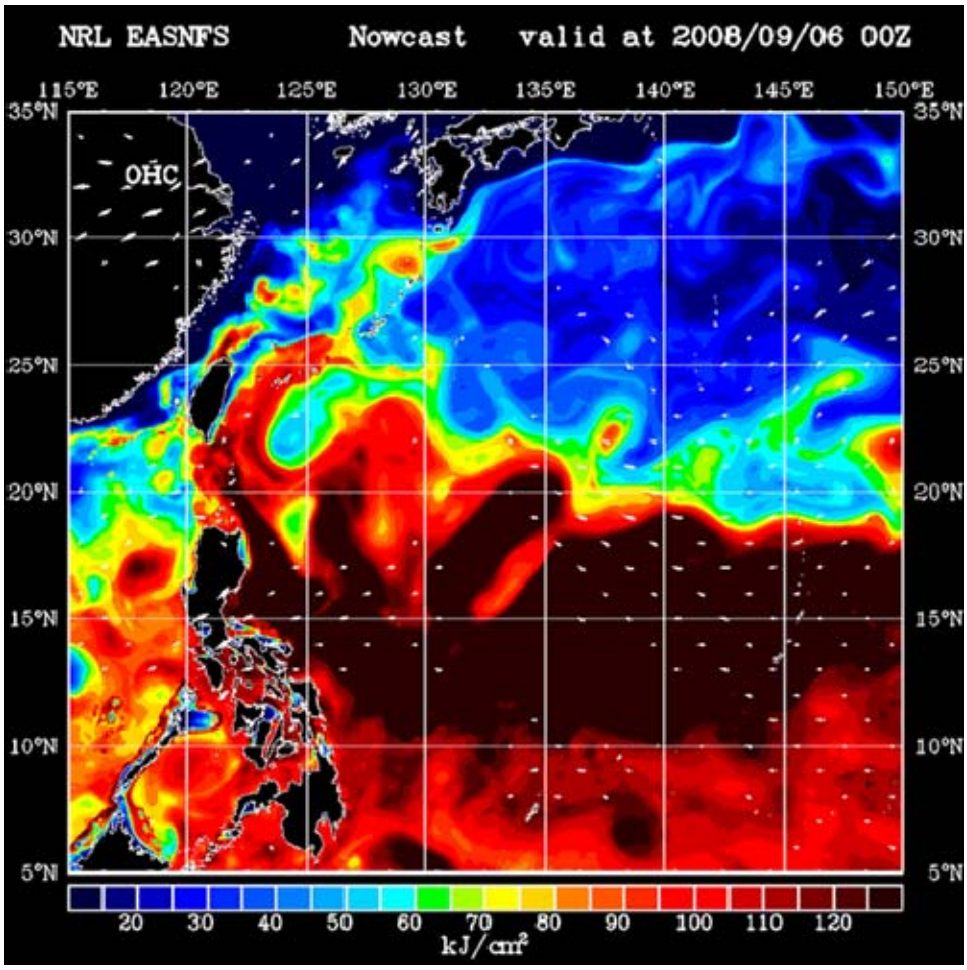

Figure 7. Analysis of OHC (kJ cm^{-2}) from the EASNFS Nowcast at 0000 UTC 06 September 2008 from the NRLSSC.

D. SUMMARY

The cases of TY Sinlaku and STY Jangmi during the TCS-08/T-PARC experiments provide unique opportunities to examine fluctuations in TC intensity as a function of variations in atmosphere and ocean conditions. In addition, the observations of OHC and mixed-layer depth (MLD) collected are compared to model-derived values at the same location that the observations were taken. Finally, forecast intensity improvements based on biases noted between the differences in observed and modeled ocean profiles will be recommended.

THIS PAGE INTENTIONALLY LEFT BLANK

II. BACKGROUND

A. OCEAN SAMPLING

1. AXBT Processing

The AXBT is the primary instrument for measuring the characteristics of the ocean column from an aircraft. During TCS-08/T-PARC, more than 200 AXBTs were deployed during WC-130J flights into several tropical circulations that varied from open waves to super typhoon intensity. When the AXBT is dropped from the airplane, its radio signal is recorded on a receiver in the plane and then several processing steps are necessary before it becomes useable data. The output from the AXBT processing system is a "FIN" file that contains one meter resolution of the ocean temperatures to a depth of 400 or 800 meters. Several important variables can then be derived from the AXBT trace (Table 1). These include the SST at the top of the profile and the MLD, which distinguishes the well-mixed upper ocean from the steady temperature decrease in the thermocline below the MLD. The SST is often used to predict the intensity to which a typhoon could potentially develop if it passes over an undisturbed area of ocean. More important to TC intensity is the OHC, which is the heat content in the ocean column from the surface down to the 26^{o}C isotherm, and has units in kJ cm^{-2}.

Table 1. Ocean parameters derived from the AXBT profile.

Parameter	Definition
SST	Sea-Surface Temperature, or skin temperature of the ocean
Z26	Depth of the 26°C isotherm, important for OHC equation
T100	Average Temperature of the top 100 meters of the ocean
OHC	Ocean Heat Content calculated for a column of water >26°C
MLD	Mixed Layer Depth
Slope	Slope of the thermocline below the MLD

In the sample data set for Typhoon Jangmi provided in Table 2, the SST is the top value of the AXBT trace. The computations for Z26, T100, and OHC were built into a post-processing program. As defined above in Table 1, the OHC is defined in Price (2009), which is also based on the hurricane heat potential defined by Leipper and Volgenau (1972), and is the heat content of an ocean column from the surface to the 26°C isotherm:

$$OHC(x,y) = \rho_0 C_p \int_{Z_{26}}^{0} T_i(x,y,z) - 26)dz$$

In this expression, sea-water density is defined as ρo = 1025 kg m-3 and heat capacity is defined as Cp = 4.0 x 103 Jkg-1 oC-1. The lower limit of integration is the depth of the 26oC isotherm, Z26. Examples of these derived variables from AXBTs collected in STY Jangmi from the aircraft flight on 25 Sept 2008 are provided in Table 2. An example of an ocean temperature profile taken from AXBT 200 in Table 2 is provided in Figure 8.

Table 2. Ocean variables measured and derived quantities from the AXBTs deployed in Typhoon Jangmi from 1856 UTC 25 September to 0118 UTC 26 September.

				Trace				Slope	T100	OHC	OHC24
AXBT#	Time (UTC)	Lat(N)	Lon(E)	Depth	SST C	26°C Depth	MLD m	°C/100m	°C	KJ/cm^2	KJ/cm^2
195	1856	12.59	137.29	146	29.56	94.71	5	4.06	27.79	73.03	160.72
196	1916	13.01	136.16	285	29.60	150.21	61	4.50	29.22	154.53	289.78
197	1946	13.30	134.35	731	29.81	152.80	67	4.01	29.42	169.19	306.26
199	2021	13.19	132.24	550	29.81	139.26	48	4.11	29.29	152.63	277.55
200	2047	11.54	132.05	397	29.54	132.46	62	4.94	29.35	152.56	278.31
201	2100	11.04	133.31	648	29.81	129.91	42	5.81	29.16	140.35	250.82
202	2117	12.09	134.02	411	29.64	153.37	51	3.36	29.29	161.94	296.88
203	2208	14.36	135.03	395	29.72	156.67	61	3.97	29.37	165.45	304.42
204	2229	15.37	135.41	408	29.86	165.32	84	5.17	29.75	188.03	336.98
205	2250	15.43	134.12	412	29.92	121.68	52	5.06	29.08	129.16	249.16
206	2314	15.46	132.31	392	28.85	154.30	60	4.00	29.49	167.58	308.21
209	2335	14.43	133.00	352	29.49	95.07	10	3.70	27.67	67.96	162.31
210	0050	11.24	135.06	681	29.69	99.84	40	7.85	28.69	109.54	203.36
211	0118	13.04	135.51	565	29.60	151.22	50	3.60	29.04	147.65	281.59

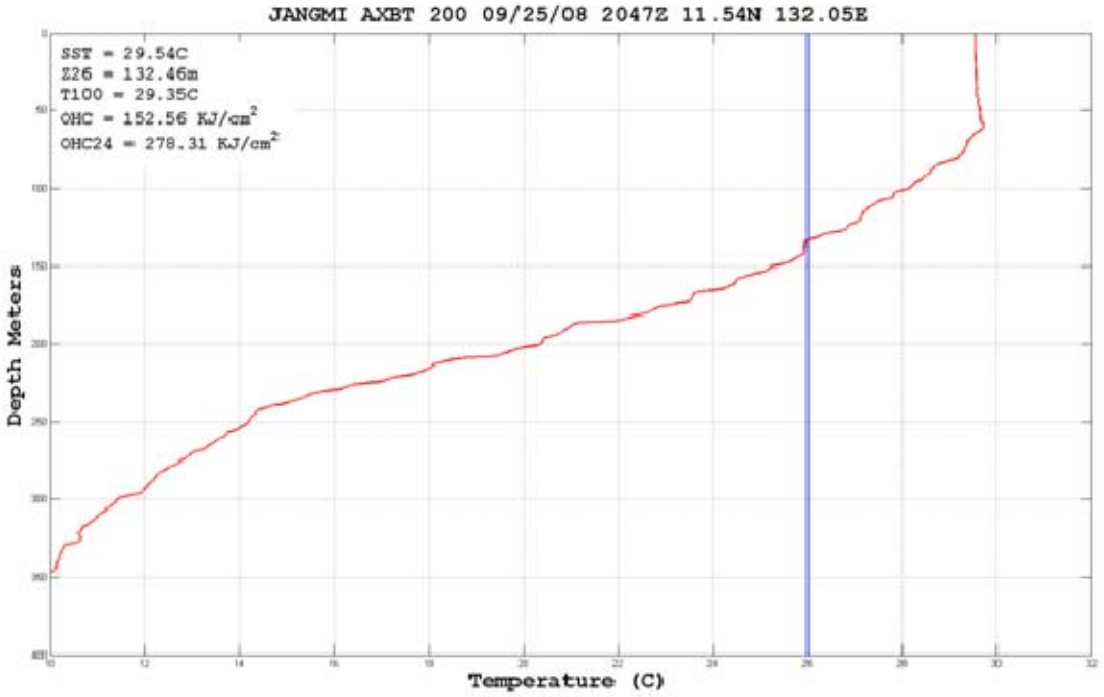

Figure 8. Vertical profile of ocean temperature (^{o}C) as measured by AXBT 200 from the 25 September 2008 Jangmi flight.

The variables measured and then derived from the AXBT profiles are vital in understanding how the ocean environment interacts with and influences the TC. Near equally as important is the comparison of *in-situ* data with satellite-sensed data for verification and documenting biases for different conditions. For example, how close is the *in-situ* SST to the remotely sensed SST? Satellite-derived SST is much more reliable over open ocean that is undisturbed by strong wind and wave action, but this is not the case when near a TC. The SST and Z26 are the boundaries of the ocean column for the OHC calculation, which makes these two variables very important for predicting storm intensity. Therefore, OHC is the most important variable considered in this study and is used as the baseline in comparing *in-situ* data with both the broad EASNFS OHC analysis from NRLSSC and the single point modeled AXBT trace comparisons. The T100 variable (Price 2009) is roughly comparable to the OHC in the deep ocean, and is the average temperature of the top 100 meters of the ocean column. As this temperature

increases, so does OHC. The MLD and Slope are both measures of the larger scale ocean environment in which near-surface features exist and give indications of how much mixing can occur at the base of the mixed layer.

The *in situ* ocean observations from the AXBTs deployed during the flights into Sinlaku and Jangmi will be used to evaluate, analyze, and verify satellite-derived and climatic data. In addition, the observations are utilized in ocean prediction models for analysis, nowcasts, and forecasts of SST, OHC, and typhoon intensity.

2. Composite AXBT Processing

For analysis of Typhoon Sinlaku four AXBT profiles (Figure 9) relative to the position of the storm (i.e., ahead, behind, and on either side) were used to identify changes to the ocean columns that the storm induced. These four AXBT positions are displayed in Figure 10 relative to the current position of TC during the flight and the underlying OHC analysis from 2 days prior to the storm arriving at this position. The variation in ocean conditions from the 12 September flight (Figure 9) reflect not only changes to the ocean column from the influence of the storm but also take into account variations due to pre-existing ocean features such as the cold eddy that TY Sinlaku had just passed over. An inspection of Figure 10 reveals why AXBT 152 had the lowest SST and most shallow MLD as it was both in the wake of the storm and on the outside edge of the cold eddy. By contrast, AXBT 156 was deployed southwest of the storm and dropped into the Kuroshio Current.

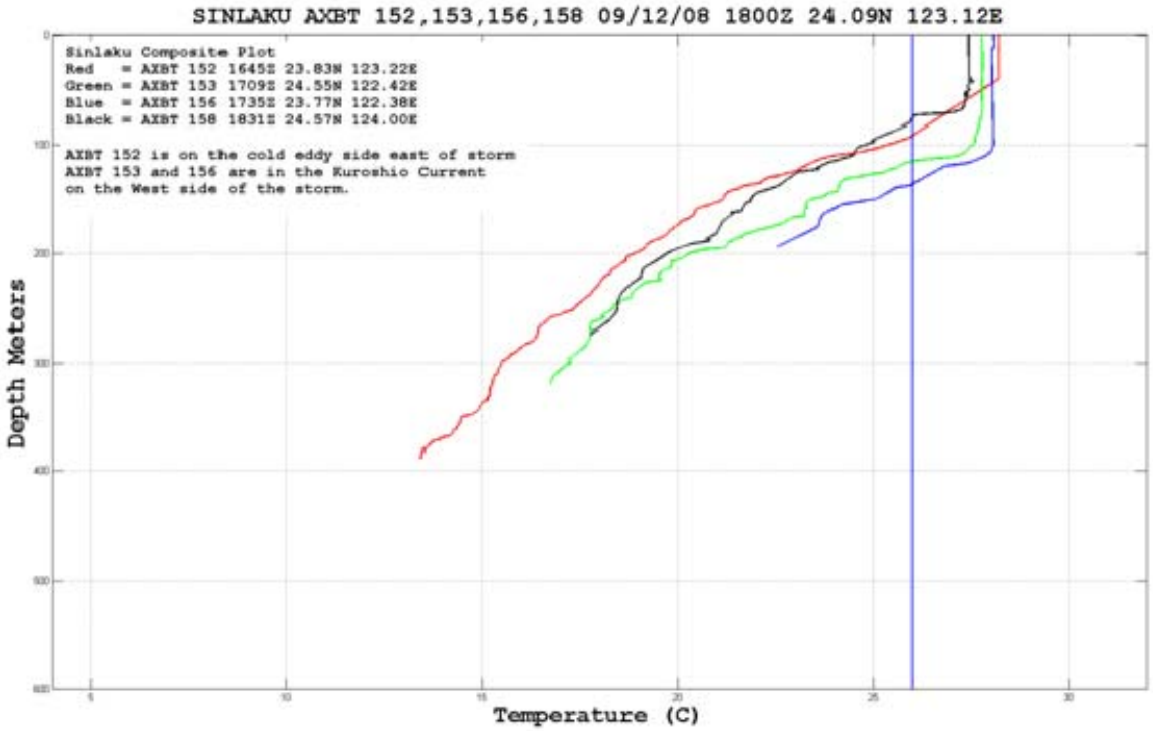

Figure 9. Plots of AXBTs 152, 153, 156, and 158 from the flight on 12 September 2008 into TY Sinlaku. Locations of the AXBTs are indicated in Figure 10. The 26 ^{o}C isotherm is indicated by the blue vertical line.

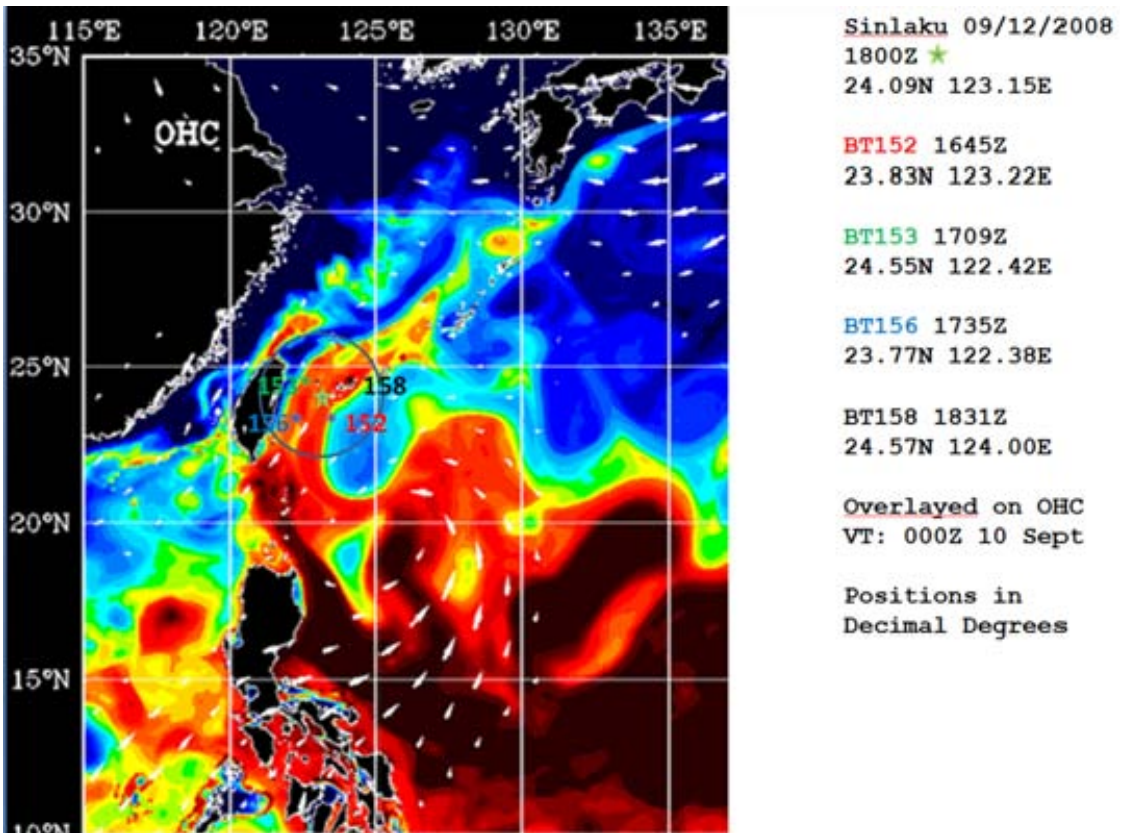

Figure 10. Locations of AXBTs 152, 153, 156, and 158 relative to the center of Typhoon Sinlaku and the EASNFS analysis of OHC at 1800 UTC 12 September 2008. The arrows indicate the direction of the atmospheric forcing on 12 September, which was two days prior to the AXBT deployments.

3. Comparison of AXBTs with EASNFS Model

The NRLSSC EASNFS model uses a mixture of climatic, satellite, and *in situ* observations to produce SST and OHC analyses and forecasts. The EASNFS model has 41 vertical levels and a horizontal resolution of 1/16 deg. Satellite altimetry from the Advanced Very High Resolution Radiometer (AVHRR) and four variables from the Navy Operational Global Atmospheric Prediction System (NOGAPS) are used to produce the ocean profile at a given position (Lin et al. 2008). Model ocean profiles are interpolated to the location of each AXBT to allow identification of cases when model and observed profiles are similar (Figure 11) or different (Figure 12). The model-derived ocean profiles produced at the same location of the AXBTs were kindly

provided by Dr. D.-S. Ko from NRLSSC. These examples of AXBT profiles from a Jangmi flight with the corresponding EASNFS ocean model profiles will be examined in Chapter III.C to evaluate the accuracy of the EASNFS model. Such analyses of AXBT-model comparisons will aid NRL SSC in making improvements to the model and inform users more about model limitations.

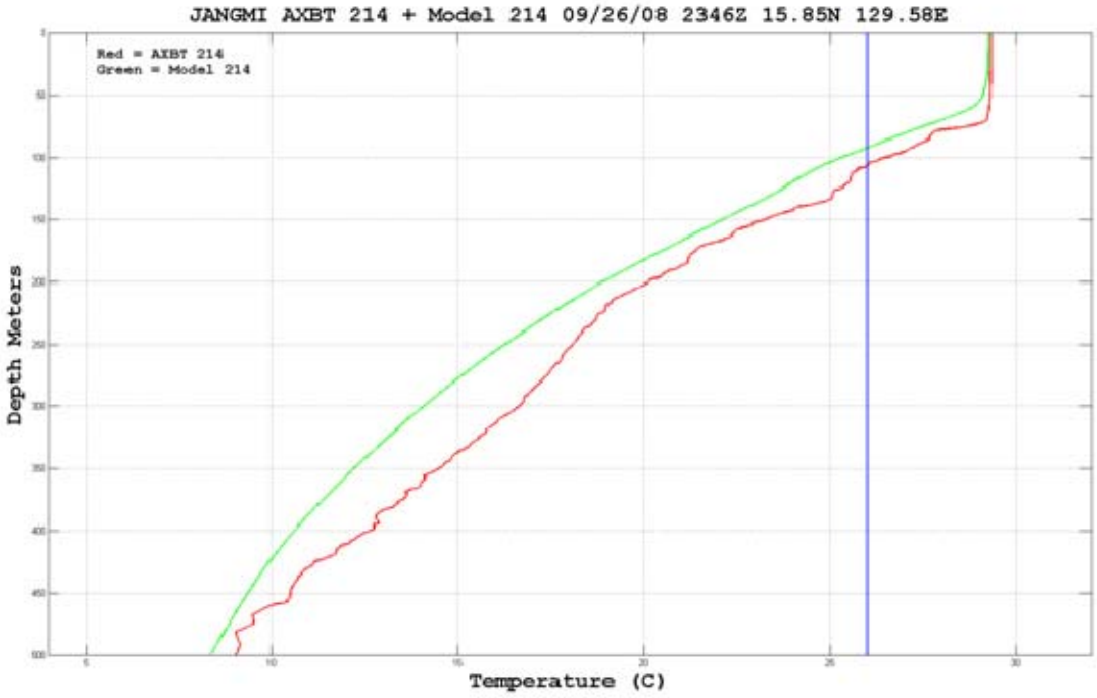

Figure 11. Comparison of Jangmi AXBT 214 with the EASNFS model profile at the same location.

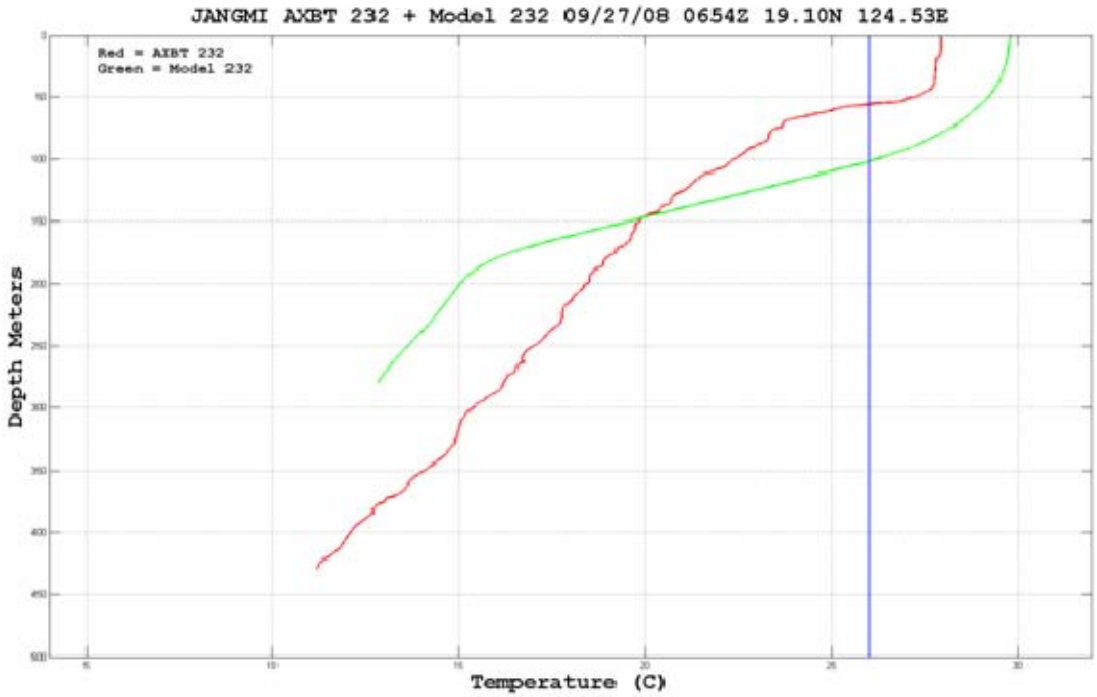

Figure 12. Comparison of Jangmi AXBT 232 with the EASNFS model profile at the same location

4. Vertical Wind Shear Analysis

The evolution of vertical wind shear over both TY Sinlaku and STY Jangmi is defined from the European Center for Medium-range Weather Forecasts (ECMWF) analyses at one-quarter degree resolution. Vertical wind shear is computed by the vector difference in winds at 200 hPa and 850 hPa averaged in a radial band between 3 degree and 5 degree radius that is centered on the storm position in the analysis.

B. DATA SUMMARY

1. TY Sinlaku (TCS-33, TY 15W)

The characteristics of Sinlaku are defined from seven Air Force WC-130J flights from 9 September 2008 through 19 September 2008. The first four flights occurred while Sinlaku was on a westward heading toward Taiwan and three more flights occurred after Sinlaku recurved and headed toward the Japanese Islands. Additional flights were also flown by the Naval Research Lab (NRL) P-3 with a total of 175 dropsondes deployed over 13 flights between the two aircraft and 67 AXBTs deployed from the WC-130J (Table 3).

Table 3. Summary of WC-130J flights in TY Sinlaku with the number of radial legs through the center, numbers of AXBTs and dropwindsondes in each flight, and the type of flight pattern.

Flight	Mission Start	Mission End	Radial Legs	AXBTs	Sondes	Pattern
0133W	09/09 0030Z	09/09 1045Z	2	11	20	Alpha
0233W	09/10 0140Z	09/10 1225Z	2	10	24	Alpha
0433W	09/11 0728Z	09/11 1828Z	2	13	25	Alpha
0533W	09/12 1138Z	09/12 2318Z	2	10	21	Alpha
0833W	09/16 2044Z	09/17 0426Z	0	8	7	Synoptic
1033W	09/17 2224Z	09/18 0713Z	3	9	32	Butterfly
1233W	09/09 0053Z	09/20 0711Z	0	6	18	Synoptic

The flight patterns flown on 9 and 10 September (Figures 13 and 14) were designed to map the structure of the developing tropical storm (TS) 15W, which became Typhoon Sinlaku at 0900 UTC 10 September. Two additional flights on 11 and 12 September (Figures 15 and 16) were conducted to continue observing the structure of the storm and collect AXBT profiles of the underlying ocean in the vicinity of the storm. Typhoon Sinlaku then approached and moved over the northern tip of Taiwan before getting caught up in the upper-level westerlies and recurving to the east. The weakened TS Sinlaku moved toward Japan and briefly strengthened to minimal typhoon intensity on 17 September before undergoing extratropical transition on 20 September. The last three flights from 17-19 September gathered observations of the re-intensification and

extratropical transition process by sampling the ocean and atmosphere in the vicinity of the storm and then to the north along the polar front boundary over Japan.

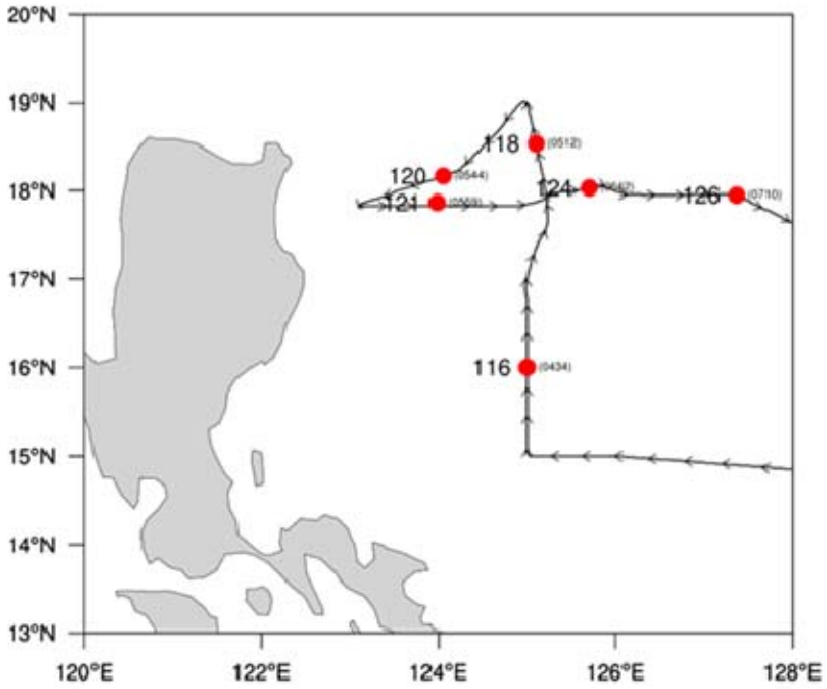

Figure 13. Flight path of the WC-130J into TS Sinlaku on 9 September 2008. Circles with numbers mark the locations of the AXBT deployments.

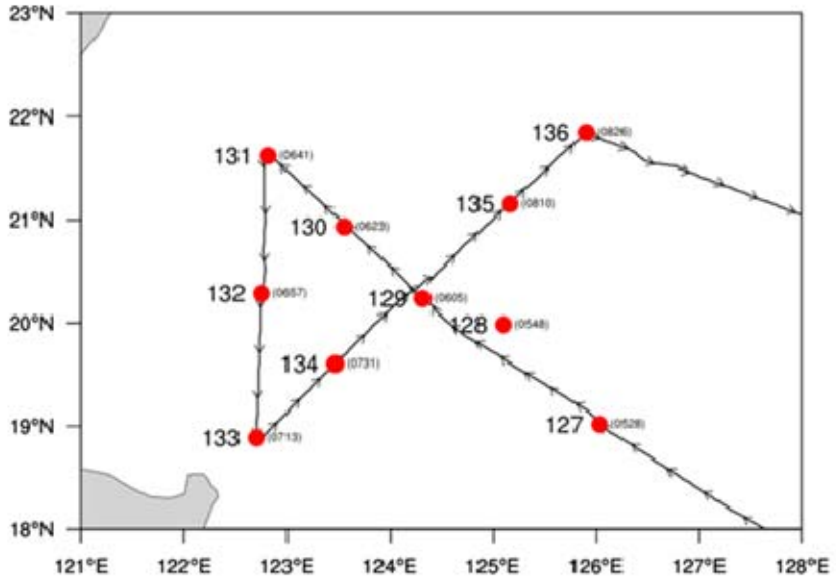

Figure 14. Flight path of the WC-130J into TS Sinlaku on 10 September 2008. Circles with numbers mark the locations of AXBT deployments.

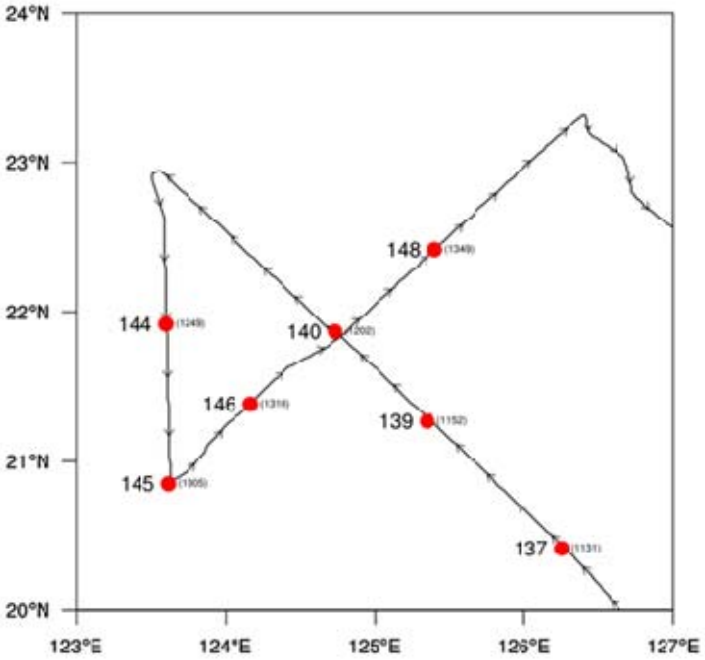

Figure 15. Flight path of the WC-130J into TY Sinlaku on 11 September 2008. Circles with numbers mark the locations of AXBT deployments.

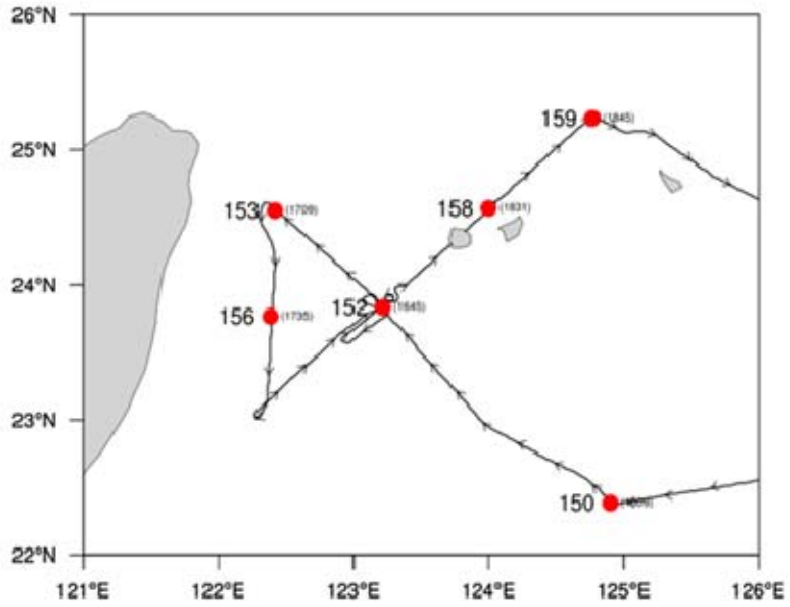

Figure 16. Flight path of the WC-130J into TS Sinlaku on 12 September 2008. Circles with numbers mark the locations of AXBT deployments.

Even as TY Sinlaku began with a north-northwestward track, it was clear that it would be passing over a complex ocean thermal environment (Figure 17). The vertical wind shear in the environment for TS Sinlaku on 9 September is given in Figure 18. Notice that TS Sinlaku was being influenced by 10–15 kt of vertical wind shear over the northern half of the storm. The average vertical wind shear over the next two days as Sinlaku intensified into a Typhoon would remain close to 10 kt.

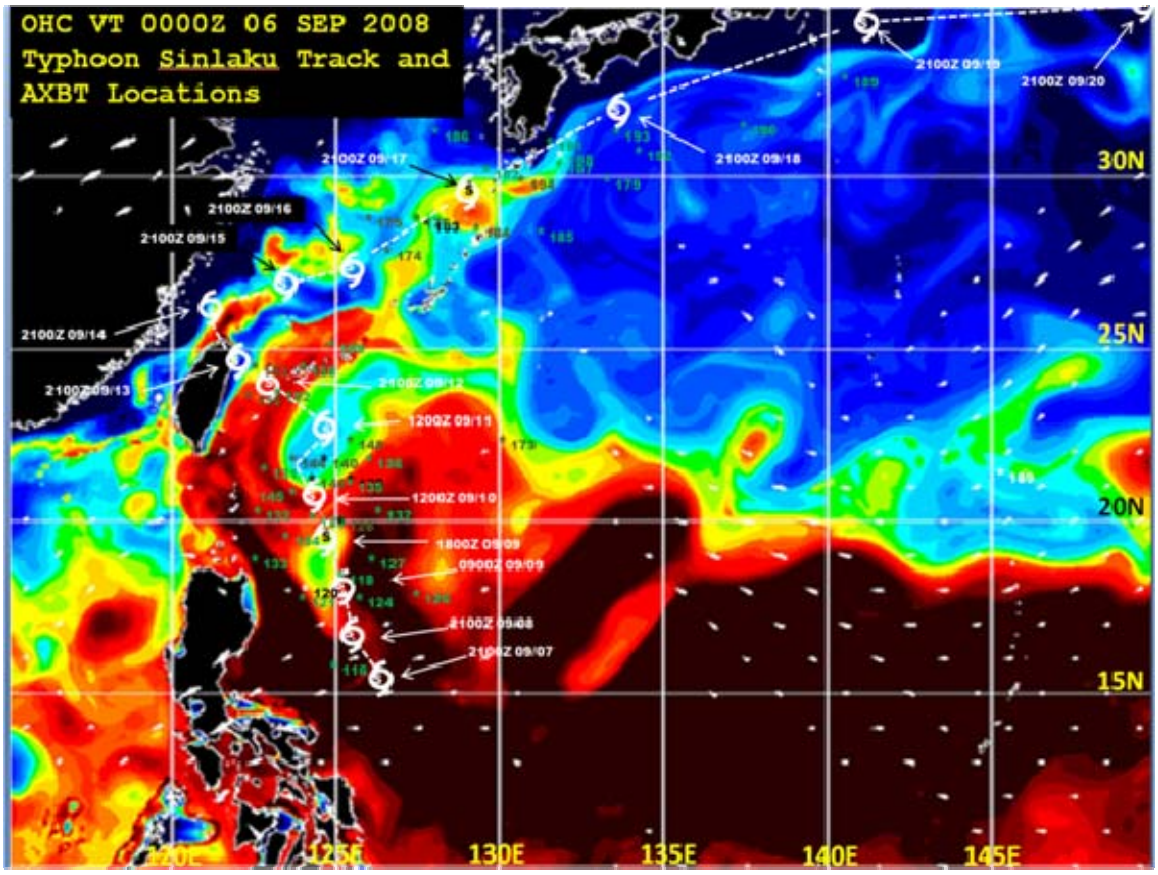

Figure 17. Ocean Heat Content (kJ cm^{-2}) at 0000 UTC 6 September 2008 superimposed with TY Sinlaku storm track and AXBT locations.

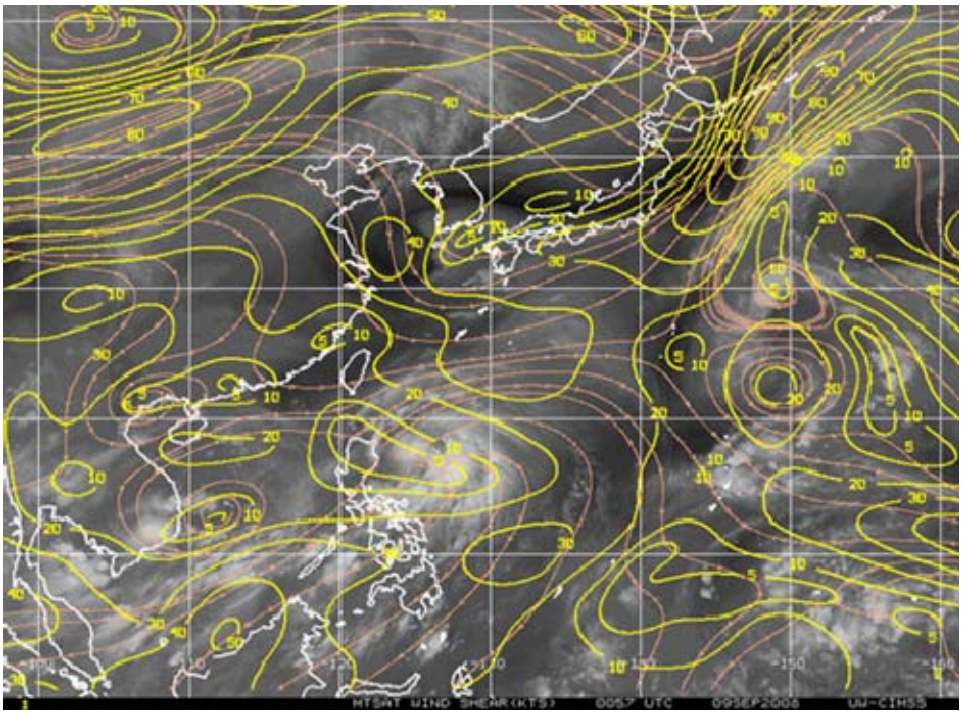

Figure 18. Vertical wind shear direction (streamlines) and isotachs (contours, kt) from the Cooperative Institute for Meteorological Satellite Studies (CIMSS) imagery and infrared satellite at 0057 UTC 9 September 2008.

2. STY Jangmi (TCS-47, STY 19W)

The characteristics of STY Jangmi are defined from three Air Force WC-130J flights from 25 through 27 September 2008. The tropical disturbance labeled TCS-47 by TCS-08/T-PARC was first identified on 16 September as a mass of thunderstorms that drifted westward for six days before it developing into a Tropical Depression (TD) late on 22 September. The environment prior to 21 September was dominated by large values of vertical wind shear due to an upper-level low to the northeast that was moving in tandem with TCS-47 (Figure 19).

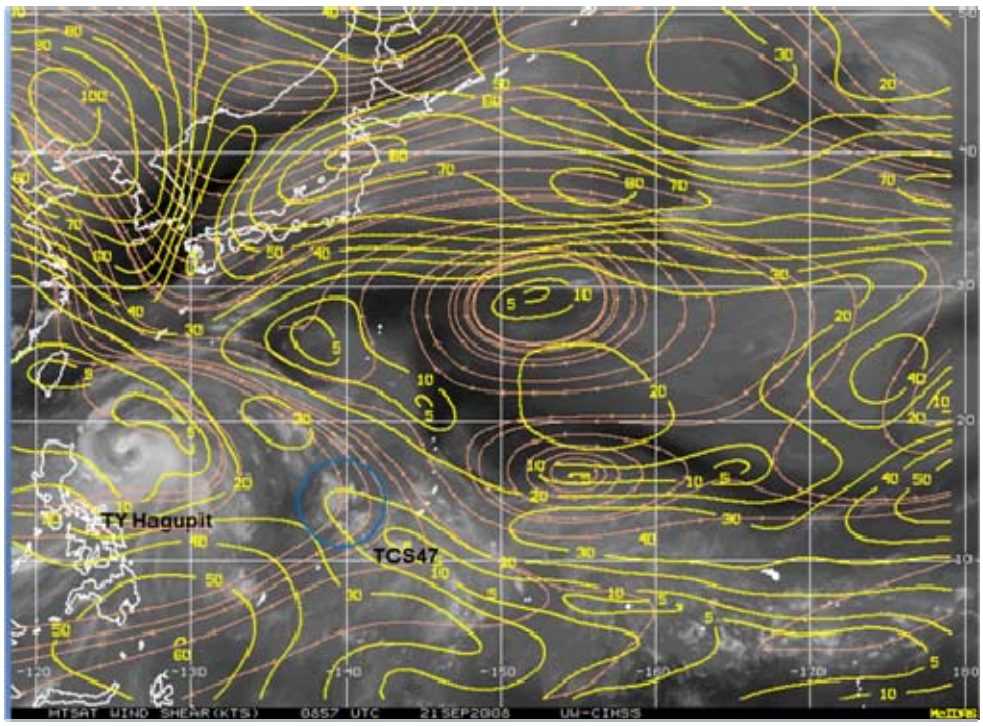

Figure 19. Vertical wind shear direction (streamlines) and isotachs (contours, kt) from the CIMSS image at 0857 UTC 21 September 2008. Note the shear streamlines across TCS-47 with large magnitude of shear.

As TCS-47 moved away from the upper-level shear on 22 September, the persistent deep convection intensified and TD19W formed. The complex OHC ocean environment for Jangmi and throughout September was similar to what Sinlaku encountered (Figure 7). Jangmi also formed over a deep, warm ocean layer and later crossed over warm and cold eddies on its track toward Taiwan. The first two WC-130J flights flown for Jangmi (Figures 20 and 21) were planned to observe intensification of Jangmi from TS to TY. Ultimately, Jangmi intensified into a STY that was the subject of the flight on 27 September (Figure 22). Jangmi was a Category 5 STY when it passed over the cold eddy east of Taiwan on the morning of 28 September. It then weakened and passed over the northern tip of Taiwan. A total of 89 dropwindsondes and 56 AXBTs were deployed during the three WC-130J flights (Table 4).

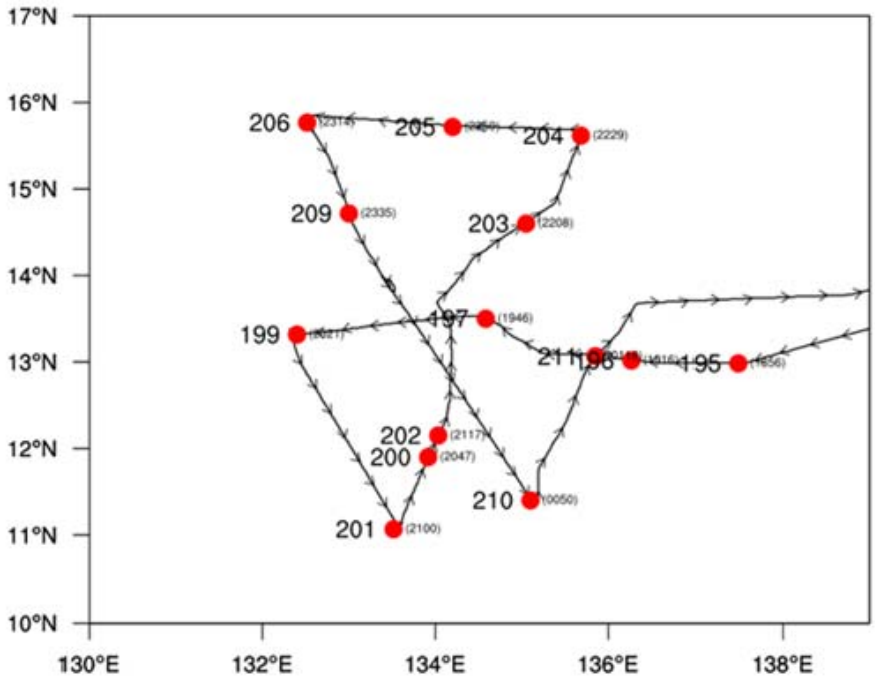

Figure 20. WC-130J Flight path into TY Jangmi on 25 September 2008. Circles with numbers mark the locations of the AXBT deployments.

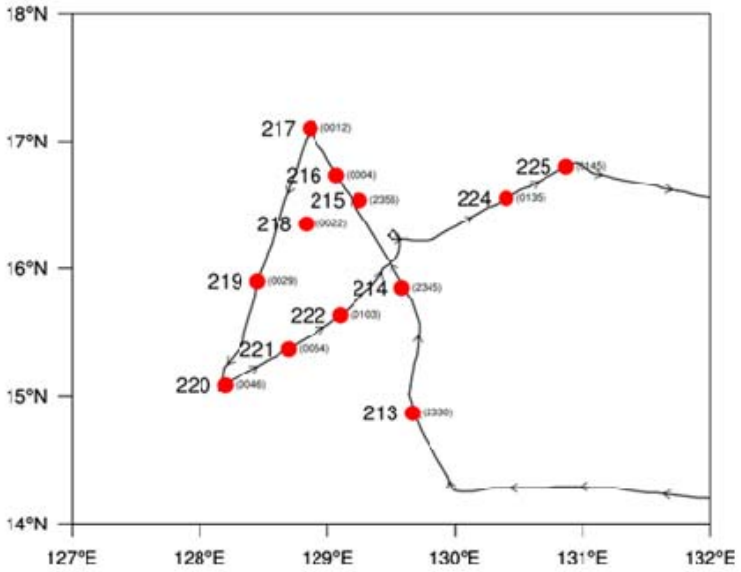

Figure 21. WC-130J Flight path into TY Jangmi on 26 September 2008. Circles with numbers mark the locations of the AXBT deployments.

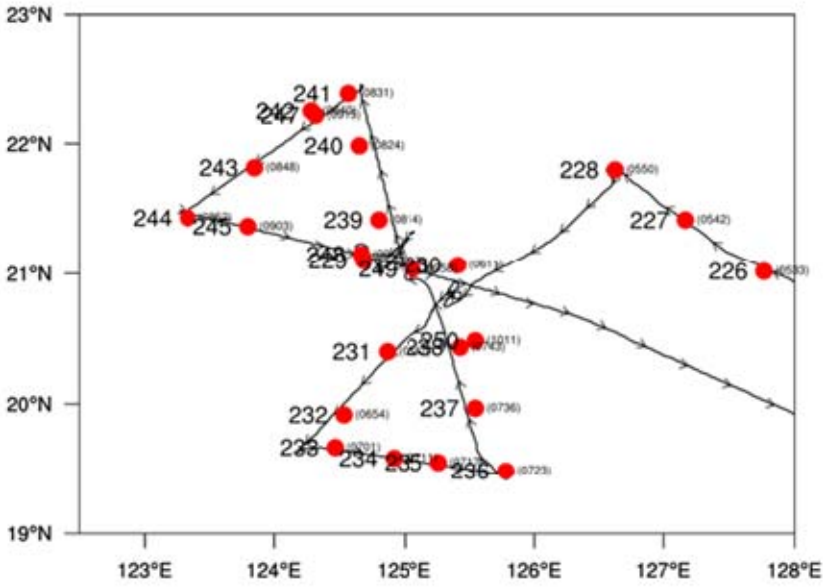

Figure 22. WC-130J Flight path into STY Jangmi on 27 September 2008. Circles with numbers mark the locations of the AXBT deployments.

Table 4. As in Table 3, except for three WC-130J flights into STY Jangmi.

Flight	Mission Start	Mission End	Radial Legs	AXBT's	Sondes	Pattern
0247W	09/24 1713Z	09/25 0320Z	3	17	26	Butterfly
0447W	09/25 2003Z	09/26 0650Z	2	14	24	Alpha
0747W	09/27 0208Z	09/27 1417Z	3	25	39	Butterfly

III. ANALYSIS

A. TY SINLAKU

1. Pretropical Depression Stage

Typhoon Sinlaku formed over the Philippine Sea approximately midway between Guam and the Philippines. Throughout the month of September, a series of warm and cold ocean eddies existed just north of the region of a deep mixed layer that existed throughout the Philippine Sea. Contained in the eddy field was a large cold eddy centered near 22^{o}N and 125^{o}E, and just east of Taiwan there was a warm tongue that was associated with the Kuroshio Current between the cold eddy and Taiwan (Figure 17).

Typhoon Sinlaku was first observed as TCS-033 on 1 September 2008 during the TCS-08 field program. On the first visual satellite image, an arc-shaped set of clouds was identified and classified as a wave in the easterly trade wind flow (Figure 23).

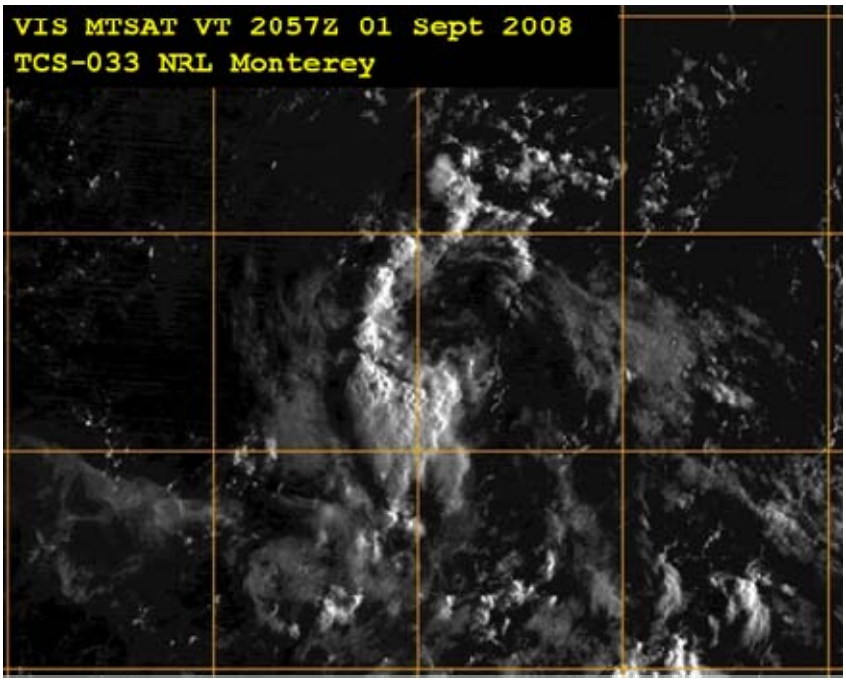

Figure 23. Visual MTSAT image at 2057 UTC 1 September 2008 of TCS-033 near 21.5^{o}N, 150.3^{o}E. Image from http:\\www.nrlmry.navy.mil/sat_products.html.

On 2 September, TCS-033 continued to move westward as a wave with brief cyclic bursts of convection that were difficult to identify on satellite imagery. There was an upper-level cold low north of TCS-033 that was producing moderate northerly vertical wind shear that continued over the wave into 3 September. On 3 September, TCS-033 turned to the southwest and began moving away from the upper-level low and farther from the shear.

At 1957 UTC 4 September, TCS-33 was near 18.5°N, 141°E with increased convection scattered along a nicely arced line that was clearly identifiable as an open wave (Figure 24). On 5 September, convection continued to increase but there was still no indication of cyclonic organization as TCS-033 continued as a low-level open wave (Figures 25 a).

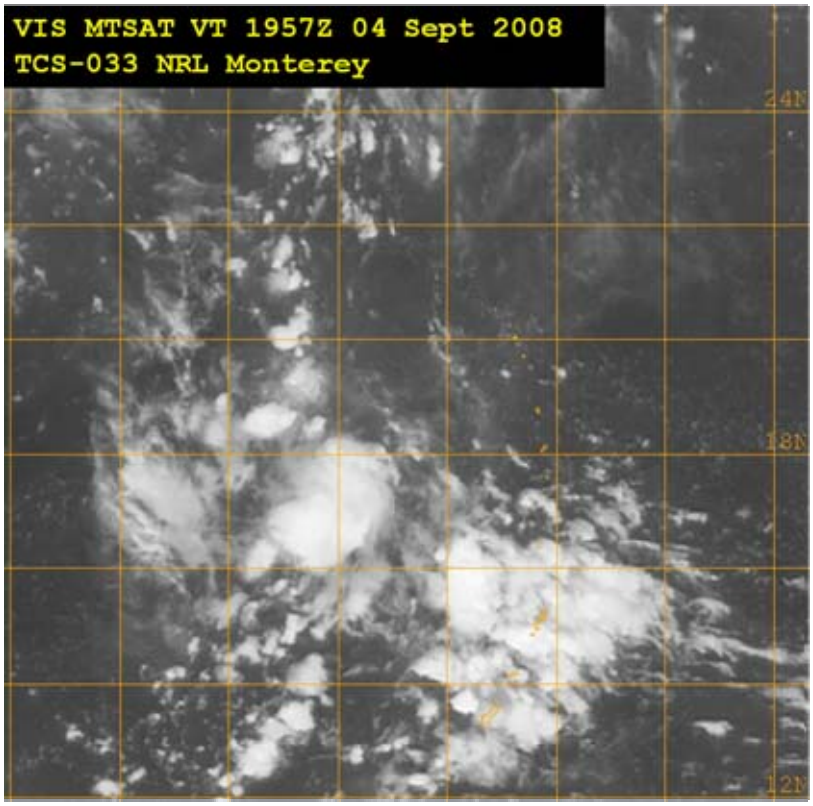

Figure 24. Infrared MTSAT imagery at 1957 UTC 4 September 2008 of TCS-033 near 18.5°N and 141°E. Image from http:\\www.nrlmry.navy.mil/sat_products.html.

On 6 September (Figure 25b), TCS-033 continued to move westward as an open wave into a favorable environment for development away from significant vertical wind shear. Convection increased through the day and by 2100 UTC the convection pattern suggested that possible cyclonic organization was taking place (Figure 26). Based on the ECMWF 850 hPa analysis at 0000 UTC 7 September (Figure 25c), it was clear that the amplitude of the low–level wave also beginning to increase.

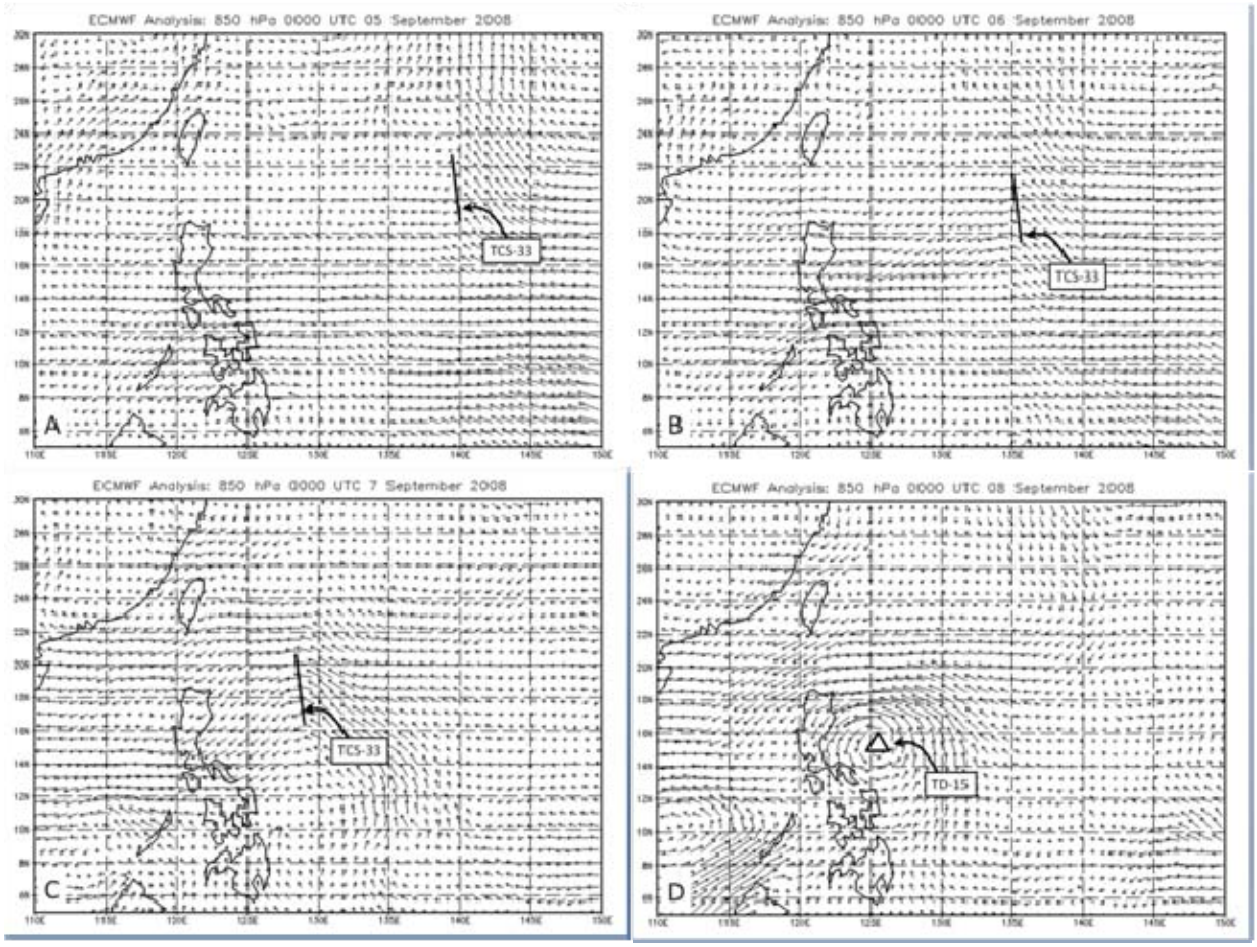

Figure 25. Analyses of 850 hPa winds from the ECMWF at (a) 0000 UTC 5 September 2008, (b) 0000 UTC 6 September 2008, (c) 0000 UTC 7 September 2008, and (d) 0000 UTC 8 September 2008.

At 2100 UTC 7 September (Figure 27), JTWC upgraded TCS-033 from a “poor” to a “fair” area for development. On the 0000 UTC 8 September ECMWF 850 hPa analysis (Figure 27d), the low-level circulation was completely closed. At the 0600 UTC

8 September update, JTWC skipped the normal TC Formation Alert (TCFA) process and issued an advisory for TD15W. Later the same day, the 1200 UTC advisory named the storm TS Sinlaku.

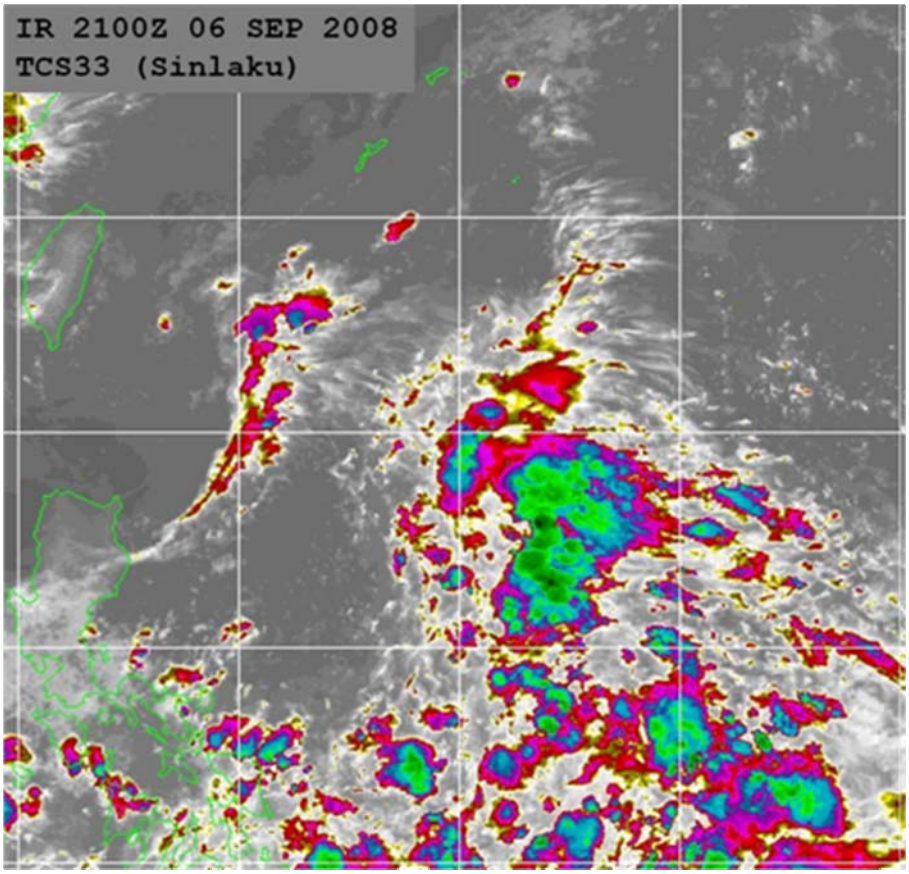

Figure 26. Color enhanced IR MTSAT imagery of TCS-033 at 2100 UTC 6 September 2008. Image from http:\\www.nrlmry.navy.mil/sat_products.html.

Along the track of TCS-033 from 1 September through 7 September, the OHC was greater than 130 kJ cm^{-2} based on the EASNFS OHC analysis (Figure 7). When TCS-033 intensified into a TD, the OHC was 125 kJ cm^{-2}. These OHC values were large enough to support a typhoon of major intensity.

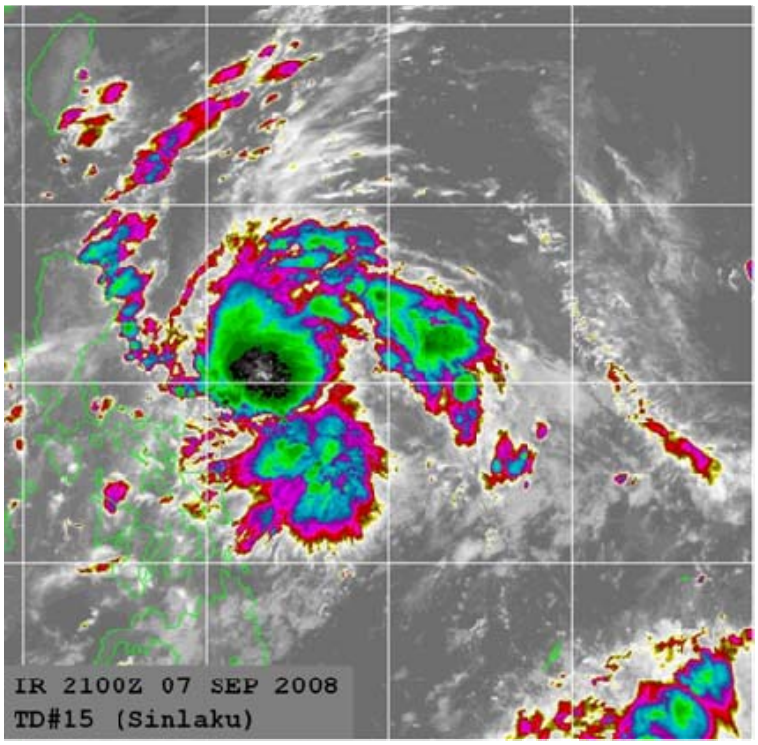

Figure 27. Color enhanced IR MTSAT image of TD15W at 2100 UTC 7 September 2008. Image from http:\\www.nrlmry.navy.mil/sat_products.html.

In a general sense, the formation of TD15W was a classic La Nina type of formation as it traveled as an open wave under the influence of enhanced trade winds for almost 2,300 km before finally forming in the western North Pacific Ocean east of the Philippines.

2. TY Sinlaku Intensification Stage (8–10 September 2008)

Sinlaku underwent a gradual intensification from a TD at 0000 UTC 8 September 2008 to 65 kts by 1200 UTC 9 September 2008 and then underwent rapid intensification after that and reached a peak intensity of 125 kt at 1800 UTC 10 September 2008 (Figure 28). During this period, the magnitude of the vertical wind shear fluctuated around 10 kt (Figure 28) and the storm moved from the region of a warm, deep tropical ocean to over a weak cold eddy on 9 September (Figures 28). The OHC values associated with the cold eddy were near 70 kJ cm^{-2} based on the EASNFS analysis.

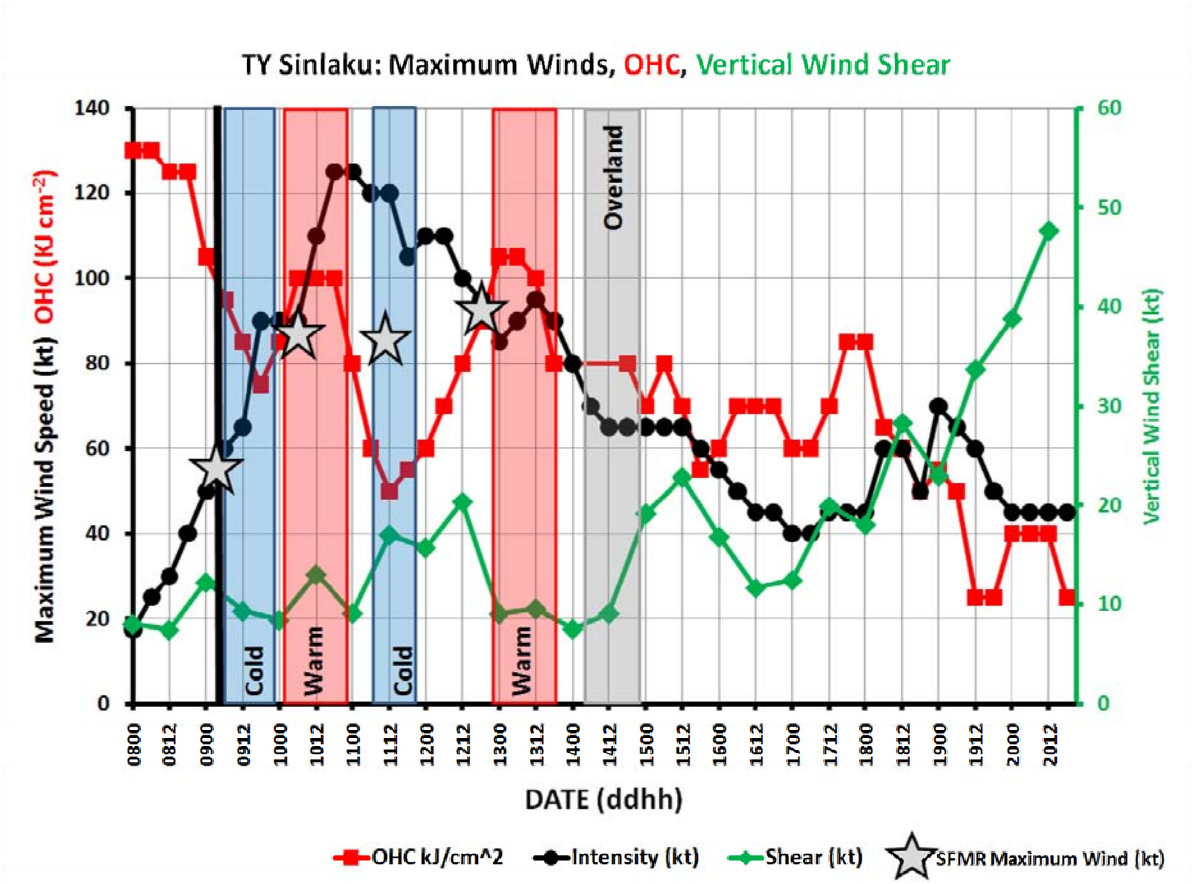

Figure 28. Typhoon Sinlaku OHC (kJ cm^{-2}) values from EASNFS analysis, intensities (kt) in 6-h increments, vertical wind shear (kt) in 12-h increments from ECMWF analysis, and SFMR maximum winds (kt). Colored boxes define periods when Sinlaku traversed significant ocean features or land.

Tropical Storm Sinlaku appeared to be organizing around an area of deep convection (Figure 29a) near the center and a second strong convective band was present along the eastern side of the circulation. Microwave imagery at 0600 UTC (Figure 29b), revealed that the center was beginning to develop a near continuous and symmetric eye wall. Although the vertical wind shear was decreasing between 0000 and 1200 UTC 9 September (Figure 28), the storm convection weakened (Figures 29a,b) on the west and northwest side as it moved over the cold eddy (Figure 30). Additionally, the outflow to the northwest was restricted (Figure 29c).

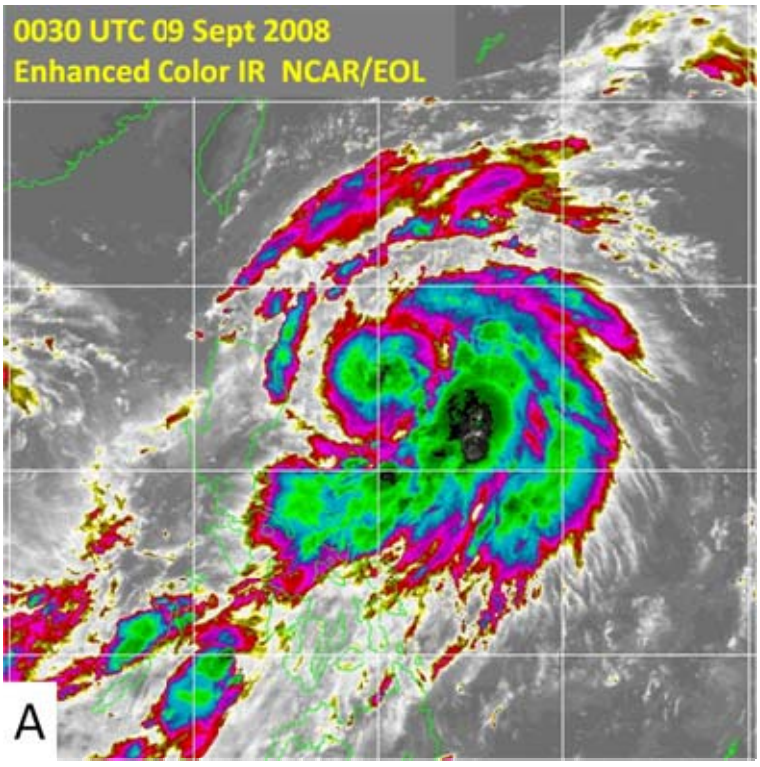
0030 UTC 09 Sept 2008
Enhanced Color IR NCAR/EOL
A

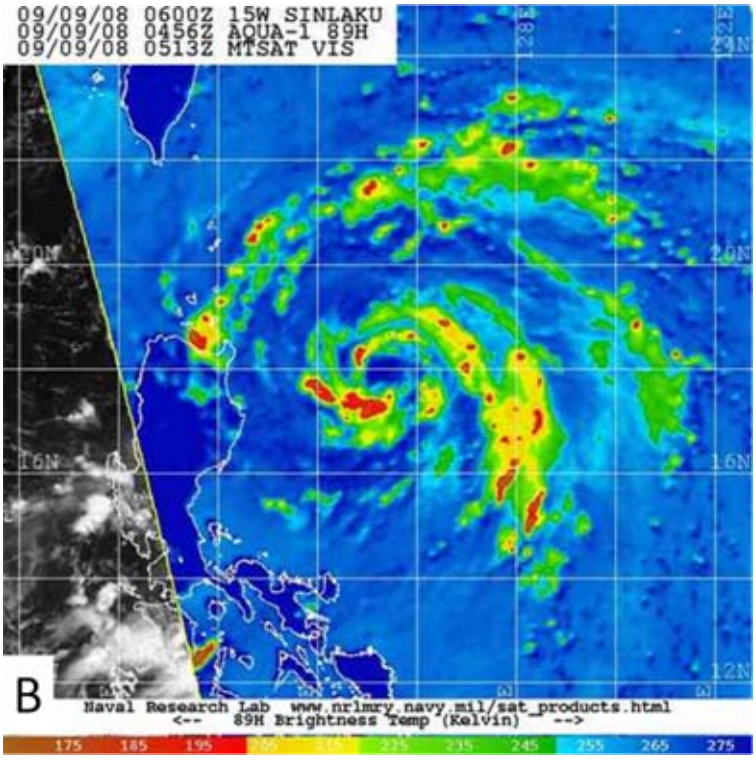
09/09/08 0600Z 15W SINLAKU
09/09/08 0456Z AQUA-1 89H
09/09/08 0513Z MTSAT VIS
20N
16N
12N
B
Naval Research Lab www.nrlmry.navy.mil/sat_products.html
<-- 89H Brightness Temp (Kelvin) -->
175 185 195 205 215 225 235 245 255 265 275

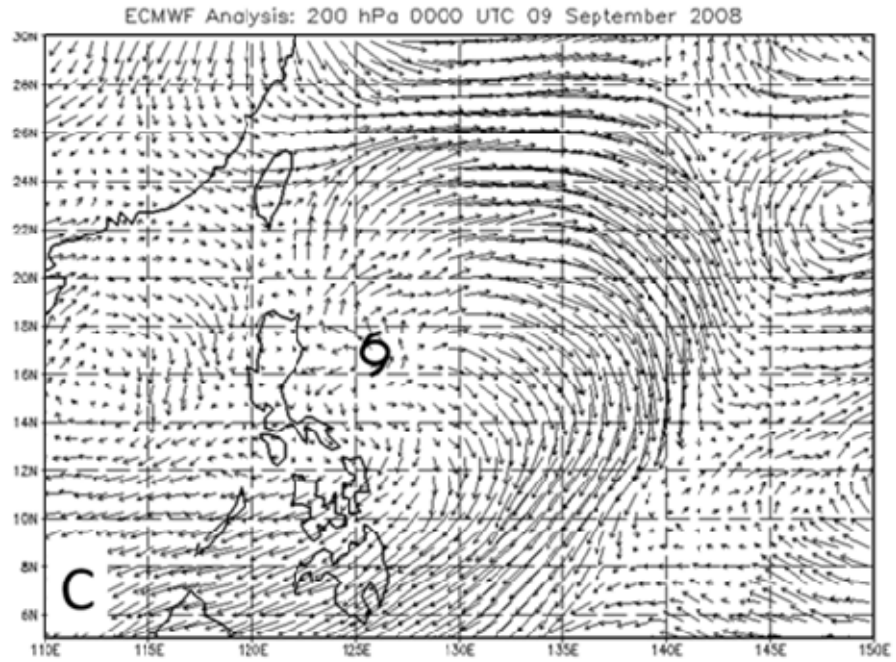

Figure 29. (a) Color-enhanced MTSAT IR image at 0030 UTC 9 September of TS Sinlaku. (b) Microwave image at 89 GHz at 0456 UTC 9 September. (c) Analyzed 200 hPa winds from ECMWF at 0000 UTC 9 September 2008. Satellite imagery from http:\\www.nrlmry.navy.mil/sat_products.html.

The first flight into Sinlaku was centered at 0530 UTC 9 September (Figure 13). During the flight, TS Sinlaku was located southeast of the cold eddy (Figure 30). The average OHC of the AXBTs deployed into the storm environment was 99.44 kJ cm^{-2} (Table 5).

Table 5. Oceanic variables derived from AXBTs on 9 September 2008.

9-Sep				Slope	T100	OHC	OHC24
AXBT#	SST C	26°C Depth	MLD m	°C/100m	°C	KJ/cm^2	KJ/cm^2
116	29.24	109.61	58	5.34	28.61	107.86	212.99
118	28.8	76.31	60	8.40	27.60	82.67	148.94
120	28.82	80.69	35	7.53	27.55	71.78	144.73
121	29.41	127.68	45	4.41	28.82	123.18	241.26
124	28.85	93.35	45	5.33	28.21	90.69	177.02
126	29.15	123.69	40	4.29	28.77	120.47	235.43

The AXBT identified as 120 (Figures 30 and 31) was deployed close to the cold eddy with an OHC value of 71.78 kJ cm^{-2} (Table 5) which verifies the EASNFS OHC analysis in Figure 30. The temperature profile for AXBT 120 (blue profile in Figure 31) differs from the other profiles, as it identifies a shallower MLD and much lower OHC value than the others in the group.

Even though TS Sinlaku was traversing a relatively cold ocean feature with OHC values between 70-80 kJ cm^{-2} (Figure 17), the OHC was still large enough to allow intensification (Mainelli et al. 2008), and Sinlaku became a typhoon by 1200 UTC 9 September 2008. However, the maximum winds of Sinlaku did not increase (Figure 28) for 12 hours beginning at 1800 UTC 9 September after passing over the cold eddy, even though the magnitude of the vertical wind shear decreased to less than 10 kt. Therefore, the pause in the rate of intensification may be attributed to a delayed effect of ocean coupling that is based on the time it takes the evaporation and cooling process to occur inside the storm (Mainelli 2000).

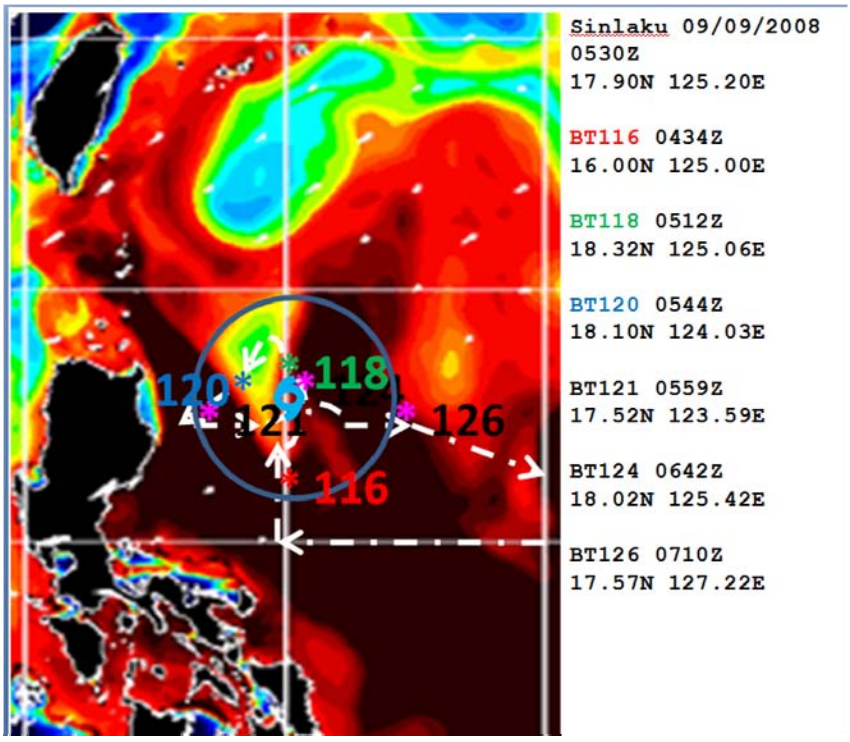

Figure 30. Analyzed OHC (shaded, kJ cm^{-2}) from the EASNFS at 0000 UTC 7 September 2008 and locations of AXBT deployments for the WC-130J flight centered at 0530 UTC 9 September 2008. The dashed lines define the flight track.

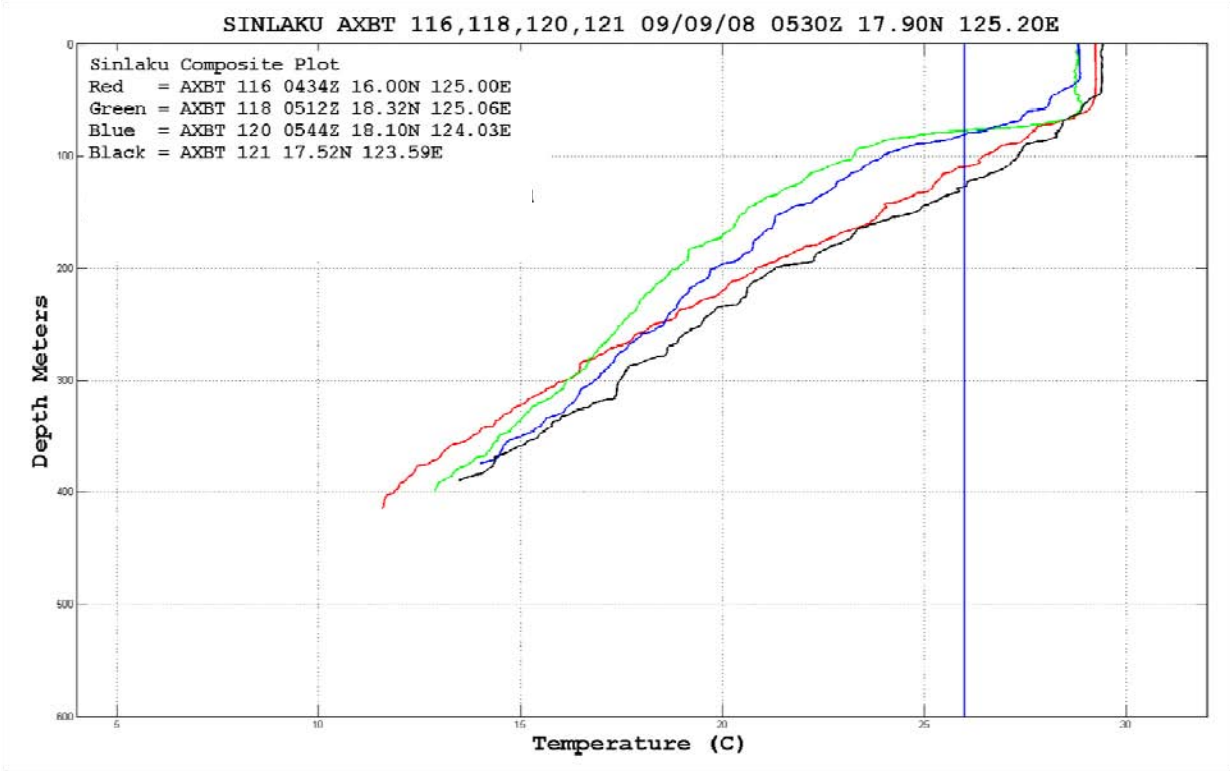

Figure 31. Temperature profiles recorded by AXBTs 116, 118, 120, and 121 from the flight on 9 September 2008 into TS Sinlaku. Locations of the AXBTs are indicated in the inset. The 26 ^{o}C isotherm is indicated by the blue vertical line.

Typhoon Sinlaku underwent its most rapid intensification from 1200 UTC 9 September to 1800 UTC 10 September (Figure 28), when the wind speed increased from 65 kt to 125 kt and the central pressure fell from 975 hPa to 935 hPa. During this intensification, Sinlaku was in an environment with less than 10 kt of vertical wind shear from the northwest and was traversing over a warm ocean region as it passed between the cold eddy from the previous day and the cold eddy just southeast of Taiwan (Figure 32).

During the second flight (Table 3) centered near 0530 UTC on 10 September, TY Sinlaku had moved to the northern edge of the cold eddy and had begun to move over the warm feature that existed to the southeast of the cold eddy near Taiwan. At this time, Sinlaku was a 90 kt typhoon just prior to undergoing rapid intensification. The EASNFS analyzed OHC values in the warm tongue close to 100 kJ cm^{-2} (Figure 32).

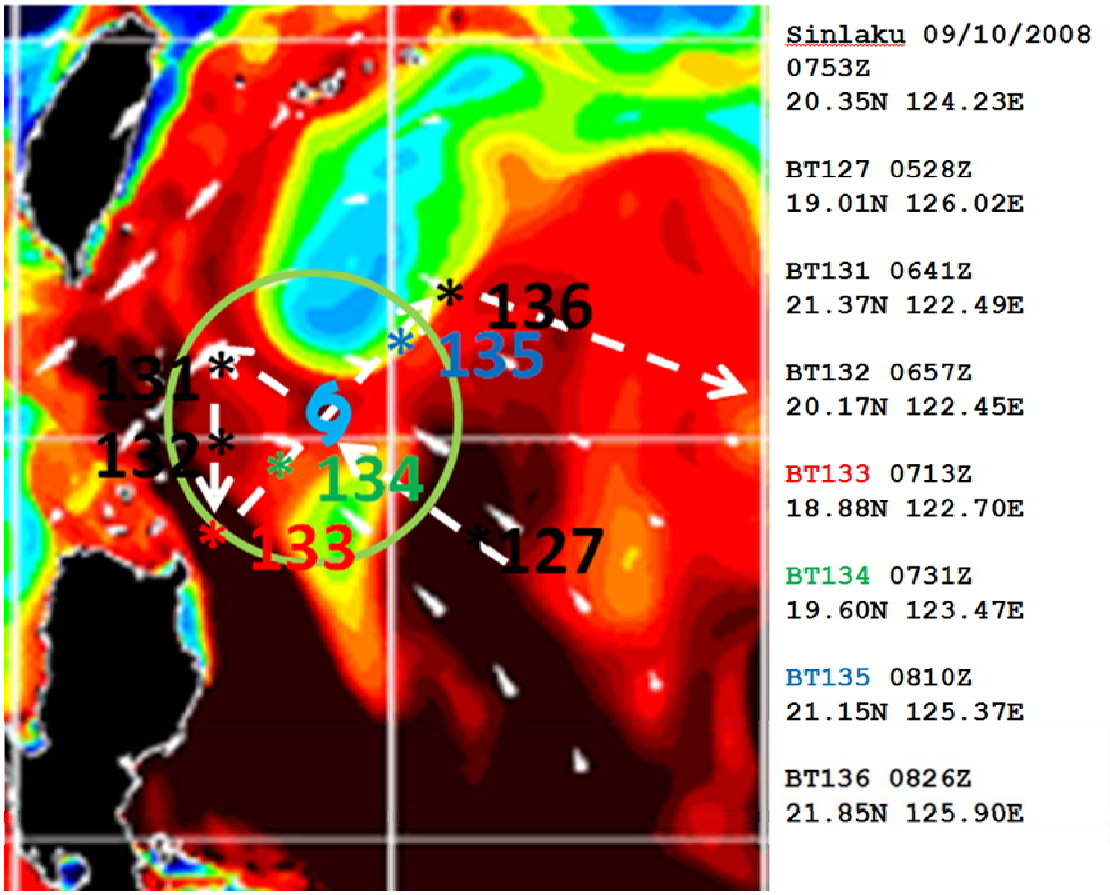

Figure 32. Composite plot at 0753 UTC 10 September 2008 with locations of AXBTs in relation to TY Sinlaku overlaid on EASNFS OHC analysis at 0000 UTC 8 September 2008. Arrows correspond to the aircraft flight path.

Some of the AXBT profiles (Figure 33) had indications of both mixing produced by the storm and of reduced OHC values related to the cold eddy to the rear of the storm. The AXBT numbered 134 (Figure 33) was deployed in the southwestern eye-wall and measured an OHC of only 18.54 kJ/cm^{-2}. This OHC likely reflects the effect of upper ocean cooling due to extreme mixing at that location.

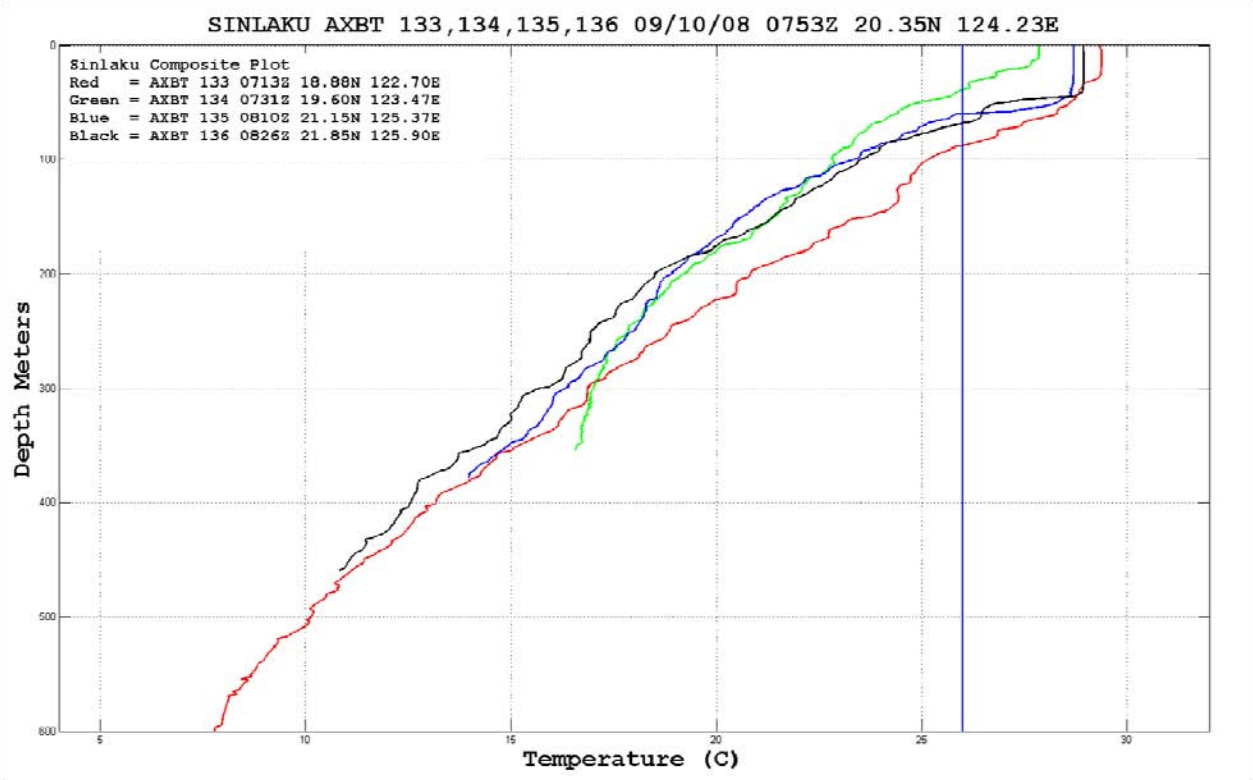

Figure 33. Temperature profiles recorded by AXBTs 133-136 from the flight on 10 September 2008 into TY Sinlaku. Locations of the AXBTs are indicated in the inset. The 26°C isotherm is indicated by the blue vertical line.

The average OHC measured by the four AXBTs 129-132 (Table 6) deployed into the warm tongue on 10 September was 80.43 kJ cm^{-2}.

Table 6. Oceanic variables derived from AXBTs on 10 September 2008.

10-Sep				Slope	T100	OHC	OHC24
AXBT#	SST C	26°C Depth	MLD m	°C/100m	°C	KJ/cm^2	KJ/cm^2
127	28.47	86.95	45	5.10	27.76	75	157.84
128	28.37	73.39	58	6.88	27.32	61.97	137.16
129	28.19	88	48	4.62	27.73	71.08	161.17
130	28.71	92.13	N/A	N/A	27.64	66.82	165.43
131	28.89	127.49	40	5.75	28.24	96.47	210.02
132	28.78	92.01	55	4.58	28.14	87.38	182.06
133	29.34	87.28	30	4.88	28.09	87.16	177.81
134	27.85	38.48	12	5.65	25.28	18.54	60.60
135	28.69	59.22	45	7.82	26.90	60.38	119.87
136	28.93	68.65	40	6.73	27.04	61.01	124.53

After traversing the warm tongue over a period of 18 h, Sinlaku reached its peak intensity of 125 kt at 1800 UTC 10 September 2008 (Figure 34a). Sinlaku formed a complete symmetric eye (Figure 34b) and its outflow became uniform in all directions (Figure 34c), which in turn was related to reduced vertical wind shear over the storm.

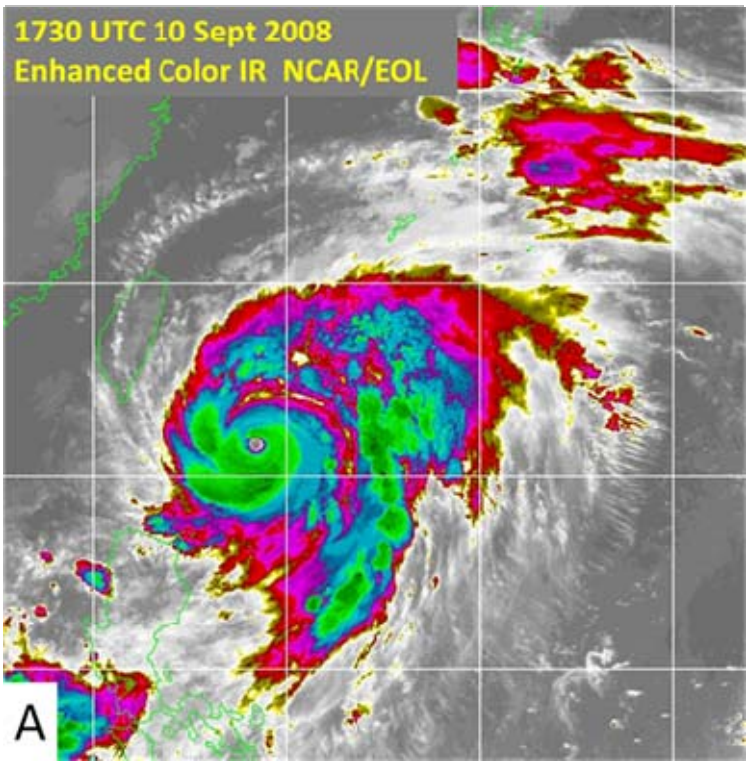

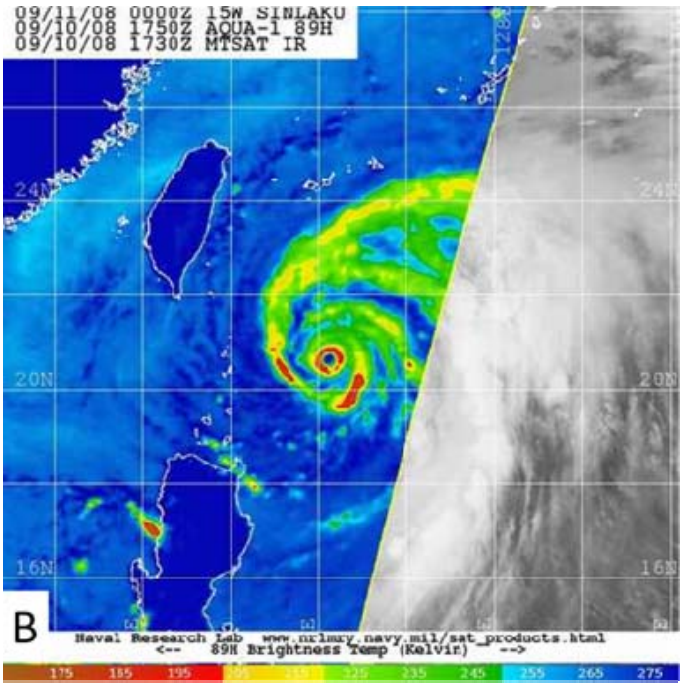

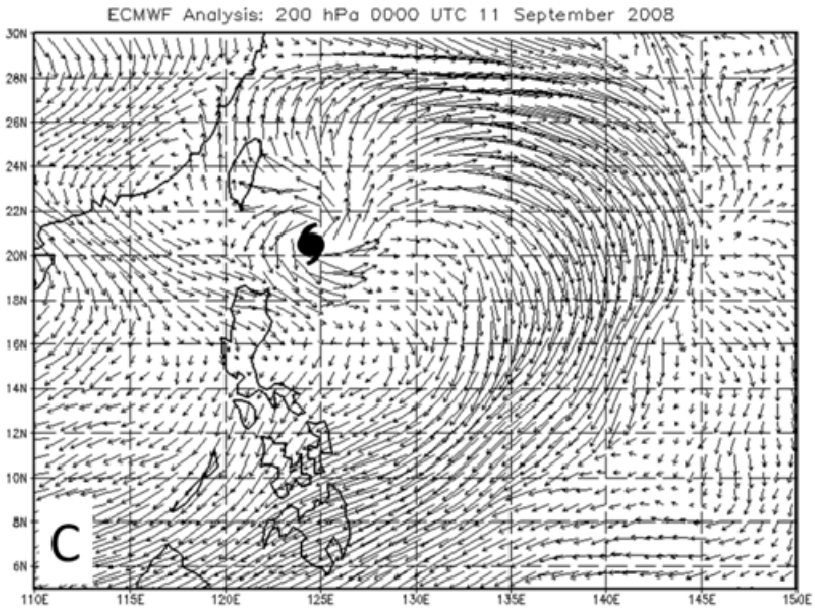

Figure 34. (a) Color-enhanced MTSAT IR image of TY Sinlaku at 1730 UTC 10 September 2008. (b) Microwave image at 89 GHz of TY Sinlaku at 1750 UTC 10 September 2008. (c) Analyzed 200 hPa winds from ECMWF at 0000 UTC 11 September 2008. Satellite imagery from http:\\www.nrlmry.navy.mil/sat_products.html.

3. TY Sinlaku Weakening Stage (11–14 September 2008)

Typhoon Sinlaku remained at peak intensity of 125 kt from 1800 UTC 10 September until 0000 UTC on 11 September (Figure 28). The magnitude of the vertical wind shear then increased to 17 kt from the northwest from 1200 UTC 11 September to 1200 UTC 12 September. A corresponding decrease in convection occurred in the northwest quadrant of the storm (Figures 35a,b). The upper-level outflow to the north became limited as the primary outflow channel (Figure 35c) was displaced to the east and equatorward due to the increased vertical wind shear. During this time of decreasing intensity and increasing vertical wind shear, TY Sinlaku was also moving over a cold eddy that was southeast of Taiwan (Figures 28 and 36).

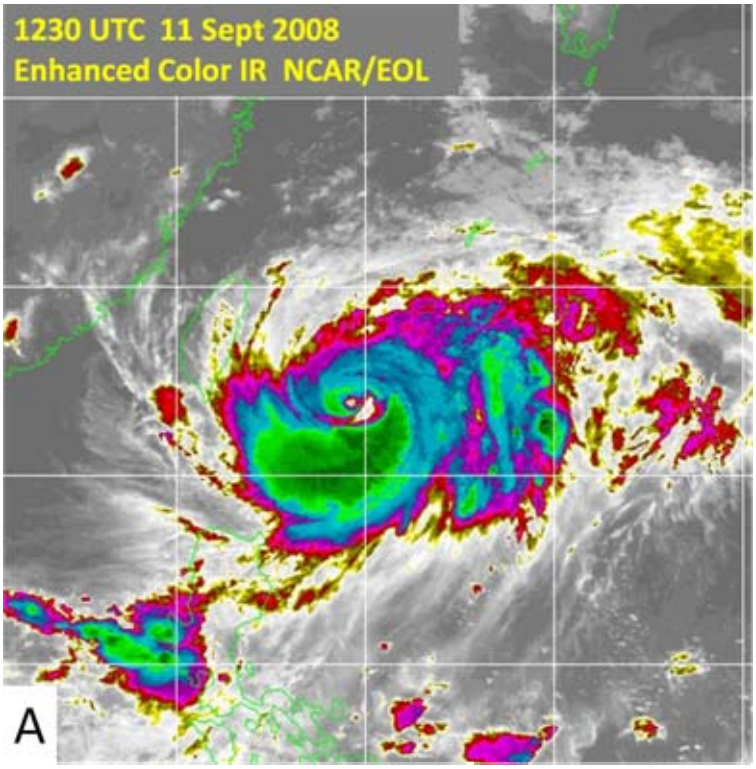

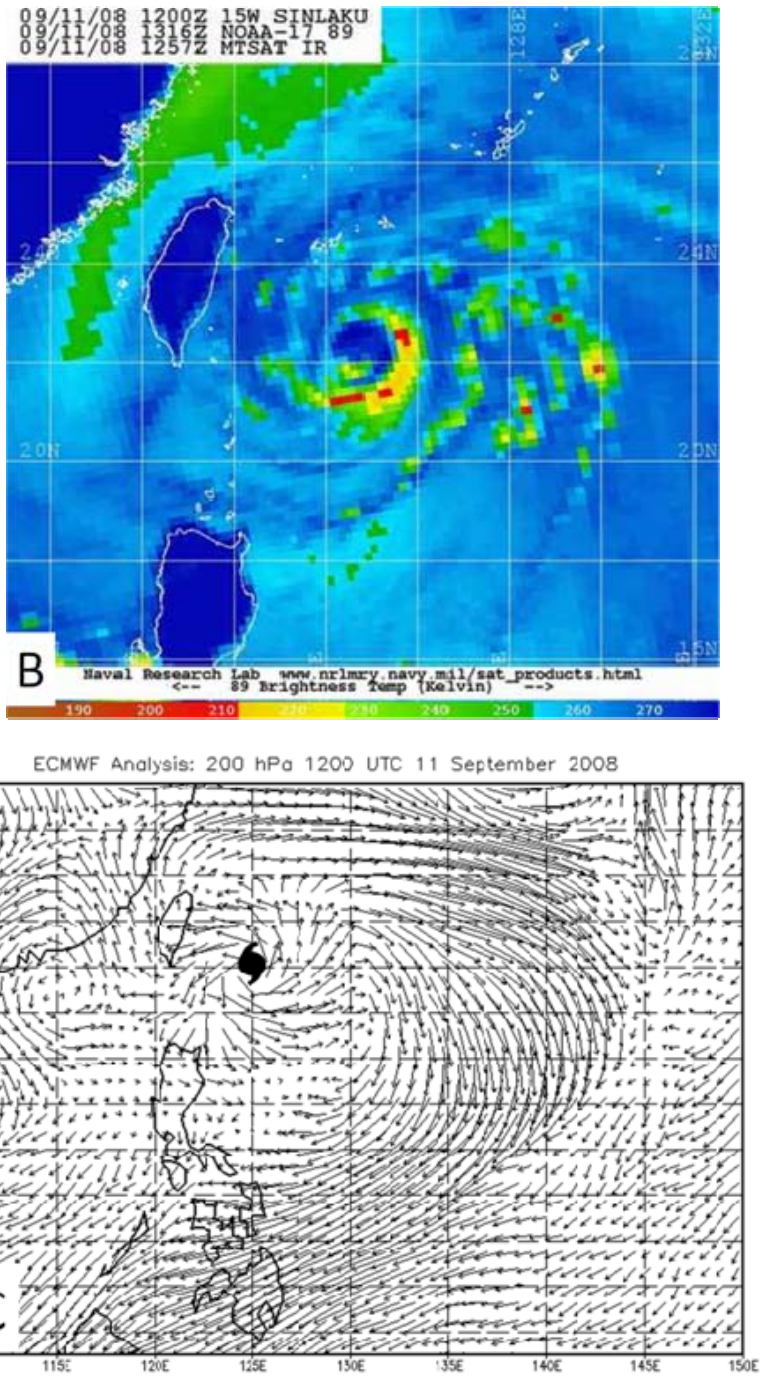

Figure 35. (a) Color-enhanced MTSAT IR image of TY Sinlaku at 1230 UTC 11 September 2008. (b) Microwave image at 89 GHz of TY Sinlaku at 1316 UTC 11 September 2008. (c) Analyzed 200 hPa winds from ECMWF at 1200 UTC 11 September 2008. Satellite imagery from http:\\www.nrlmry.navy.mil/sat_products.html.

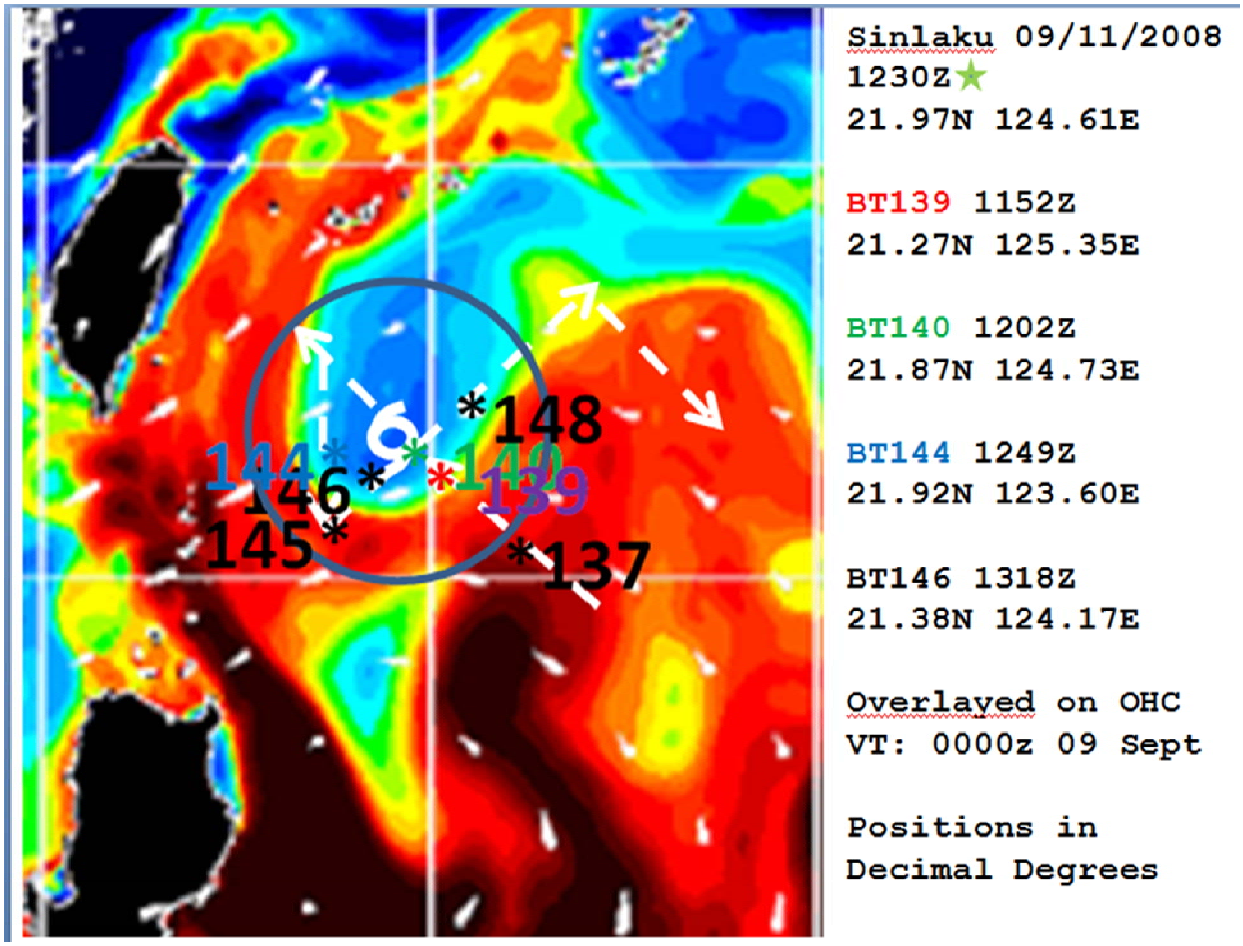

Figure 36. Location of TY Sinlaku at 1230 UTC 11 September 2008 with locations of AXBTs overlaid on EASNFS OHC analysis at 0000 UTC 9 September 2008. The dashed lines define the aircraft flight track.

The third aircraft mission into TY Sinlaku was centered at 1230 UTC 11 September 2008 (Figure 15) when Sinlaku was traversing the cold eddy (Figure 36). All the AXBTs in the near-Sinlaku environment had OHC values less than 60 kJ cm^{-2} (Figure 37 and Table 7), which was the threshold for major typhoon intensification defined by Mainelli et al. (2008). Only AXBT 137, which was deployed in the warm tongue to the southeast of Sinlaku had an OHC well above 60 kJ cm^{-2} (Figure 38).

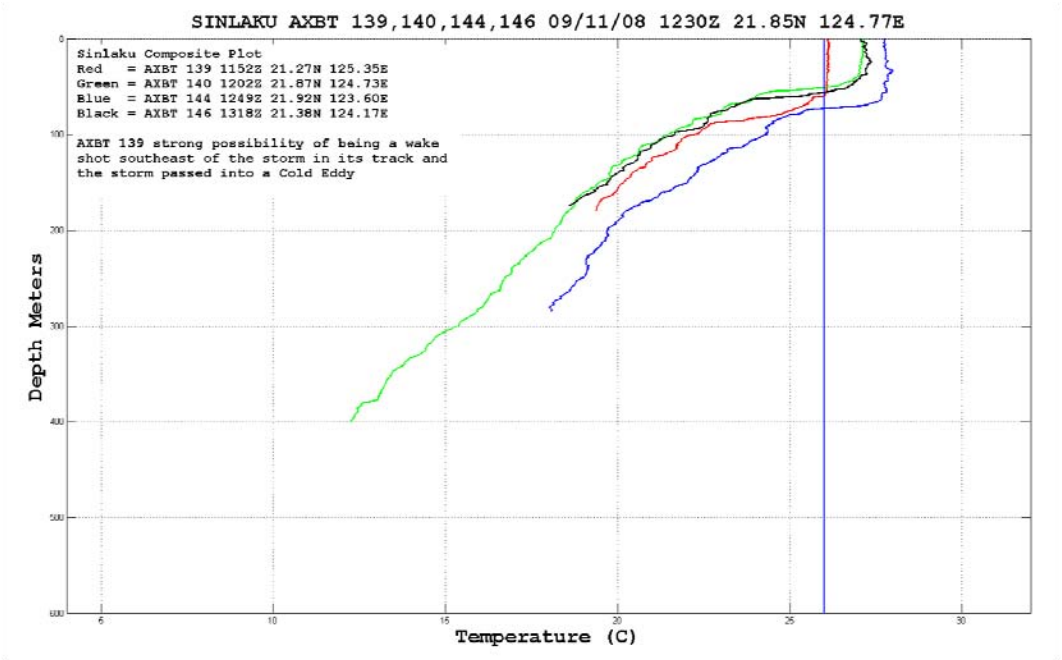

Figure 37. Temperature profiles recorded by AXBTs 139, 140, 144, and 146 deployed during the flight into TY Sinlaku on 11 September 2008. Locations of the AXBTs are indicated in the inset. The 26°C isotherm is indicated by the blue vertical line.

Table 7. Oceanic variables derived from AXBTs on 11 September 2008.

11-Sep				Slope	T100	OHC	OHC24
AXBT#	SST C	26°C Depth	MLD m	°C/100m	°C	KJ/cm^2	KJ/cm^2
137	28.53	111.6	80.6	5.99	28.33	97.5	203.55
139	26.11	59.5	59	6.11	25.33	2.31	62.33
140	27.15	50.49	38.7	7.05	25.08	20.46	64.61
144	27.75	72.44	63	6.24	26.91	50.73	118.78
145	28.04	72.93	54	6.14	27.08	51.11	129.6
146	27.07	56.96	38	6.87	25.37	24.44	73.30
148	27.45	77.03	59	7.81	26.57	43.21	110.58

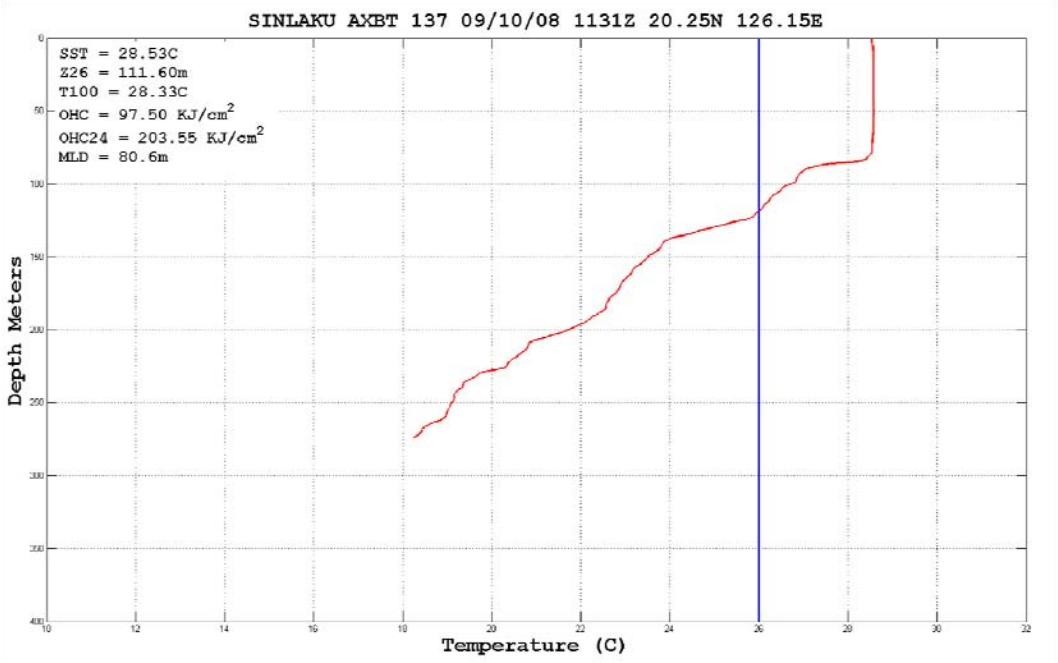

Figure 38. Vertical temperature profile from AXBT 137 with a deep warm layer.

The AXBT 144 (Figure 37) was deployed ahead of Sinlaku on the edge of the cold eddy and had the highest OHC of 97.5 kJ cm^{-2} and largest MLD in the near-Sinlaku environment. The AXBT 139 (Figure 37) was deployed immediately behind the storm center in the cold eddy and had an OHC of only 2.31 kJ cm^{-2}. Therefore, the AXBT data verified the EASNFS analysis (Figure 36) and indicated that the ocean environment ahead of Sinlaku would be more favorable for intensification than existed over the cold eddy the storm had just traversed.

By 1200 UTC 12 September 2008, the vertical wind shear increased to a maximum near 20 kt (Figure 28) and the storm intensity decreased to below 100 kt (Figure 28). However, Sinlaku was just beginning to traverse the warm tongue associated with the Kuroshio Current between Taiwan and the cold eddy to the southeast of Taiwan (Figure 39). The WC-130J flight that was centered near 1800 UTC 12 September deployed two AXBTs (numbers 153 and 156, Figure 39) ahead of the storm in this warm feature. The MLD and OHC values for AXBT 156 (Table 8 and Figure 40) in the center of the warm tongue were much larger than the values in regions closer to

Sinlaku. After the flight on 12 September, Sinlaku's intensity increased from 85 kt to 100 kt between 0600-1200 UTC 13 September (Figure 28) as Sinlaku moved over the warm ocean environment measured by AXBTs 153 and 156. Furthermore, the vertical wind shear decreased to below 10 kt during this period. This intensification occurred prior to Sinlaku making landfall on Taiwan.

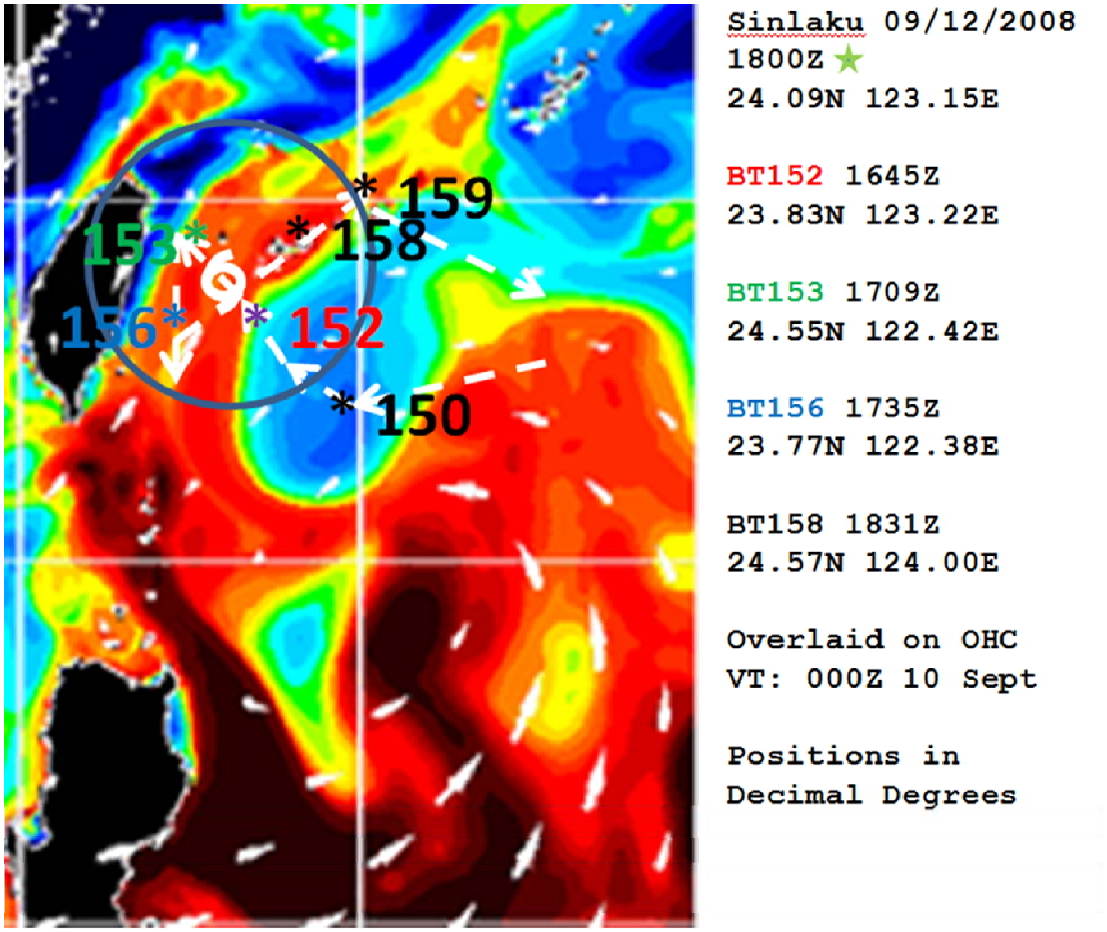

Figure 39. Location of TY Sinlaku at 1800 UTC 12 September 2008 with locations of AXBTs in relation to the storm and overlaid on EASNFS OHC analysis from 0000 UTC 10 September 2008. The dashed lines define the aircraft flight track.

Table 8. Oceanic variables derived from AXBTs on 12 September 2008.

12-Sep				Slope	T100	OHC	OHC24
AXBT#	SST C	26°C Depth	MLD m	°C/100m	°C	KJ/cm^2	KJ/cm^2
150	25.38	NA	40	7.18	NA	NA	NA
152	28.23	91.57	41	6.66	27.46	60.32	144.29
153	27.80	114.19	75	5.26	27.77	79.20	182.65
156	28.09	136.79	100	5.94	28.07	101.62	222.69
158	27.45	75.38	64	5.83	26.91	41.98	121.27
159	28.38	111.39	67	5.57	28.15	89.90	193.97

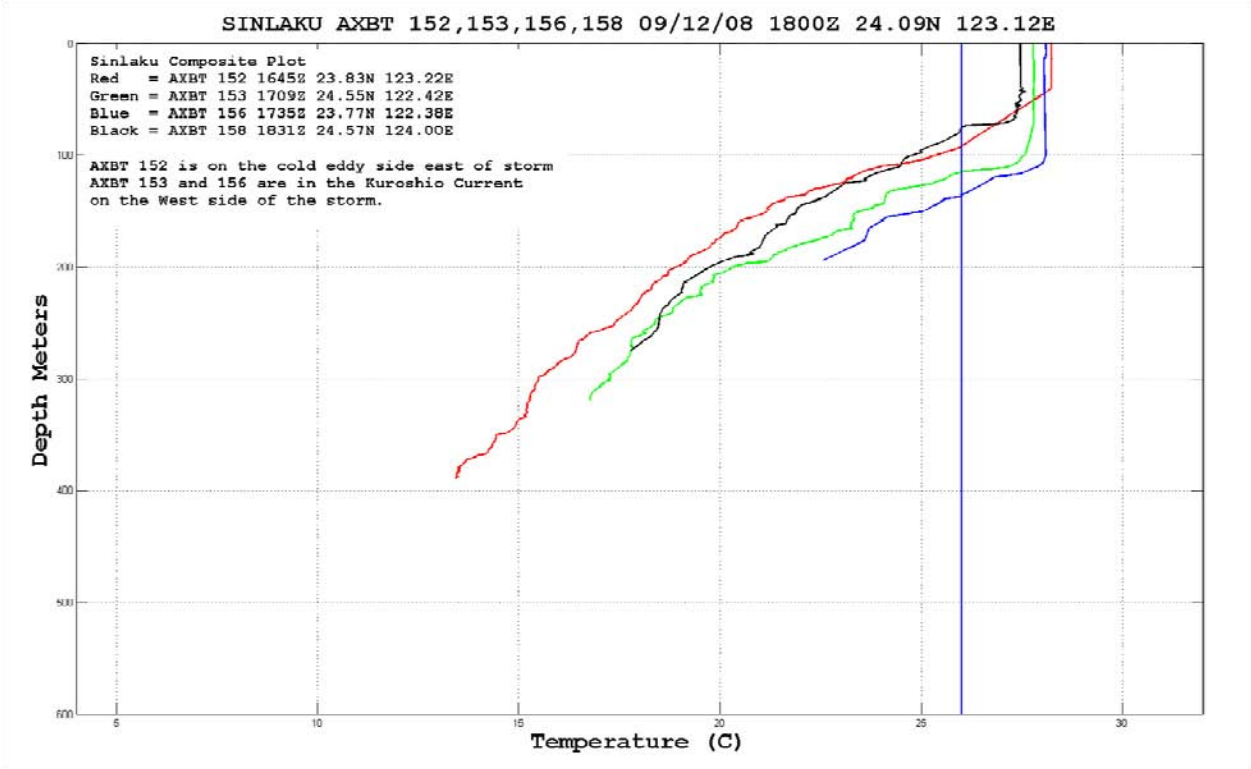

Figure 40. As in Figure 9, with AXBT 153 (Green) with an OHC of 79.20 kJ cm^{-2} and a MLD of 75 m, and AXBT 156 (Blue) with an OHC of 101.62 kJ cm^{-2} and a MLD of 100 m that represent ocean conditions in the deep, warm Kuroshio Current.

4. TY Sinlaku Over Taiwan and Extratropical Transition

Typhoon Sinlaku approached Taiwan as a 100 kt storm and moved over the northern tip of the island from 1800 UTC 13 September to 1200 UTC 14 September. A combination of friction over land, interaction with the topography of Taiwan's Central

Mountain Range, and continued light northwesterly vertical wind shear contributed to weakening from 100 kt to 65 kt by 1200 UTC 14 September. Soon after passing north of Taiwan, TS Sinlaku encountered stronger westerly winds associated with a midlatitude trough. On 15 September, the vertical wind shear increased to 20 kt (Figure 28) and by 0600 UTC 16 September, Sinlaku had weakened to 40 kt as it moved into the westerlies. While moving on a northeastward track west of the Ryukyu Island chain, TS Sinlaku slowed down and moved over an ocean region influenced by the Kuroshio Current with OHC values between 60-80 kJ cm^{-2} (not shown). Between 1200 UTC 18 September to 1200 UTC 19 September 2008, Sinlaku intensified from 45 kt to a minimal typhoon of 70 kt even though it was in a high vertical wind shear environment. Soon after this reintensification, Sinlaku underwent extratropical transition.

5. Typhoon Sinlaku Summary

The open wave TCS-033 that was to become TY Sinlaku moved under the influence of easterly trades in a moderate vertical wind shear environment for five days from 1 September to 6 September. On 6 September, TCS-033 entered a more favorable atmospheric environment with reduced vertical wind shear that allowed it to develop into TD15W on 7 September 2008. During this TC formation the vertical wind shear values were less than 10 kt. The ocean over which the pre-Sinlaku wave passed was characterized by a deep, warm mixed layer with higher than normal SST. The OHC where TY Sinlaku formed was greater than 125 kJ cm^{-2}, which is typical for the deep, warm ocean layer of the tropical western North Pacific.

The average vertical wind shear was near 9 kt from 0000 UTC 8 September to 0000 UTC 11 September, and Sinlaku intensified steadily through this period (Figure 28). A short pause in intensification occurred when Sinlaku remained at 90 kt for about 12 hours between 1200 UTC 9 September and 0000 UTC 10 September as the storm traversed a cold eddy (Figure 28). The first of four flights into Sinlaku was centered near 0500 UTC 9 September 2008 as Sinlaku was passing from an ocean environment with OHC greater than 120 kJ cm^{-2} and over the first weak cold eddy along its path. In the

center of the cold eddy, the OHC was near 70 kJ cm^{-2}, and this agreed closely with the EASNFS analyzed OHC from 7 September 2008 taken two days prior to that flight.

On 10 September 2008, TY Sinlaku was passing over a warm ocean feature that existed between the two cold eddies. The EASNFS analysis of OHC from 8 September 2008 was between 90-100 kJ cm^{-2} for this region. The AXBTs deployed during the second flight into Sinlaku had OHC values that averaged 80.43 kJ cm^{-2}. However, this average excluded two AXBTs (numbers 135 and 136) that were on the outer edge of the cold eddy and AXBT 134 (Table 6) that was deployed in the southwest eye-wall of the storm. The EASNFS OHC analysis may have been biased too warm with respect to this feature, as this analysis was prior to the storm arrival and thus may not reflect the influence of the mixing of the upper ocean by the storm.

Following 11 September when Sinlaku reached a peak intensity of 125 kt, it then entered into a 36-hour period of increased vertical wind shear (Figure 28) and weakened to near 85 kt. At the same time, Sinlaku passed over a more intense cold eddy than the previous one on 9 September. The EASNFS analyzed OHC at 9 September was between 35-40 kJ cm^{-2}. The average OHC from the AXBTs from the third flight into Sinlaku as the storm passed over the cold eddy was 41.34 kJ cm^{-2}, which again agreed with the EASNFS analysis.

During 1200 UTC 12 September to 1800 UTC 13 September, TY Sinlaku regained 100 kt intensity as it traversed over a region of high OHC and the vertical wind shear decreased to near 8 kt (Figure 28). Based on the 10 September 2008 EASNFS analysis, the warm region had OHC values between 85-95 kJ cm^{-2} which was in good agreement with the average OHC value of 90.24 kJ cm^{-2} from the three AXBTs that were deployed in the same area (Table 8).

Sinlaku then weakened to a tropical storm while passing over the northern tip of Taiwan from 1800 UTC 13 September to 1200 UTC 14 September. During this period, Sinlaku encountered vertical wind shears greater than 20 kt and weakened to a minimal 40 kt storm on 16 September after recurving to the northeast.

In the TY Sinlaku case, it was clear that vertical wind shear values of less than 10 kt and high OHC allowed the storm to undergo steady intensification. Between 1200

UTC 11 September and 1200 UTC 12 September, vertical wind shear increased to above 15 kt and the storm then weakened. The storm weakening appeared to begin about 12 h earlier (Figure 28) when Sinlaku traversed the cold eddy southeast of Taiwan. Just before reaching Taiwan, the storm passed over a warm ocean feature with OHC values around 100 kJ cm^{-2}. The vertical wind shear also decreased to 8 kt during this time, which allowed the storm to increase in intensity from 85 to 95 kt (Figure 28).

Throughout the pre-recurvature period of TY Sinlaku, vertical wind shear and varying ocean conditions seemed to be well-correlated with the fluctuations in the storm intensity. During periods of low vertical wind shear and warm ocean conditions, wind speeds increased regularly. Under low vertical wind shear and cold ocean conditions, the storm slowly weakened. In moderate vertical wind shear up to 12 kt and with very warm ocean conditions, the storm was able to intensify or maintain strength. However, vertical wind shear greater than 12 kt was always associated with weakening.

B. STY JANGMI

1. Pretropical Depression Stage

STY Jangmi was first observed as TCS-047 on 16 September 2008 during the TCS-08 field program. The TCS-047 system was an organized mass of thunderstorms (Figure 41) at 12^{o}N, 168^{o}E moving at 10 kt under the influence of the easterly trade winds.

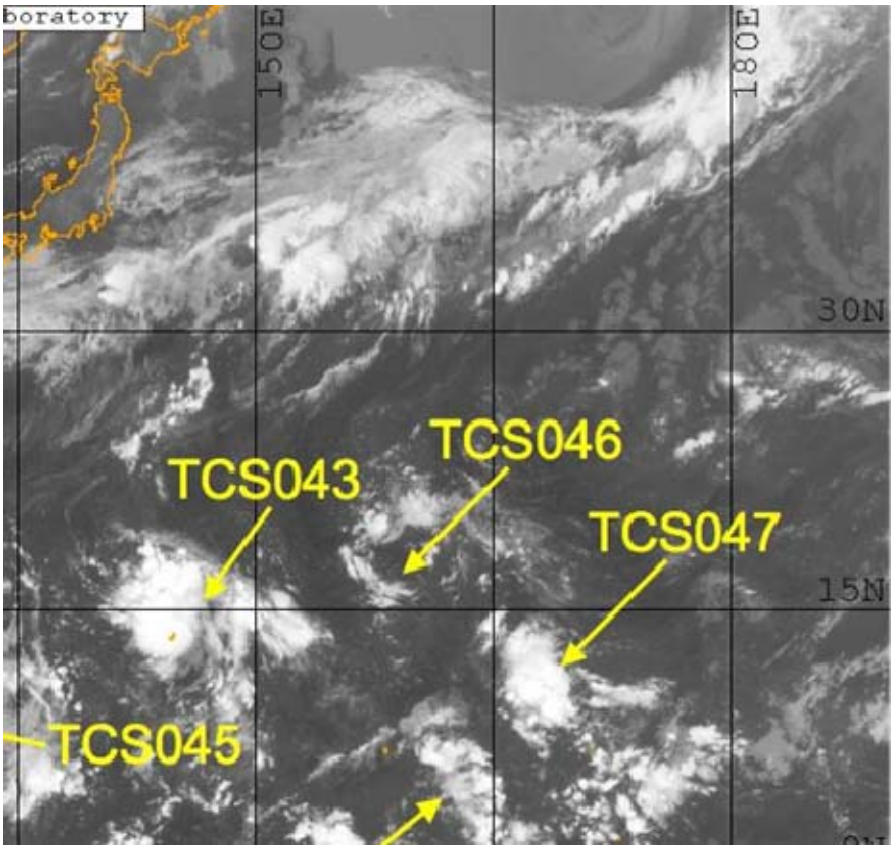

Figure 41. Infrared MTSAT image at 1830 UTC 16 September 2008 with various tropical systems identified with TCS labels by the TCS-08 project. The pre-Jangmi disturbance is TCS-047. Satellite imagery from http://www.nrlmry.navy/sat_products.html.

From 17 September to 22 September, TCS-047 continued to travel westward (Figure 42) at roughly 10 kt. While still identified as a wave in the easterlies (Figure 42a), the wind circulation of TCS-047 weakened considerably on 19 September (Figure 42b) as it moved in tandem with an upper-level low (not shown) and continued to be affected by persistent 15 kt northerly vertical wind shear.

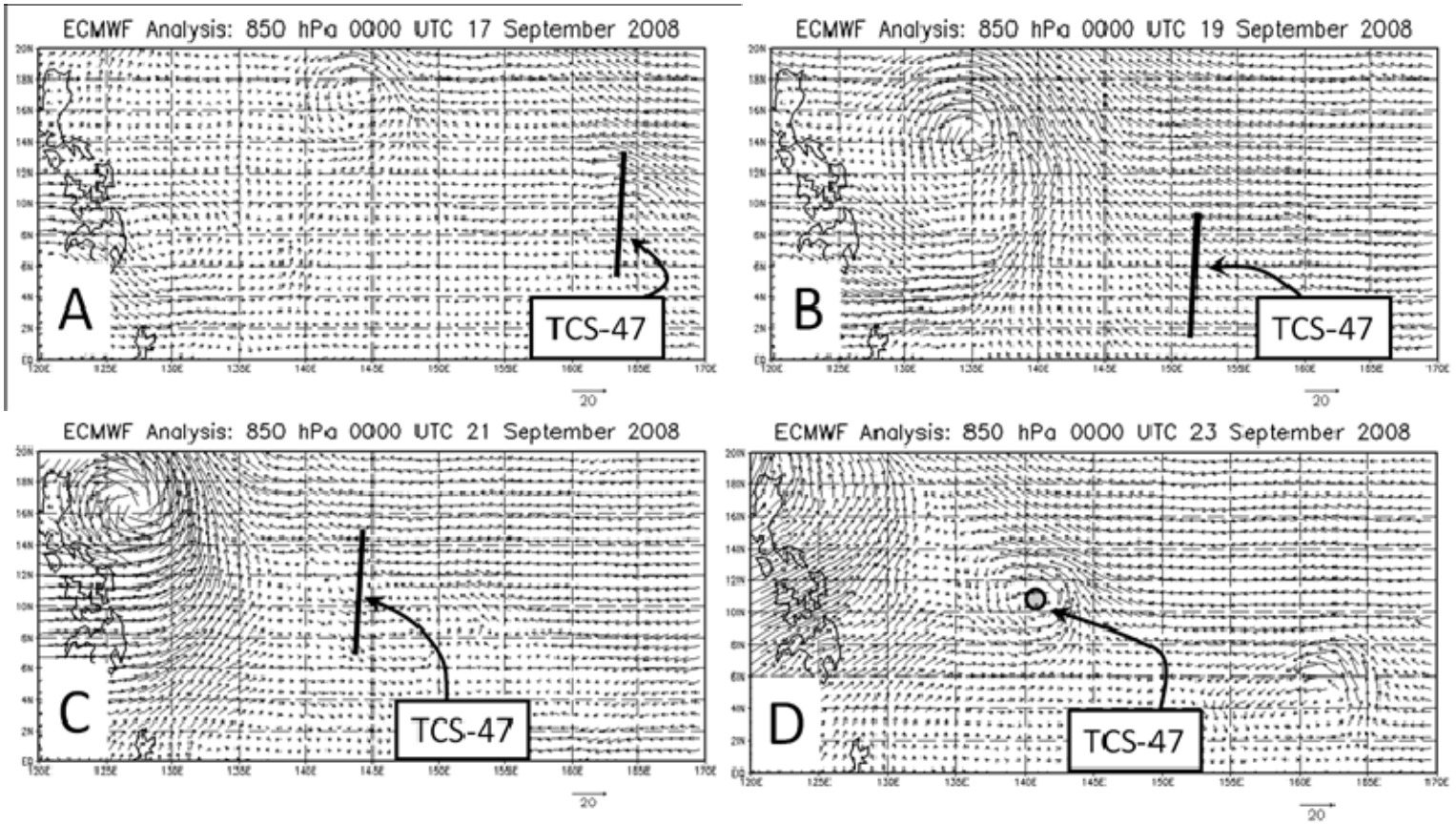

Figure 42. Analyses of 850 hPa winds from ECMWF at (a) 0000 UTC 17 September 2008, (b) 0000 UTC 19 September 2008, (c) 0000 UTC 21 September 2008, and (d) 0000 UTC 23 September 2008.

On 20 September 2008, the organized cloud pattern in an area of southerly winds was the first indication of a possible low-level cyclonic circulation. The northerly vertical wind shear associated with the upper-level cold low inhibited intensification, but the low-level circulation persisted into 21 September (Figure 42c). However, the upper-level low remained to the northeast of TCS-047 through 22 September 2008 (Figure 43).

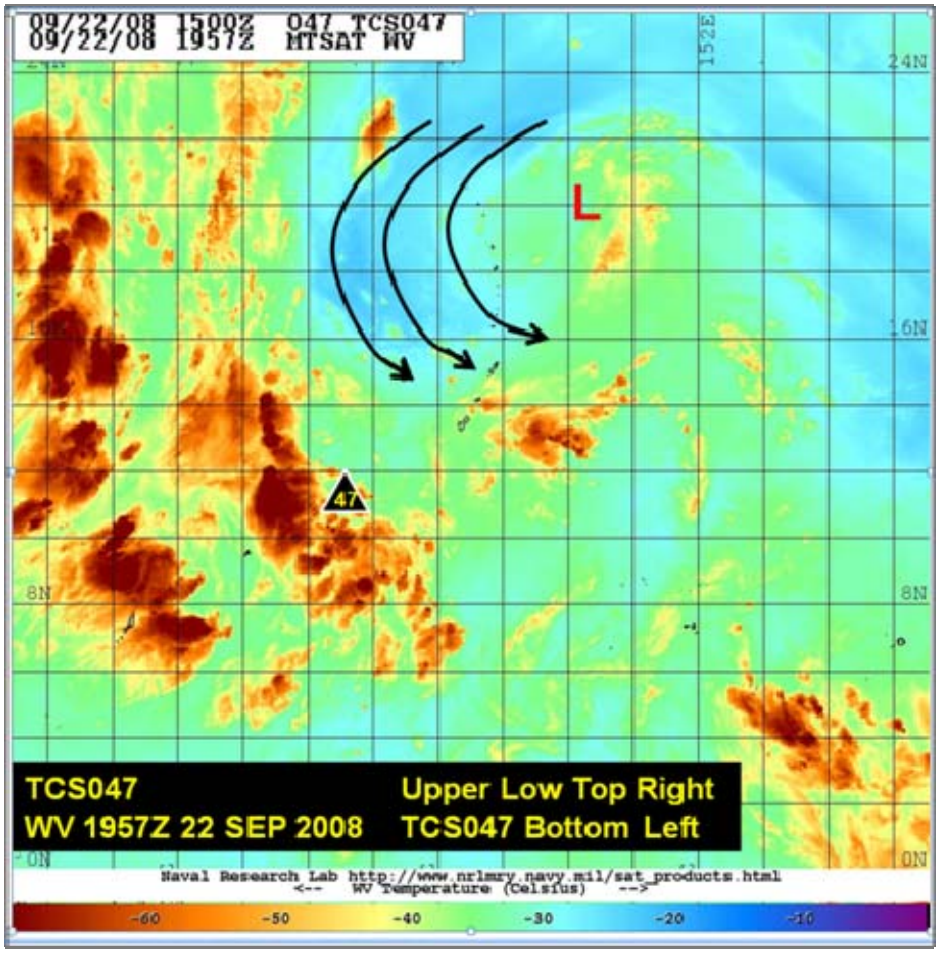

Figure 43. Water vapor MTSAT image at 1957 UTC 22 September 2008. The location of TCS-047 is defined the triangle symbol near 11°N, 140°E. The upper-level cold low is defined by the letter "L" and the vertical wind shear pattern is identified by the curved arrows. Satellite imagery from http:\\www.nrlmry.navy.mil/sat_products.html.

As TCS-047 continued to move westward, the vertical wind shear associated with the upper-level low was reduced late on 22 September. On 23 September, TCS-047 fully separated from the upper-level low, which allowed development of deep persistent convection (Figure 44) and the formation of a closed low-level circulation (Figure 42d). The continued progression of the eastward-moving mass of thunderstorms, which eventually became TD19W on 23 September 2008, may be an example of the Marsupial Pouch Theory proposed by Dunkerton et al. (2008). However, the formation was also assisted as the disturbance moved westward into a region of equatorial westerlies allowing for increased moisture inflow and out of the relatively drier air flow from the easterly trades.

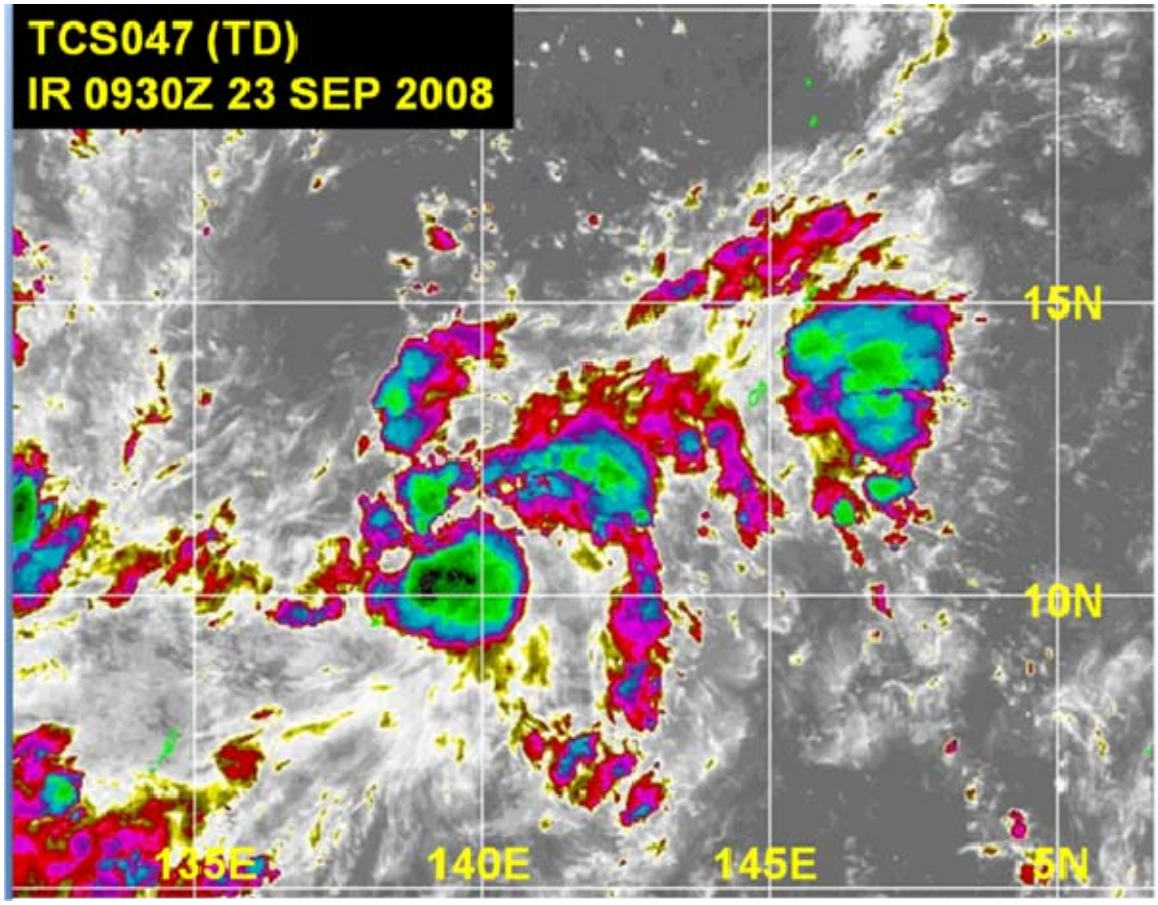

Figure 44. Color enhanced IR MTSAT image at 0930 UTC 23 September 2008 of TCS-047. Imagery from NRL-Monterey at http://www.nrlmry.navy/sat_products.html.

At 1800 UTC 23 September the Joint Typhoon Warning Center (JTWC) issued a TCFA for TCS-047 located near 11^{o}N, 140^{o}E. During 0600-1800 UTC 23 September the reduction in vertical wind shear to below 10 kt is considered to be a major factor as TCS-047 became a TD by 2100 UTC 23 September 2008. In a manner similar to the formation TY Sinlaku, the formation of TD19W was a classic La Nina type of formation as it traveled under the influence of enhanced trade winds for almost 2,700 km before finally forming in the western North Pacific Ocean.

2. TS Jangmi (24 and 25 September 2008)

As mentioned in previous sections, TC intensity is influenced by many factors. Under favorable atmospheric conditions (low vertical wind shear) and a steady forward motion of 2 to 6 m s^{-1} over a very warm ocean layer, OHC is an important factor in determining the maximum intensity a TC may attain (Lin et al. 2008). Based on EASNFS analysis, Jangmi traversed over a deep, warm ocean layer (Figure 45) from 23 September through 25 September, with OHC values from 130-150 kJ cm^{-2}, which arise because the average Z26 was greater than 130 meters and the average SST was near 30.5^{o}C. During this period, the forward motion of Jangmi slowed from 10 kt to about 7.5 kt and turned to a more north-northwest direction (Figure 45).

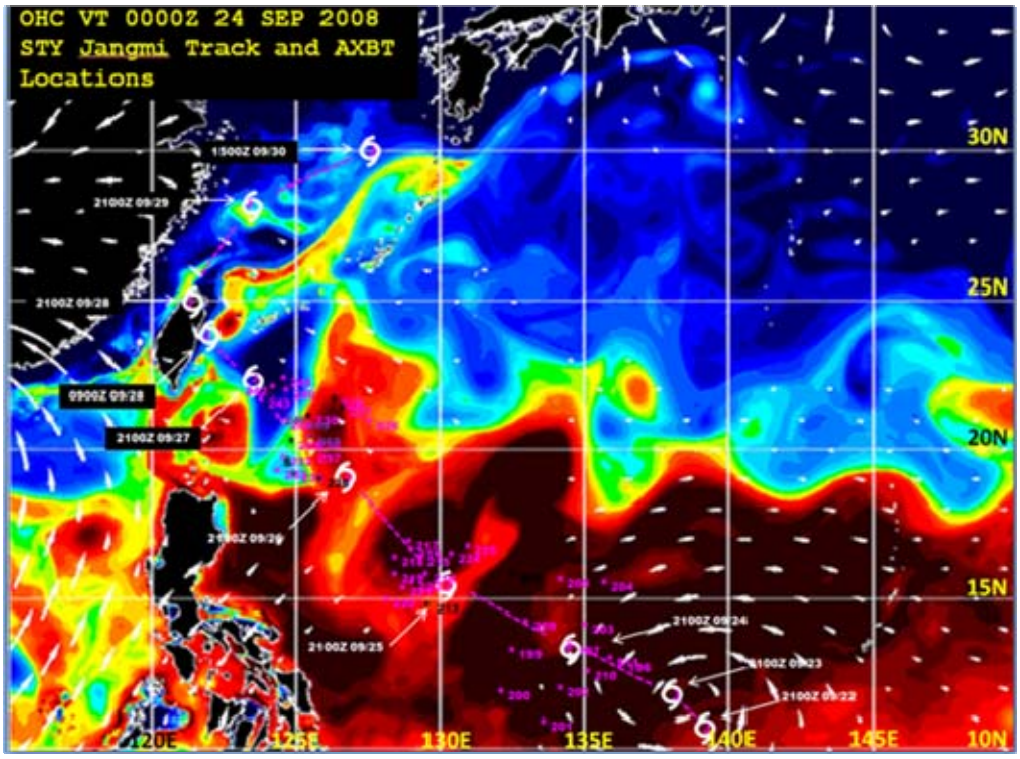

Figure 45. The track of STY Jangmi and AXBT locations overlaid on NRL EASNFS OHC analysis at 0000 UTC 24 September 2008.

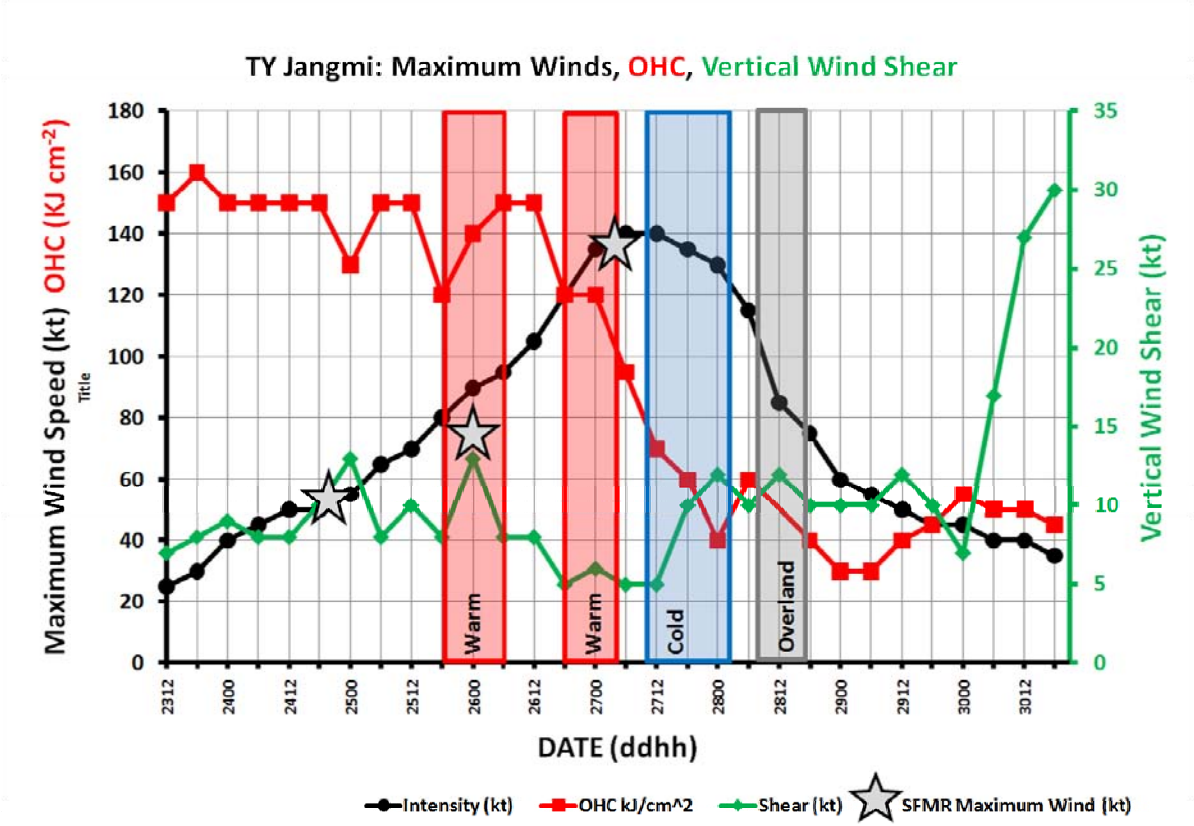

Figure 46. STY Jangmi OHC (kJ cm^{-2}) values from EASNFS analysis, intensities (kt) in 6-h increments, vertical wind shear (kt) in 12-h increments from ECMWF analysis, and SFMR maximum winds (kt). Colored boxes define periods when Jangmi traversed significant ocean features or land.

On 24 September, Jangmi intensified from a TD to a TS as vertical wind shear continued to decrease due to the increasing separation between the storm and the upper-level low (Figures 46 and 47a-c). Upper-level outflow from Jangmi increased overall but was still restricted to the north (Figures 47a and 47c). Between 1800 UTC 24 September and 0000 UTC 25 September, the vertical wind shear increased to over 10 kt and the rate of intensification slowed (Figure 46). The vertical wind shear was from the north and resulted in reduced outflow and convection over the northern half of the storm (Figures 48a-c). However, increased equatorial outflow existed (Figure 48c) and Jangmi was still over a region of high OHC (Figure 45) as it gradually intensified to a TS.

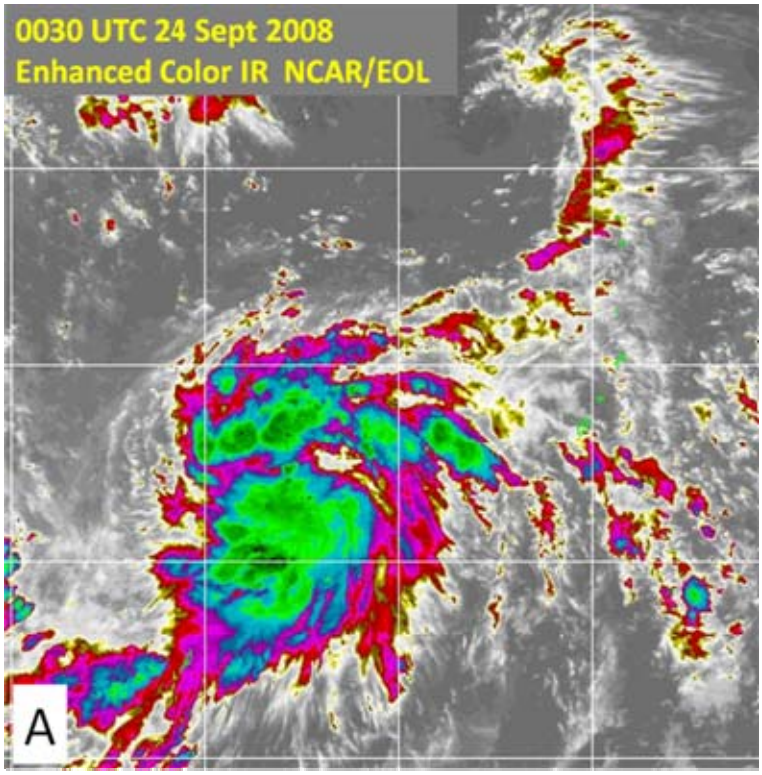
0030 UTC 24 Sept 2008
Enhanced Color IR NCAR/EOL
A

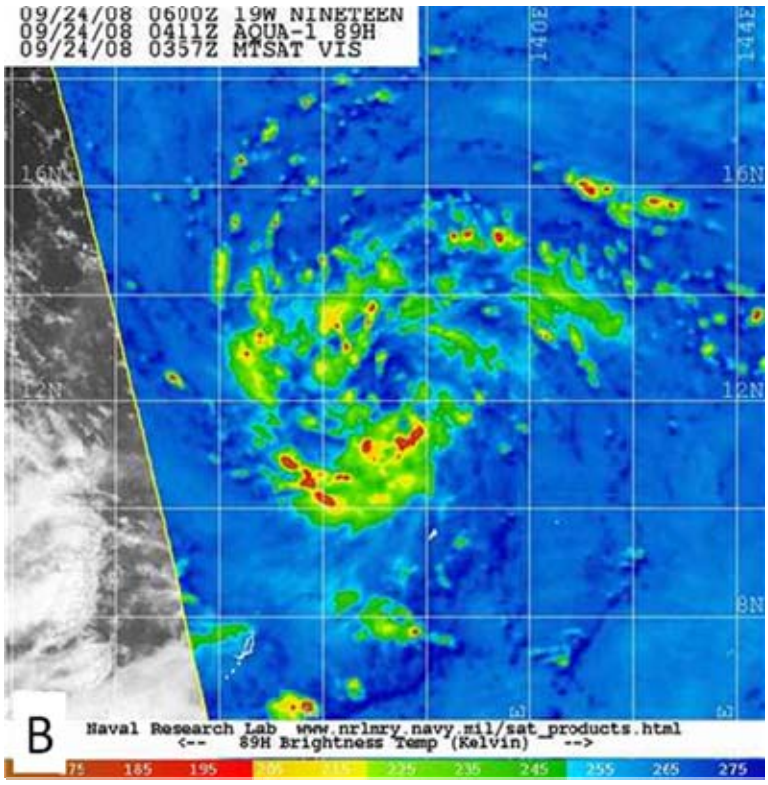
09/24/08 0600Z 19W NINETEEN
09/24/08 0411Z AQUA-1 89H
09/24/08 0357Z MTSAT VIS
16N
12N
8N
B
Naval Research Lab www.nrlmry.navy.mil/sat_products.html
<-- 89H Brightness Temp (Kelvin) -->
185
195
235
245
255
265
275

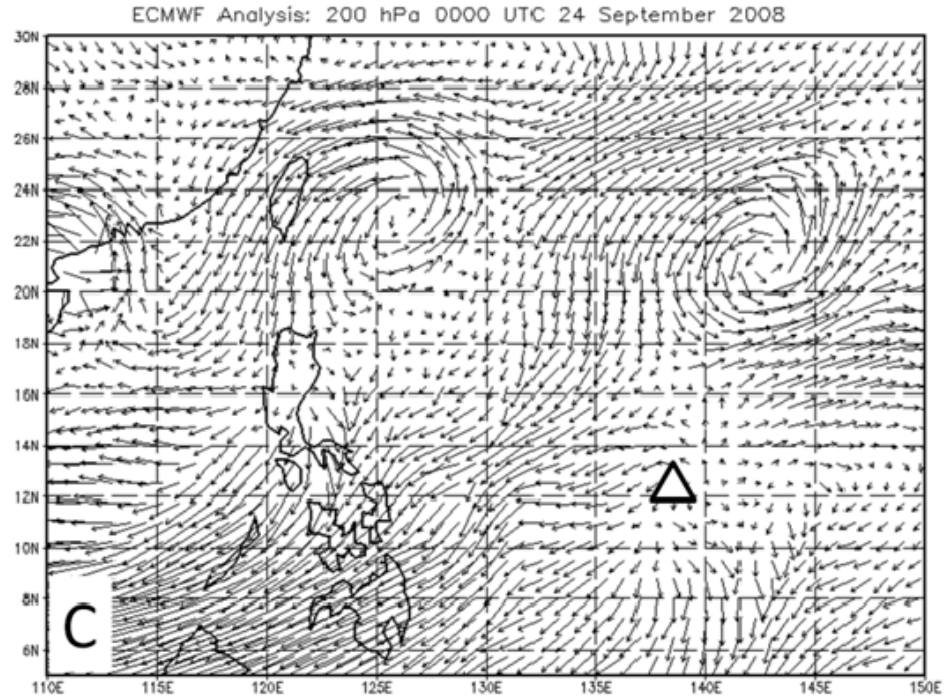

Figure 47. (a) Color-enhanced MTSAT IR image of TD 19W at 0030 UTC 24 September 2008. (b) Microwave image at 89 GHz of TD Jangmi at 0411 UTC 24 September 2008. (c) Analyzed 200 hPa winds from ECMWF at 0000 UTC 24 September 2008. Satellite imagery from http:\\www.nrlmry.navy.mil/sat_products.html.

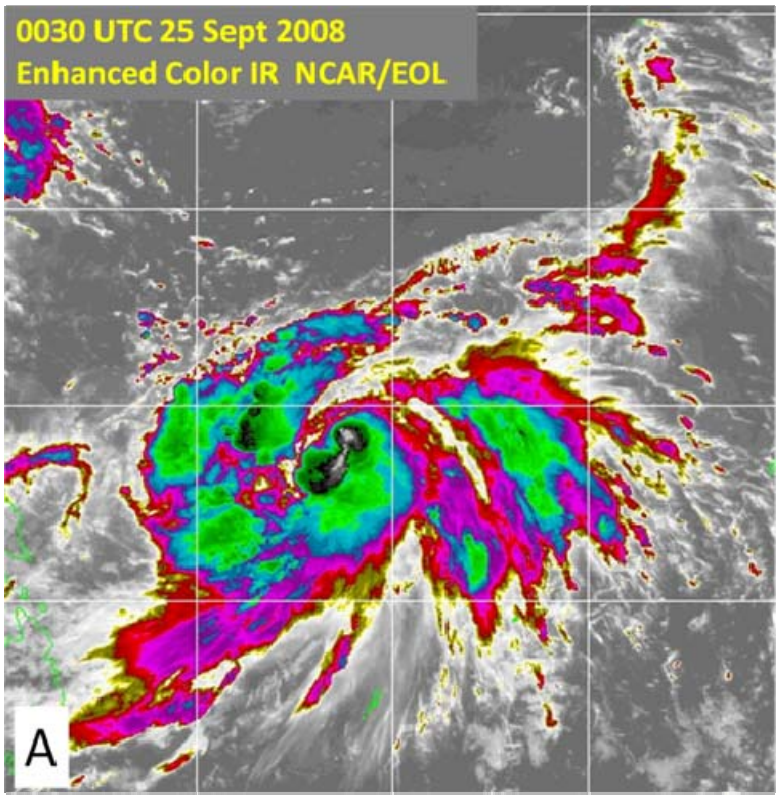
0030 UTC 25 Sept 2008
Enhanced Color IR NCAR/EOL
A

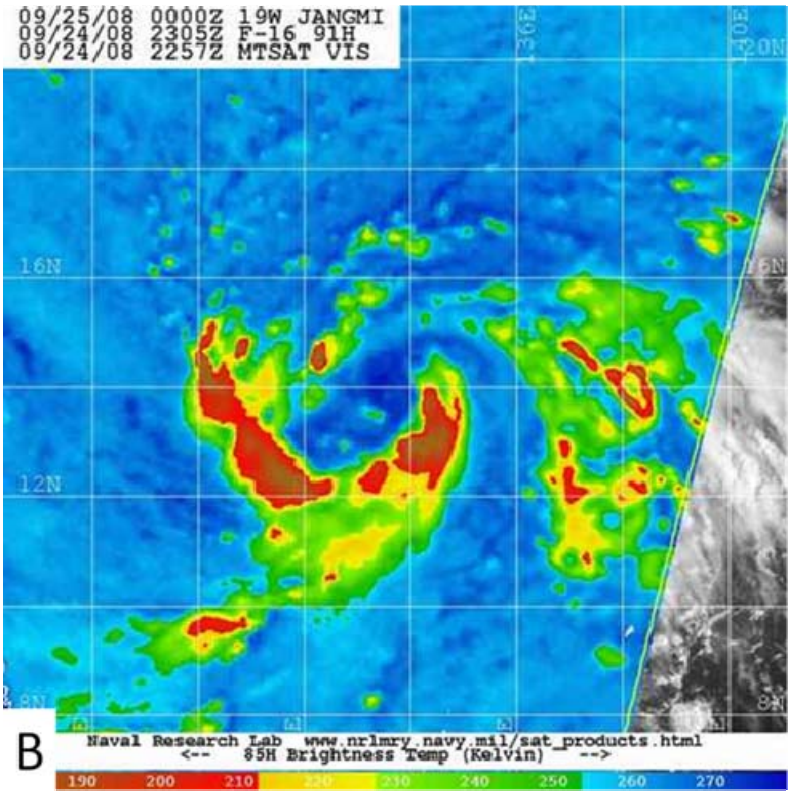
09/25/08 0000Z 19W JANGMI
09/24/08 2305Z F-16_91H
09/24/08 2257Z MTSAT VIS
16N
12N
B
Naval Research Lab www.nrlmry.navy.mil/sat_products.html
<-- 85H Brightness Temp (Kelvin) -->
190 200 210 220 230 240 250 260 270

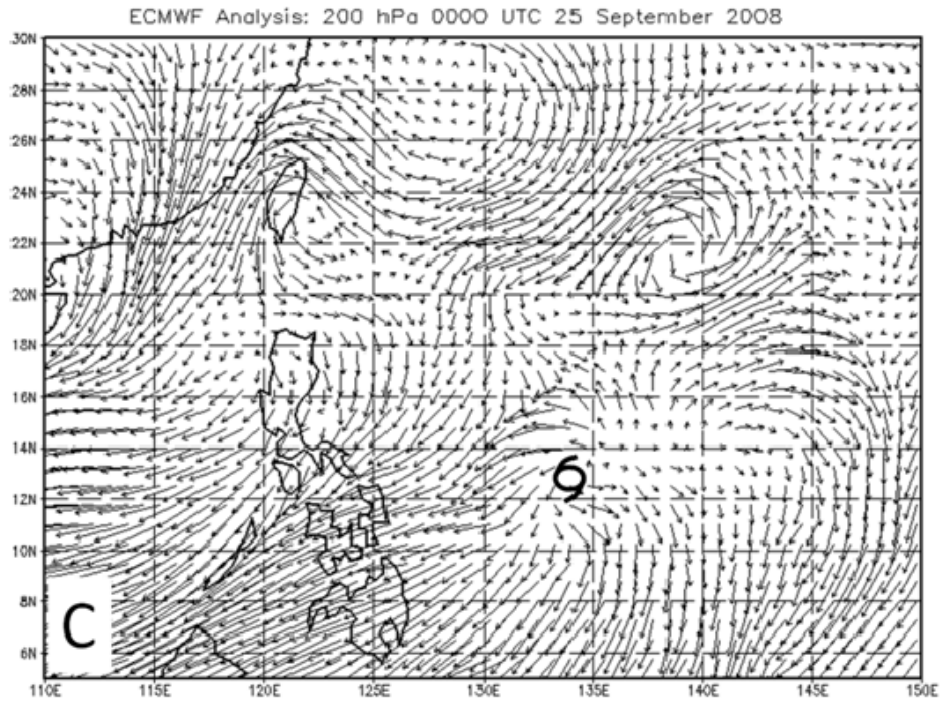

Figure 48. (a) Color-enhanced MTSAT IR image of TS Jangmi at 0030 UTC 25 September 2008. (b) Microwave image at 91 GHz of TS Jangmi at 2305 UTC 24 September 2008. (c) Analyzed 200 hPa winds from ECMWF at 0000 UTC 25 September 2008. Satellite imagery from http:\\www.nrlmry.navy.mil/sat_products.html.

After 0000 UTC on 25 September, the vertical wind shear over TS Jangmi was again reduced to below 10 kt and the storm intensified from TS to TY by 1200 UTC 25 September (Figure 46). The OHC values from the AXBTs deployed during the first Jangmi aircraft mission centered near 2143 UTC 24 September 2008 (Figure 20) were in fair agreement with the EASNFS analysis (Figures 49 and 50, Table 9). The average OHC for the 13 AXBTs deployed in the vicinity of Jangmi (Figure 49) was 146.7 kJ cm^{-2} (Table 9) and the EASNFS values were above 130 kJ cm^{-2}. The four AXBTs in Figure 50 were deployed in the vicinity of TY Jangmi. Whereas three of these AXBTs had MLDs around 50 m and OHC values near 150 kJ cm^{-2}, AXBT 209 was deployed northwest of the storm and had an OHC value of 67.96 kJ cm^{-2} (Table 9). The AXBT 209 had a high SST, but was well within the 35-50 kt wind field radius of the storm.

Thus, the temperature profile had a well-mixed layer at the surface with a steep thermocline slope to a T26 at a shallow depth, which resulted in its greatly reduced OHC value (Table 9).

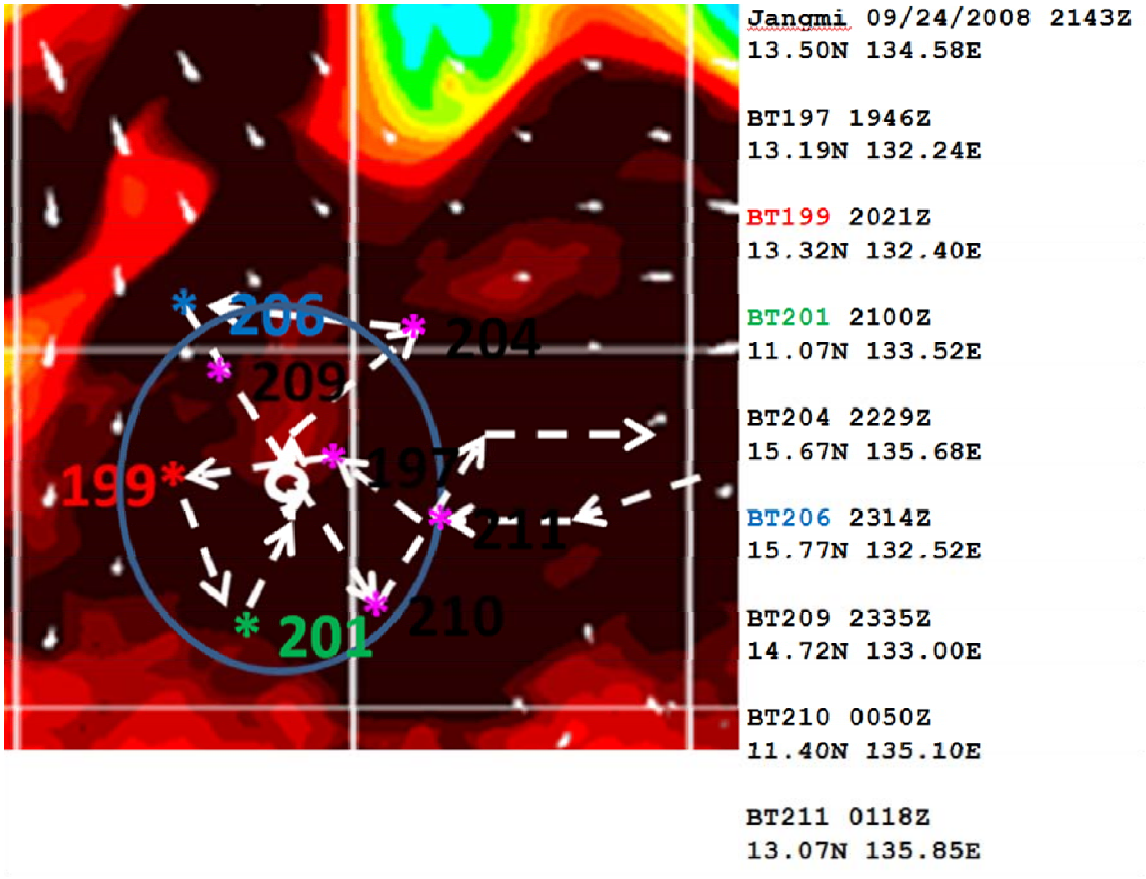

Figure 49. Composite plot of AXBTs in relation to TY Jangmi at 2143 UTC 24 September 2008 and overlaid on the EASNFS OHC analysis at 0000 UTC 23 September 2008. Arrows correspond to the aircraft flight track.

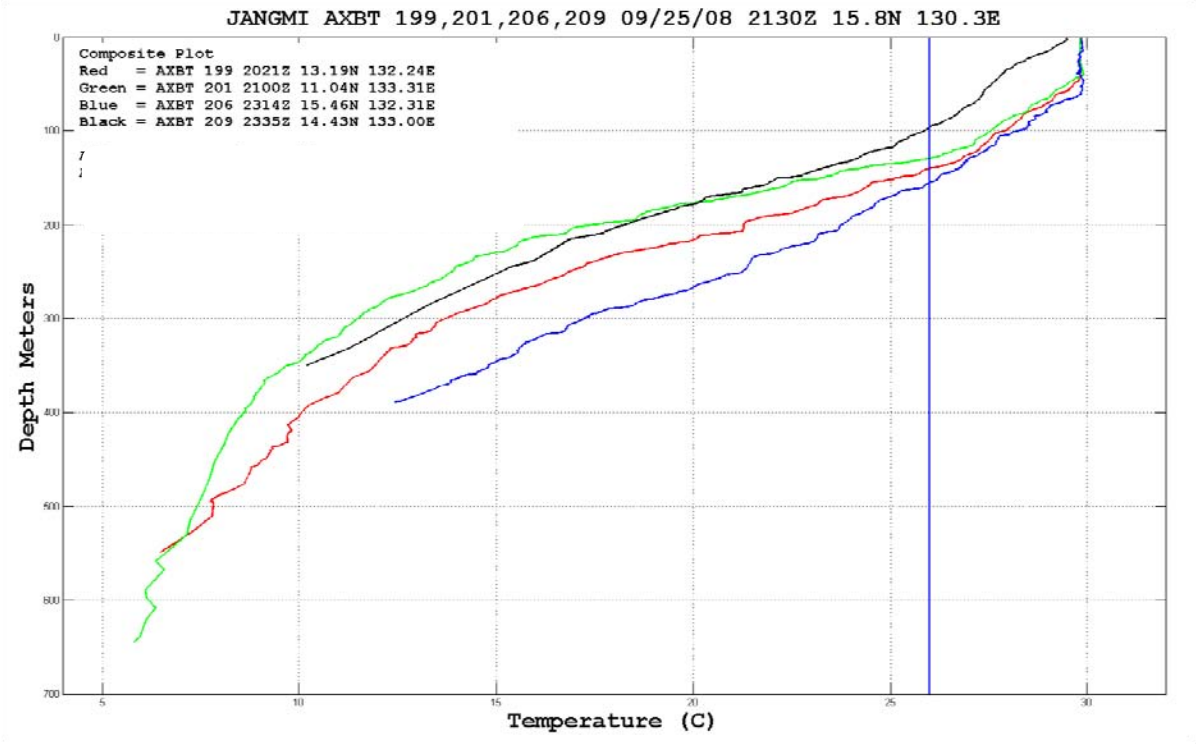

Figure 50. Temperature profiles from AXBTs 199, 201, 206, and 209 during the 24 September 2008 flight into TY Jangmi. Locations of the AXBTs are indicated in the inset. The 26°C isotherm is indicated by the blue vertical line.

Table 9. Oceanic variables derived from AXBTs on 24-25 September 2008.

25-Sep				°C/100m	°C	kJ/cm^2	kJ/cm^2
AXBT#	SST C	26°C Depth	MLD m	Slope	T100	OHC	OHC24
195	29.56	94.71	5	4.06	27.79	73.03	160.72
196	29.6	150.21	61	4.5	29.22	154.53	289.78
197	29.81	152.8	67	4.01	29.42	169.19	306.26
199	29.81	139.26	48	4.11	29.29	152.63	277.55
200	29.54	132.46	62	4.94	29.35	152.56	278.31
201	29.81	129.91	42	5.81	29.16	140.35	250.82
202	29.64	153.37	51	3.36	29.29	161.94	296.88
203	29.72	156.67	61	3.97	29.37	165.45	304.42
204	29.86	165.32	84	5.17	29.75	188.03	336.98
205	29.92	121.68	52	5.06	29.08	129.16	249.16
206	28.85	154.3	60	4	29.49	167.58	308.21
209	29.49	95.07	10	3.7	27.67	67.96	162.31
210	29.69	99.84	40	7.85	28.69	109.54	203.36
211	29.6	151.22	50	3.6	29.04	147.65	281.59

Although Jangmi then moved over a region with reduced OHC values near 80-90 kJ cm^{-2} (Figure 45) during 1200 UTC 25 to 0000 UTC 26 September, these values were still above the threshold value of 60 kJ cm^{-2} defined by Mainelli et al. (2008) and the storm intensified from 70 kt to 90 kt.

3. Jangmi 26 September 2008

Typhoon Jangmi's cloud pattern on satellite became more symmetrical and expanded in area with deep convective bands in all quadrants except in the northwest by 0030 UTC 26 September (Figure 51a). Microwave imagery at 2252 UTC 25 September (Figure 51b) indicated that Jangmi had formed a nearly complete eyewall and outflow the was distributed uniformly in all directions (Figure 51c).

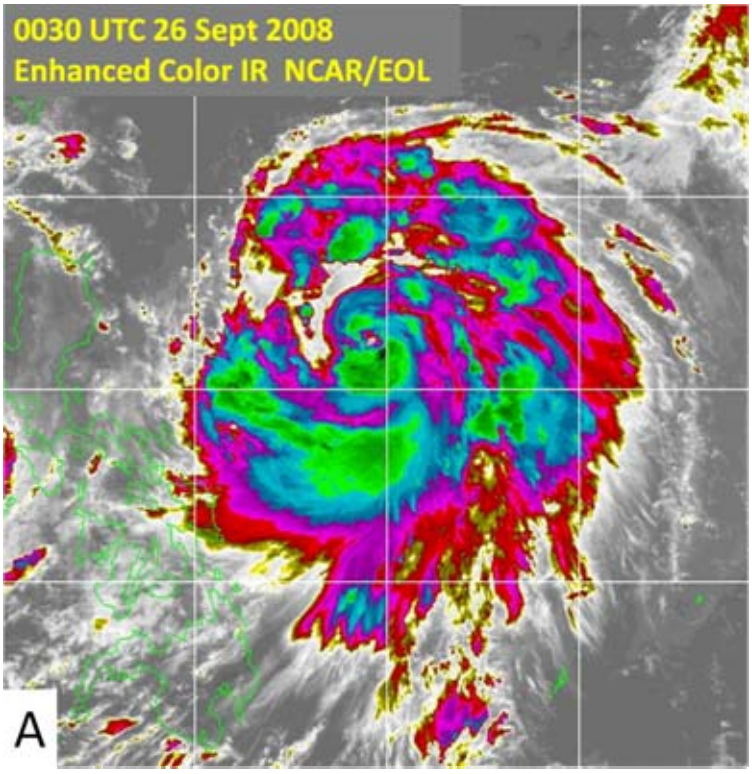

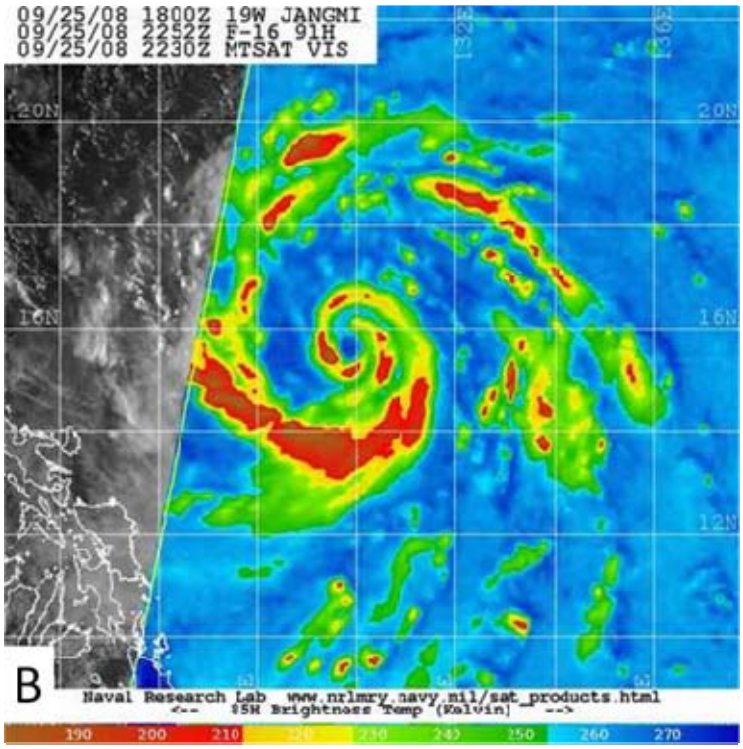

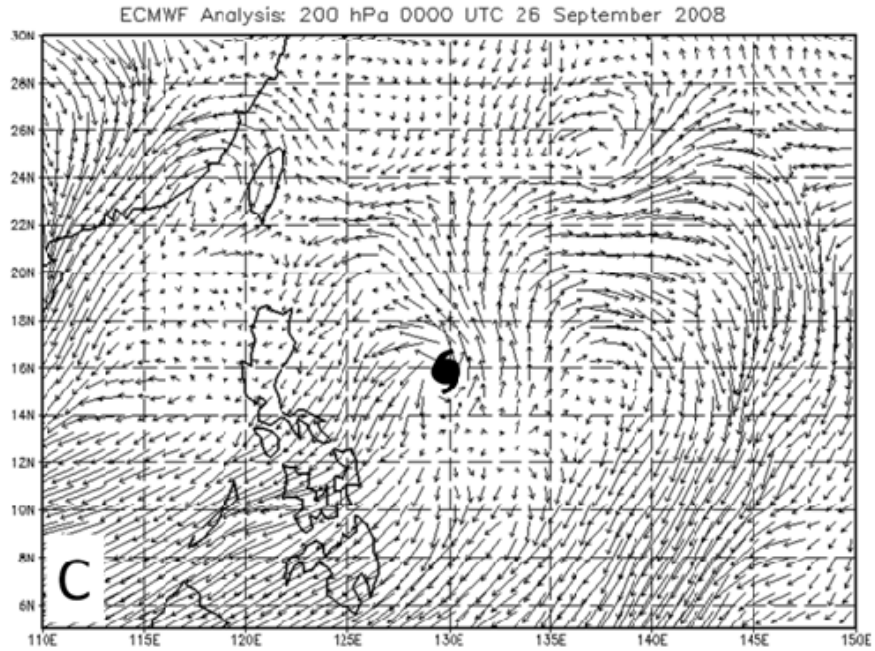

Figure 51. (a) Color-enhanced MTSAT IR image of TY Jangmi at 0030 UTC 26 September 2008. (b) Microwave image at 91 GHz of TY Jangmi at 2252 UTC 25 September 2008, and (c) Analyzed 200 hPa winds from ECMWF at 0000 UTC 26 September 2008. Satellite imagery from www.nrlmry.navy.mil/sat_products.html.

Typhoon Jangmi passed over a warm eddy that had an OHC of 120 kJ cm^{-2} according to the EASNFS analysis. During the second flight into Jangmi between 1800 UTC 25 September and 0600 UTC 26 September (Figure 21), the average OHC for the 12 AXBTs deployed into the vicinity of the storm (Figure 45) was 132.35 kJ cm^{-2} (Table 10).

Table 10. Oceanic variables derived from AXBTs on 25–26 September 2008.

26-Sep				^{o}C/100m	^{o}C	kJ/cm^2	kJ/cm^2
AXBT#	SST C	26^{o}C Depth	MLD m	Slope	T100	OHC	OHC24
213	29.25	96.69	67	8.05	28.49	101.58	197.34
214	29.32	106.06	69	8.06	28.83	116.03	220.59
215	29.49	121.9	67	6.92	29.05	130.18	238.79
216	29.47	148.57	78	5.13	29.3	158.65	294.95
217	29.56	162.47	80	4.42	29.47	177.52	329.09
218	29.55	145.19	72	5.01	29.35	159.16	296.39
219	29.48	125.12	54	5.53	28.95	127.64	242.98
220	28.92	94.81	56	6.35	28.13	86.81	177.6
221	29.45	171.36	122	6.88	29.44	201.64	358.39
222	29.32	120.93	62	6.03	28.82	118.28	228.7
224	29.22	111.63	72	6.82	28.85	117.96	222.76
225	29.07	92.76	64	5.93	28.26	92.78	183.67

The first leg of the flight centered around 0000 UTC 26 September 2008 was along the storm track and AXBTs 213 and 214 were deployed to the southeast and behind the storm and AXBTs 215 and 216 were deployed to the northwest and in front of the storm (Figure 52). Notice the clear progression of deepening MLD and increasing OHC (Figure 53) in the profiles from southeast to the northwest as the profiles behind the typhoon are indicating the mixing of the upper ocean. The profiles 215 and 216 to the northwest have not been affected as much, as they were deployed ahead of the storm and in the center of the warm eddy on the EASNFS analysis.

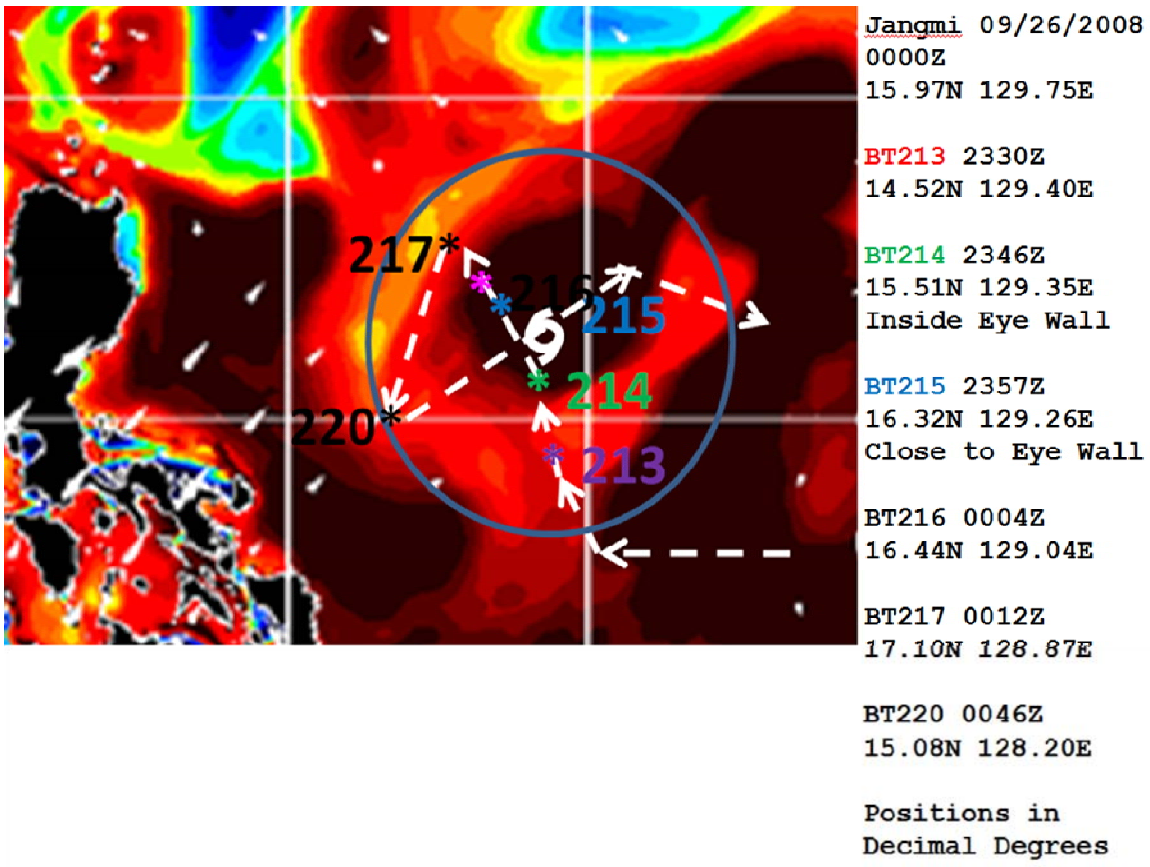

Figure 52. Composite plot of AXBTs in relation to TY Jangmi at 0000 UTC 26 September 2008 and overlaid on the EASNFS OHC analysis at 0000 UTC 24 September 2008. Arrows correspond to the aircraft flight track.

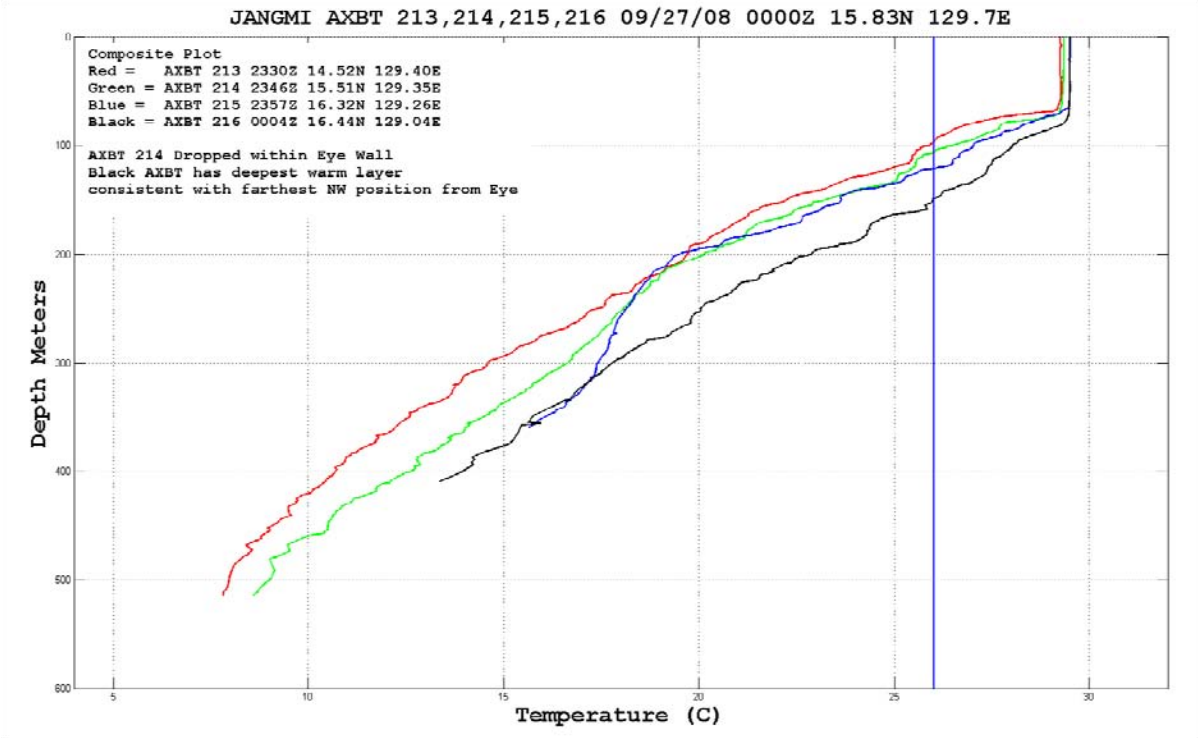

Figure 53. Temperature profiles from AXBTs 213-216 deployed during the 26 September 2008 flight in TY Jangmi. Locations of the AXBTs are indicated in the inset. The 26°C isotherm is indicated by the blue vertical line.

The second leg of the flight centered around 0105 UTC 26 September 2008 was from the southwest to the northeast across the center of the storm (Figure 21) with deployment of AXBTs 221, 222, 224 and 225 (Figure 54). The AXBT 221, which was farthest to the southwest, had a significantly deeper MLD and higher OHC than the other three profiles (Figure 55). That is, AXBT 221 was deployed in a region of the storm where mixing and wave action should have been the weakest as the storm was moving in a northwest direction.

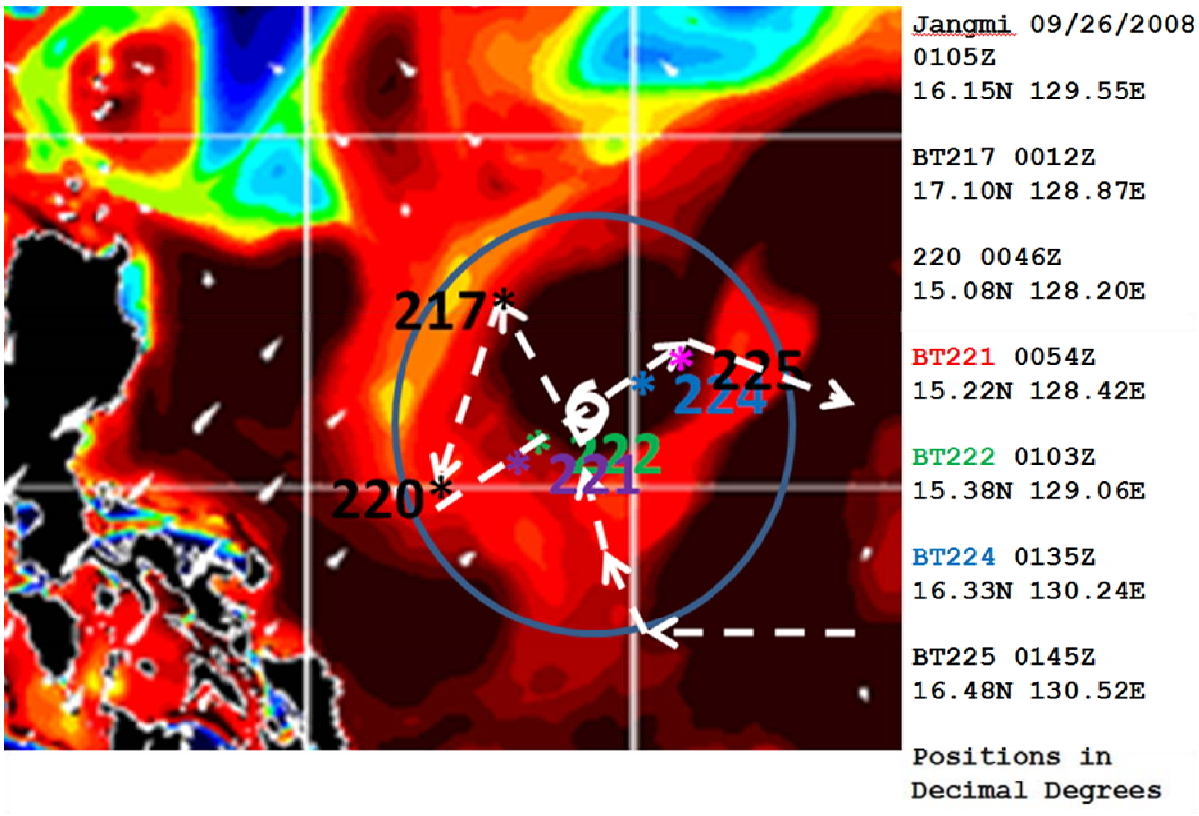

Figure 54. Composite plot of AXBTs in relation to TY Jangmi at 0015 UTC 26 September 2008 overlaid on EASNFS OHC analysis at 0000 UTC 24 September 2008. Arrows correspond to the aircraft flight track.

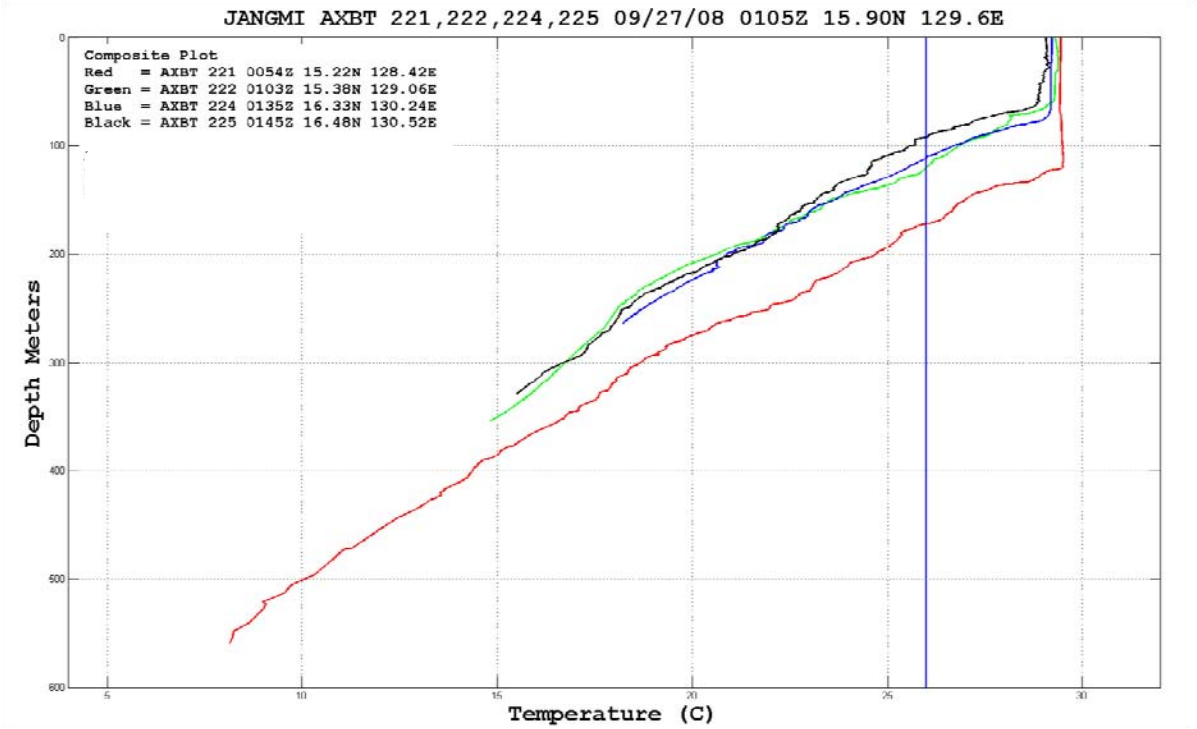

Figure 55. Temperature profiles from AXBTs 221, 222, 224, and 225 deployed during the 26 September 2008 flight into TY Jangmi. Locations of the AXBTs are indicated in the inset. The 26°C isotherm is indicated by the blue vertical line.

Coincident with the passage over the warm eddy, the vertical wind shear began to decrease sharply to below 10 kt (Figure 46). Both of these factors are considered to have contributed to the rapid increase in maximum wind speed from 95 kt to 135 kt by 0000 UTC on 27 September (Figure 56a). The central pressure of Jangmi dropped from 952 hPa to 922 hPa during this period. During the period between 0000 UTC 26 September to 0000 UTC 27 September, the cloud pattern changed from the ragged appearance of a minimal typhoon (Figure 51a) to the completely symmetric eye surrounded by a broad distribution of very cold cloud tops (Figure 56a).

4. Jangmi 27 September 2008

The vertical wind shear decreased to 6 kt (Figure 46) from 0000 UTC 27 September 2008 to 1800 UTC 27 September 2008. During this period, TY Jangmi intensified into a STY with peak winds over 140 kt and a central pressure of 918 hPa at 1200 UTC 27 September 2008. Strong, upper-level outflow existed in all directions (Figure 56c). Furthermore, at the time of minimum wind shear, Jangmi was passing over a warm ocean eddy (Figures 45 and 46). Jangmi maintained maximum intensity from 0600 to 1200 UTC 27 September 2008.

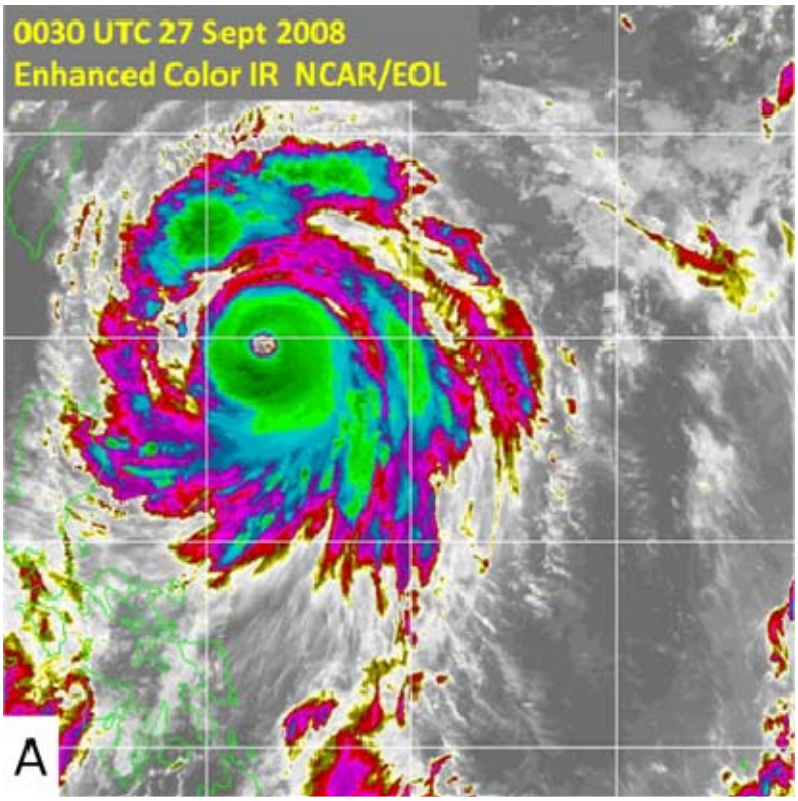

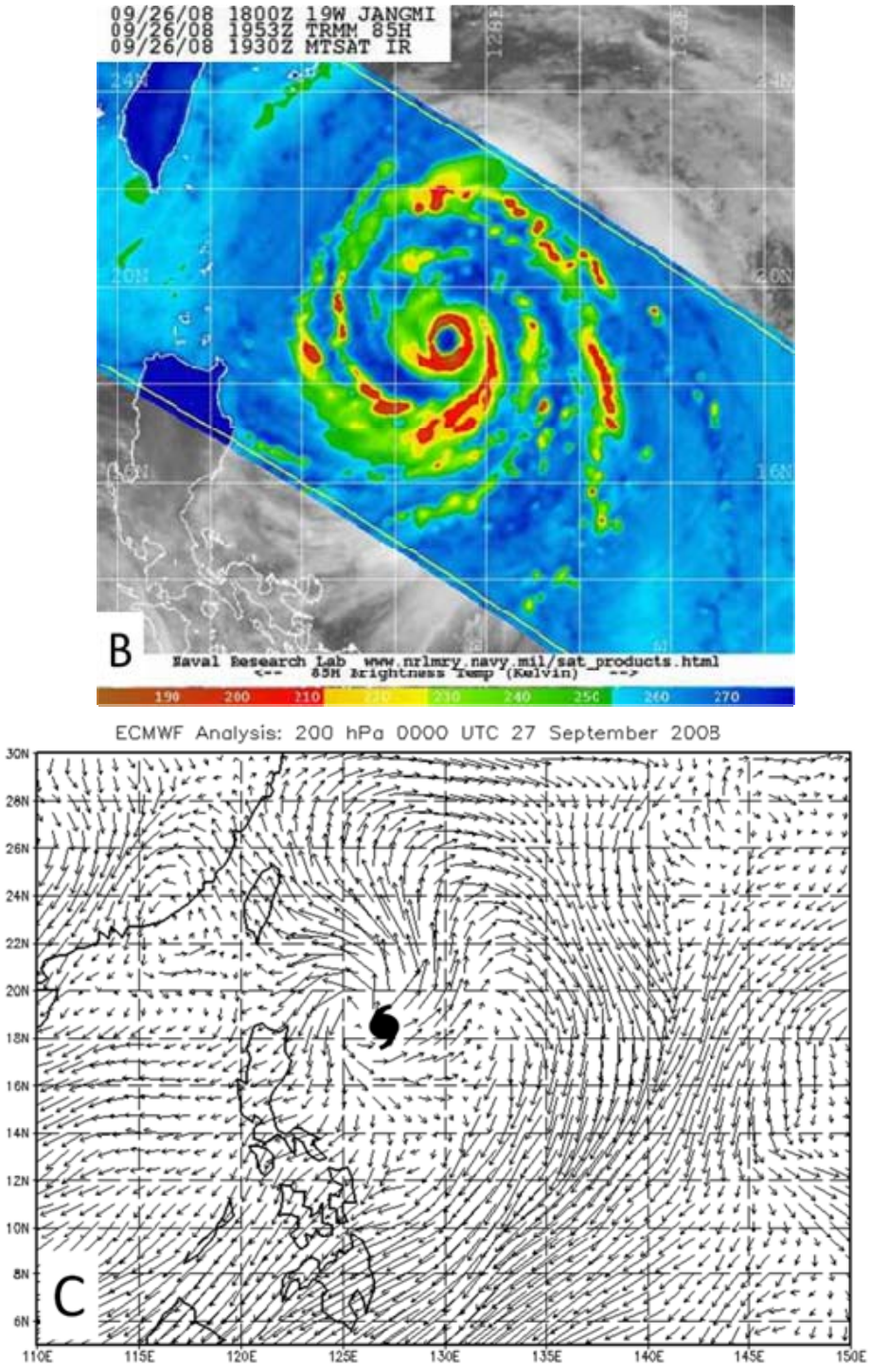

Figure 56. (a) Color-enhanced MTSAT IR image of STY Jangmi at 0030 UTC 27 September 2008. (b) Microwave image at 85 GHz of STY Jangmi at 1953 UTC 26 September 2008, and (c) Analyzed 200 hPa winds from ECMWF at 0000 UTC 27 September 2008. Imagery from www.nrlmry.navy.mil/sat_products.html.

During the ensuing 18 h, Jangmi moved over an adjacent cold eddy (Figure 45) and the wind shear increased to over 10 kt from the north by 0000 UTC 28 September (Figure 46). However, Jangmi had slowly begun to weaken to 135 kt by 1800 UTC 27 September 2008 as it began to traverse the cold eddy and before the vertical wind shear increased. This time sequence suggests that the ocean interaction with the storm exhibits a delay related closely to the evaporation and rainfall time cycle (Mainelli 2000).

The EASNFS OHC values associated with the cold eddy were near 50 kJ cm^{-2} (Figure 57). The OHC values from the AXBTs deployed on the flight centered near 0800 UTC 27 September 2008 were 50–70 kJ cm^{-2} (Figure 58 and Table 11). Note that AXBT 241, which was deployed in the wake of the storm, had an SST of 26.43°C and thus the OHC was only 6.4 kJ cm^{-2}.

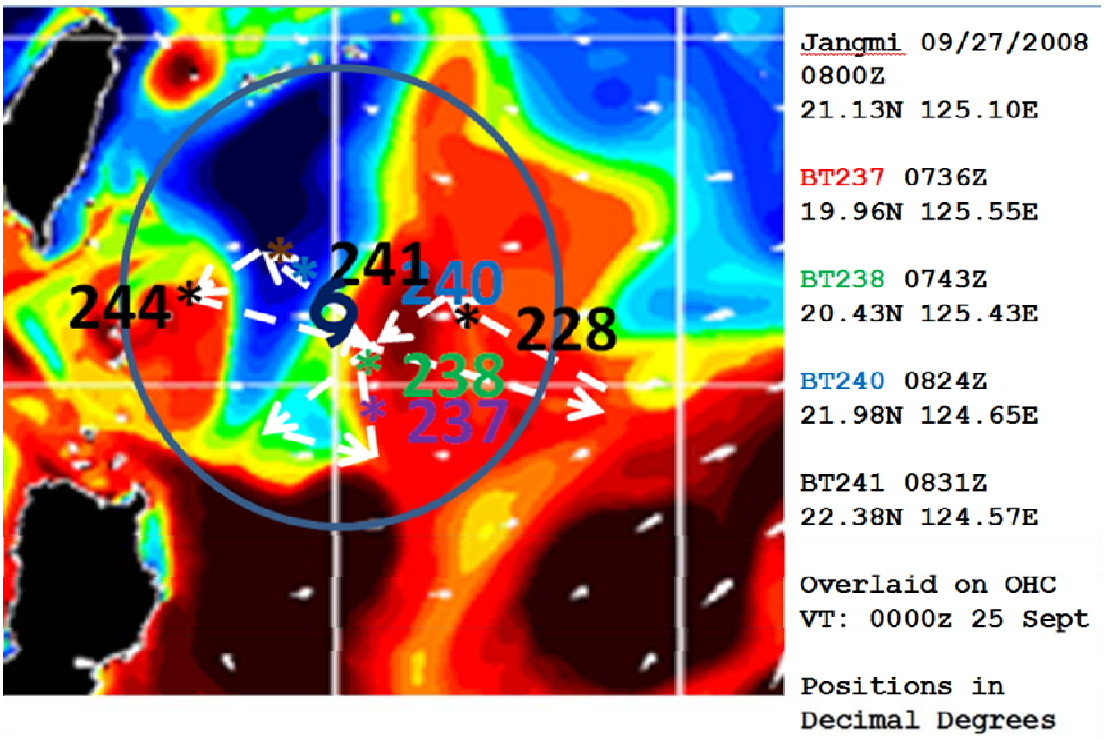

Figure 57. Composite plot of AXBTs in relation to STY Jangmi at 0800 UTC 27 September 2008 overlaid on the EASNFS OHC analysis at 0000 UTC 25 September 2008. Arrows correspond to the aircraft flight track.

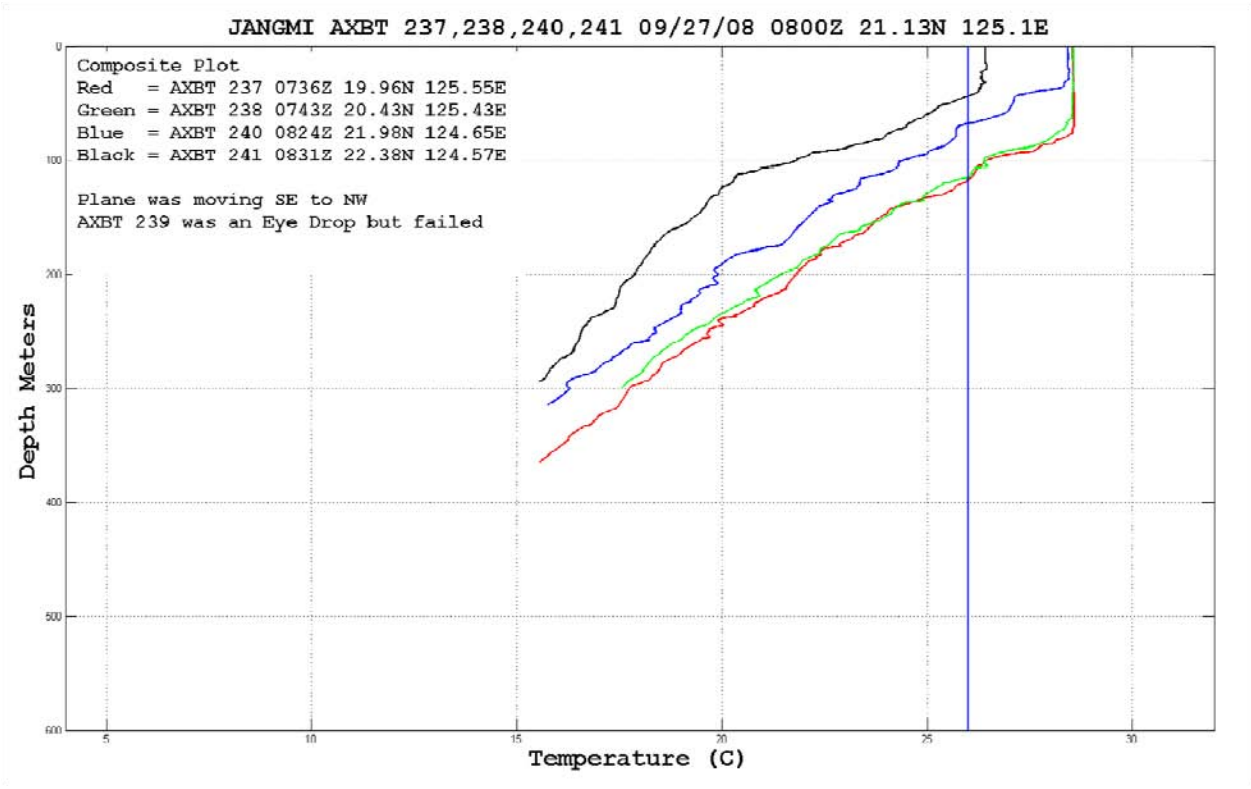

Figure 58. Temperature profiles from AXBTs 237, 238, 240, and 241 deployed in Jangmi during the 27 September 2008 flight. Locations of the AXBTs are indicated in the inset. The 26 ^{o}C isotherm is indicated by the blue vertical line.

Table 11. Oceanic variables derived from AXBTs on 27 September 2008.

27-Sep				Slope	T100	OHC	OHC24
AXBT#	SST C	26°C Depth	MLD m	°C/100m	°C	kJ/cm^2	kJ/cm^2
226	28.97	75.42	50	6.06	27.71	77.25	154.31
227	29.03	88.63	56	5.89	28.13	88.68	179.19
228	28.96	98.54	60	6.16	28.42	98.7	NA
229	26.5	131	100	NA	NA	NA	NA
230	28.46	132.55	102	7.45	28.37	113.9	NA
231	28.56	81.84	60	6.42	27.69	73.9	151.44
232	27.93	55.24	43	7.59	25.91	38.35	88.35
233	27.85	69.74	37	6.82	26.44	39.12	103.77
234	27.75	63.57	40	6.61	26.3	40.43	97.6
235	M	M	M	NA	NA	NA	NA
236	28.54	45.6	10	5.6	26	25.87	82.75
237	28.54	117.85	79	6.25	28.36	97.68	206.2
238	28.55	115.81	65	5.41	28.25	92.96	199.11
239	M	M	M	NA	NA	NA	NA
240	28.42	67.44	35	5.71	27.02	49.04	123.88
241	26.43	43.61	40	6.89	25.13	6.4	55.35
242	28.18	105.2	70	5.04	27.75	72.14	168.32
243	28.23	94.76	35	5.09	27.6	66.02	150.82
244	M	M	M	NA	NA	NA	NA
245	M	M	M	NA	NA	NA	NA
246	M	M	M	NA	NA	NA	NA
247	28.28	105.07	75	5.22	28.14	89.1	192.22
248	28.24	108.96	80	6.14	28.23	89.76	184.3
249	28.32	107.44	78	6.12	28.07	86.08	186.11
250	27.88	98.78	70	5.59	27.55	63.22	149.95

After 1800 UTC 27 September, the combination of the cold eddy and increased vertical wind shear contributed to a rapid weakening of Jangmi from 135 kt to 110 kt prior to making landfall on Taiwan. By 0000 UTC 28 September, a reduction in the convection is evident on both the IR and microwave images (Figures 59a and 59b) on the northwest side of the storm as it passed over the cold eddy.

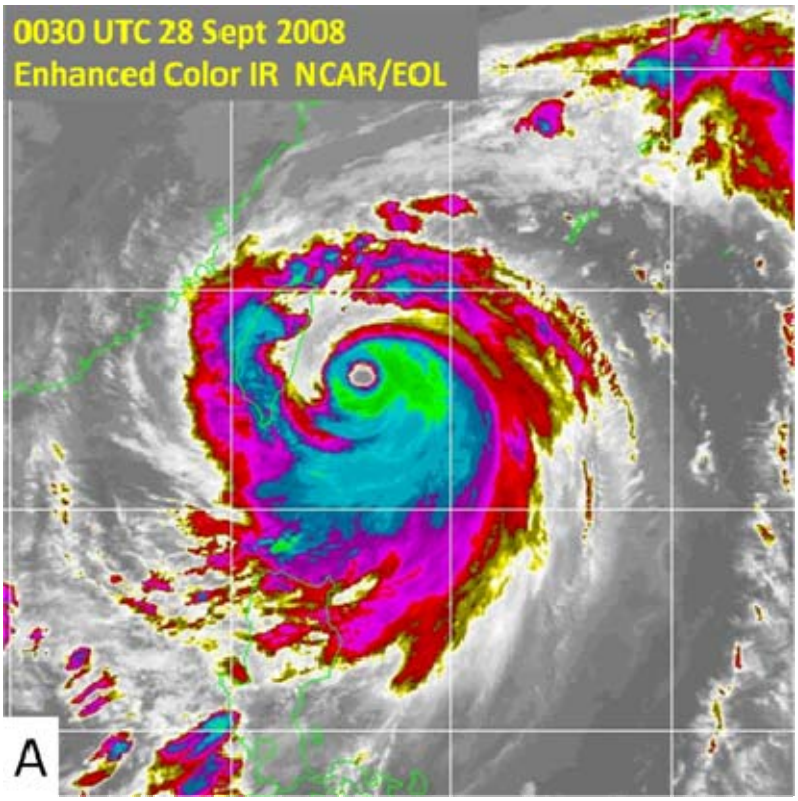
0030 UTC 28 Sept 2008
Enhanced Color IR NCAR/EOL
A

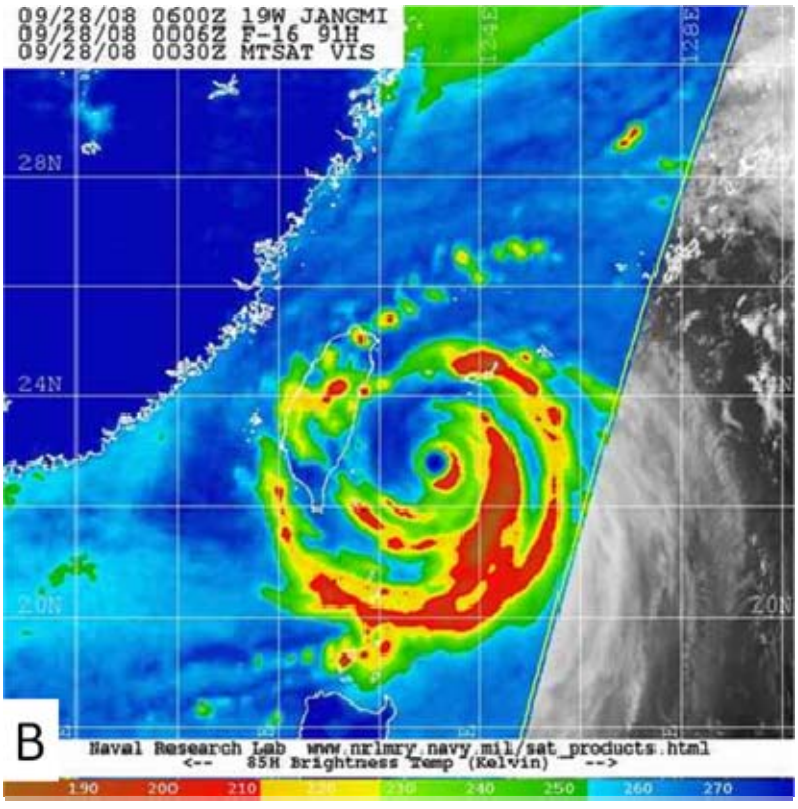
09/28/08 0600Z 19W JANGMI
09/28/08 0006Z F-16 91H
09/28/08 0030Z MTSAT VIS
28N
24N
20N
B
Naval Research Lab www.nrlmry.navy.mil/sat_products.html
<-- 85H Brightness Temp (Kelvin) -->
190 200 210 230 240 250 260 270

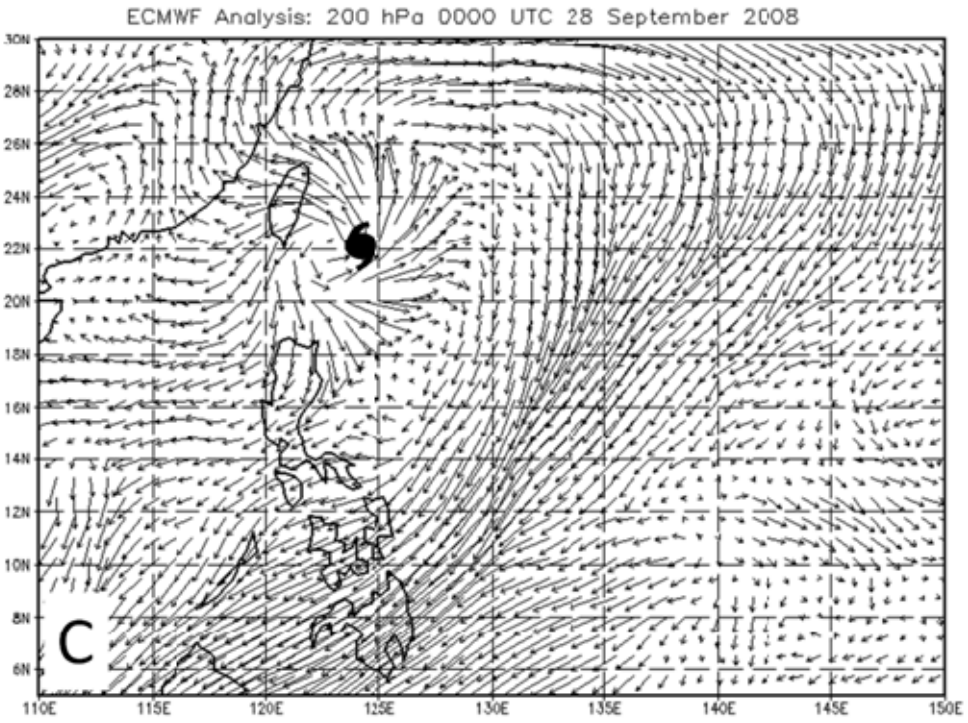

Figure 59. (a) Color-enhanced MTSAT IR image of STY Jangmi at 0030 UTC 28 September 2008. (b) Microwave image at 91 GHz of STY Jangmi at 0006 UTC 28 September 2008. (c) Analyzed 200 hPa winds from ECMWF at 0000 UTC 28 September 2008. Satellite imagery from www.nrlmry.navy.mil/sat_products.html.

5. Jangmi 28 September 2008

The combined effects of colder water and increased vertical wind shear weakened Jangmi from 135 kt to 100 kt by 0900 UTC 28 September 2008 when Jangmi encountered the northeast tip of Taiwan. Jangmi brushed over the northern tip of Taiwan and was in contact with the island for roughly 9 hours as it continued to weaken to 75 kt.

Just after passing over Taiwan, the storm weakened to a TS and it turned to the east-northeast on 29 September before undergoing extratropical transition on 30 September. This stage of Jangmi will not be discussed.

6. Super Typhoon Jangmi Summary

As TCS-047 moved from 12^{o} N, 168^{o} E to 11^{o} N, 140^{o} E in the easterly trades, the OHC along the path gradually increased from 85 kJ cm^{-2} in the central Pacific to 120 kJ cm^{-2} in the western Pacific. This entire track segment had OHC values large enough to support major typhoon intensities. However, vertical wind shear was a primary factor in the delay of the formation of TD Jangmi until 23 September 2008. On 23 September, the vertical wind shear was reduced to 5–7 kt for 12 hours, which allowed TD formation. According to the EASNFS OHC 0000 UTC analyses during 23 to 25 September, the OHC values along Jangmi's track increased from around 120 kJ cm^{-2} to 150 kJ cm^{-2}. Again, moderate vertical wind shear above 10 kt apparently slowed intensification of the storm during these two days. A critical period from 1200 UTC 26 September to 1200 UTC 27 September occurred when vertical wind shear values were again reduced to 5-7 kt and Jangmi underwent rapid intensification (Figure 46) while passing over an ocean area with extremely high values (>150 kJ cm^{-2}) of OHC. During a second period with low vertical wind shear, Jangmi passed over a cold eddy and weakened prior to the onset of increased vertical wind shear. The OHC values of 30-50 kJ cm^{-2} from the AXBTs in the cold eddy were below the 60 kJ cm^{-2} threshold (Lin et al. 2008) that is required to sustain a major typhoon according to Lin et al. (2008).

The influence of vertical wind shear on the storm from this particular case can be divided into three categories. Vertical wind shear values larger than 12 kt seemed to be strong enough to weaken the TC. Values of vertical wind shear between 8 and 12 kt slowed intensification, but in the high OHC environment of Jangmi's path the storm was able to gradually intensify from TD to TS on 25 September (Figure 46). Finally, when the wind shear was less than 8 kt around 0000 UTC 27 September, Jangmi was able to rapidly intensify from a TS to a STY over a region of high OHC values (Figure 46). Gradual weakening began on 1200 UTC 27 September as Jangmi started to move over the cold eddy even though for the next 12 hours the vertical wind shear remained low. During this period, it is considered that the low OHC values contributed to the decrease in the storm intensity.

C. COMPARISON OF TY SINLAKU AND STY JANGMI

1. Formation

The two storms formed over the Philippine Sea after traveling as open waves across large distances in the easterly trade winds under moderate vertical wind shear. In both cases, formation occurred over ocean water with a very high OHC and during a period of reduced vertical wind shear (below 10 kt) at the time of formation. Jangmi formed farther southeast than Sinlaku and had a much longer path over warm water before it reached the eddy zone around 18^{o}N. An important difference existed in forward translation speed as Jangmi, which was moving at 6 m s^{-1}, was moving quite a bit faster than Sinlaku, which was moving at 3 m s^{-1}, as both traversed the same region of high OHC. The forward translation speed of Jangmi was at the upper end of the scale listed in Lin et al. (2009) for effective coupling to ocean heat and moisture fluxes.

2. Vertical Wind Shear

The response to the vertical wind shear environment was very similar for both storms such that when the shear increased to above 12 kt each storm weakened. Reduced vertical wind shear (below 8 kt) was associated with intensification except when a storm was traversing a cold eddy or when passing over Taiwan (Figures 28 and 56).

3. Ocean Heat Content

As noted previously, STY Jangmi had a much longer path over very warm waters before it reached the eddy zone around 18^{o}N. However, Jangmi also moved approximately twice as fast as Sinlaku. When Sinlaku and Jangmi were located near 20^{o}N, 125^{o}E, both had intensities of 90 kt. The faster translation speed of Jangmi and higher vertical wind shear prevented Jangmi from becoming more intense than 90 kt. Beyond this location, both storms followed a similar path. On 6 September 2008 (Figure 17), Sinlaku passed over a weak cold eddy near 19^{o}N, 125^{o}E. Jangmi did not pass over this feature on 24 September as it moved farther to the north and east. For a 12-h period that coincided with the passage over the cold eddy, Sinlaku did not intensify. Two weeks

later on 24 September 2008, the warm eddies were warmer and the cold eddy east of Taiwan was larger and colder. On 27 September, Jangmi passed over the warm eddy that had intensified since Sinlaku's passage, which allowed Jangmi to intensify into a supertyphoon.

D. COMPARISON OF IN SITU AXBT DATA WITH EASNFS MODEL PROFILES

Several sets of AXBTs were deployed along the tracks of TY Sinlaku and STY Jangmi. The *in situ* AXBT profiles were compared to profiles from the gridded EASNFS analysis from NRLSSC that had been interpolated to the locations of the AXBT deployments.

Comparisons for each storm were made for three variables: SST, MLD, and OHC (Table 12). During the 9-12 September aircraft deployments into TY Sinlaku, 29 SST samples were taken. The EASNFS average SST was 0.70^{o}C warmer than the AXBT average SST. For the 27 samples of MLDs, the EASNFS MLD was 18.09 m shallower than the AXBT MLD average depth. For the 28 samples of OHC, the EASNFS OHC was 12.7 kJ cm^{-2} higher than the AXBT OHC.

Table 12. Statistical comparison of EASNFS analyzed ocean parameters with AXBT data obtained during the flights into TY Sinlaku from 9-12 September 2008.

Sinlaku	AXBT	EASNFS	Sample Size	Difference
Ave SST (^{o}C)	28.204	28.901	29	0.697
Ave MLD (m)	51.678	33.592	27	-18.086
Ave OHC (kJ cm^{-2})	69.473	82.176	28	12.703

During the aircraft deployments into STY Jangmi on 25–27 September, 45 samples of SST data were available (Table 13). The EASNFS average SST was 0.26^{o}C higher than the AXBT average SST. For the 44 samples AXBT-measured MLDs, the EASNFS MLD average depth was 17.25 m shallower than the AXBT MLD. For the 44 samples of OHCs, the EASNFS OHC was 11.6 kJ cm^{-2} lower than the AXBT OHC.

Table 13. Statistical comparison of EASNFS analyzed ocean parameters with AXBT data obtained during the flights into STY Jangmi from 25-27 September 2008.

Jangmi	AXBT	EASNFS	Sample Size	Difference
Ave SST (^{o}C)	28.98	29.05	45	0.07
Ave MLD (m)	59.909	42.659	44	-17.25
Ave OHC (kJ cm^{-2})	109.168	97.544	44	-11.624

Overall, the largest EASNFS-AXBT OHC difference in TY Sinlaku was nearly equal in magnitude, but opposite in sign, to the EASNFS-AXBT OHC difference in STY Jangmi. Recall from Chapter III.C.3. TY Sinlaku passed over a weak cold eddy on 9-10 September and that Jangmi did not pass over this feature two weeks later. The EASNFS analysis may not have accurately resolved these different ocean conditions. Although the overall EASNFS-AXBT differences in Jangmi indicated a negative OHC bias for the EASNFS analysis, the AXBTs deployed in the cold eddy during the third flight on 27 September had lower OHC values than the EASNFS analysis, with the AXBT average OHC values 6.46 kJ cm^{-2} lower than the EASNFS average. As Sinlaku passed over this region two weeks earlier, the mixing produced by Sinlaku may not have been reflected in the EASNFS analysis.

Combining both storms (Table 14), the EASNFS average MLD was 17.5 meters shallower than the AXBT average MLD. This bias may be related to the use of climatology data that are part of the EASNFS analysis input. Overall, the warm SST bias tended to offset the shallow MLD bias in the OHC calculation. The overall EASNFS average OHC for all locations in both storms was only 2.16 kJ cm^{-2} lower than the AXBT average OHC.

Table 14. Comparison of EASNFS and AXBT parameters as in Tables 12 and 13, with both storms combined into one group sample.

Total	AXBT	EASNFS	Sample Size	Difference
Ave SST (^{o}C)	28.676	28.992	74	0.316
Ave MLD (m)	56.779	39.211	71	-17.568
Ave OHC (kJ cm^{-2})	93.731	91.568	72	-2.163

To compare these results with observations from an undisturbed ocean environment, the AXBT profiles from the flight on 25 September 2008 that were deployed outside of the influence of Jangmi were also compared with the EASNFS profiles (Table 15). The model-AXBT differences outside of the storm environment (Table 15) were much smaller than the total differences (Table 13). The model biases may be related to unresolved mixing caused by the two tropical cyclones. The average MLD for the EASNFS profiles outside the storm environment was 4.923 m shallower than the AXBT-based MLD, but much less than the 17.5 m average from the total data set.

Table 15. Statistical comparison of EASNFS analyzed ocean parameters with AXBT profiles obtained during the flight into STY Jangmi on 25 September 2008.

Sept 25th	AXBT	EASNFS	Sample Size	Difference
Ave SST (^{o}C)	29.636	29.469	13	-0.170
Ave MLD (m)	52.923	48	13	-4.923
Ave OHC (kJ cm^{-2})	146.659	126.498	13	-20.161

A subset of four AXBTs from the 13 deployed during the flight on 25 September (numbers 197, 199, 206, and 209) were compared at different points around the storm. In this subset, AXBT 209 (Figure 60d) appears to be in a region within the influence of the storm that was well mixed (Figure 49). In this subset, the EASNFS average SST was 0.13^{o}C lower than the AXBT average. The EASNFS average MLD was 0.75 m deeper than the AXBT average depth. The EASNFS average OHC was 15.21 kJ cm^{-2} lower than the AXBT average, and the EASNFS average Z26 depth was 15.89 m less than the AXBT average, which helps explain the difference in the OHC. The four profile comparisons (Figure 60) have very similar thermocline slopes once the differences in MLD are taken into account. In this subset, the EASNFS analysis bias from the use of climatology seems to be much less when compared to the total set. In the case of AXBTs 197, 199, and 206, the EASNFS analysis MLD is still shallow when compared to the AXBT profiles, as was typical of a majority of the comparisons.

Overall, in the environment outside the direct influence of the storm, the EASNFS profiles were much closer to the AXBT profiles. Although some evidence exists of a climatology bias in the EASNFS analysis, the MLD and slopes were in much better agreement with most of the AXBT profiles than in the regions within the direct influence of the storm.

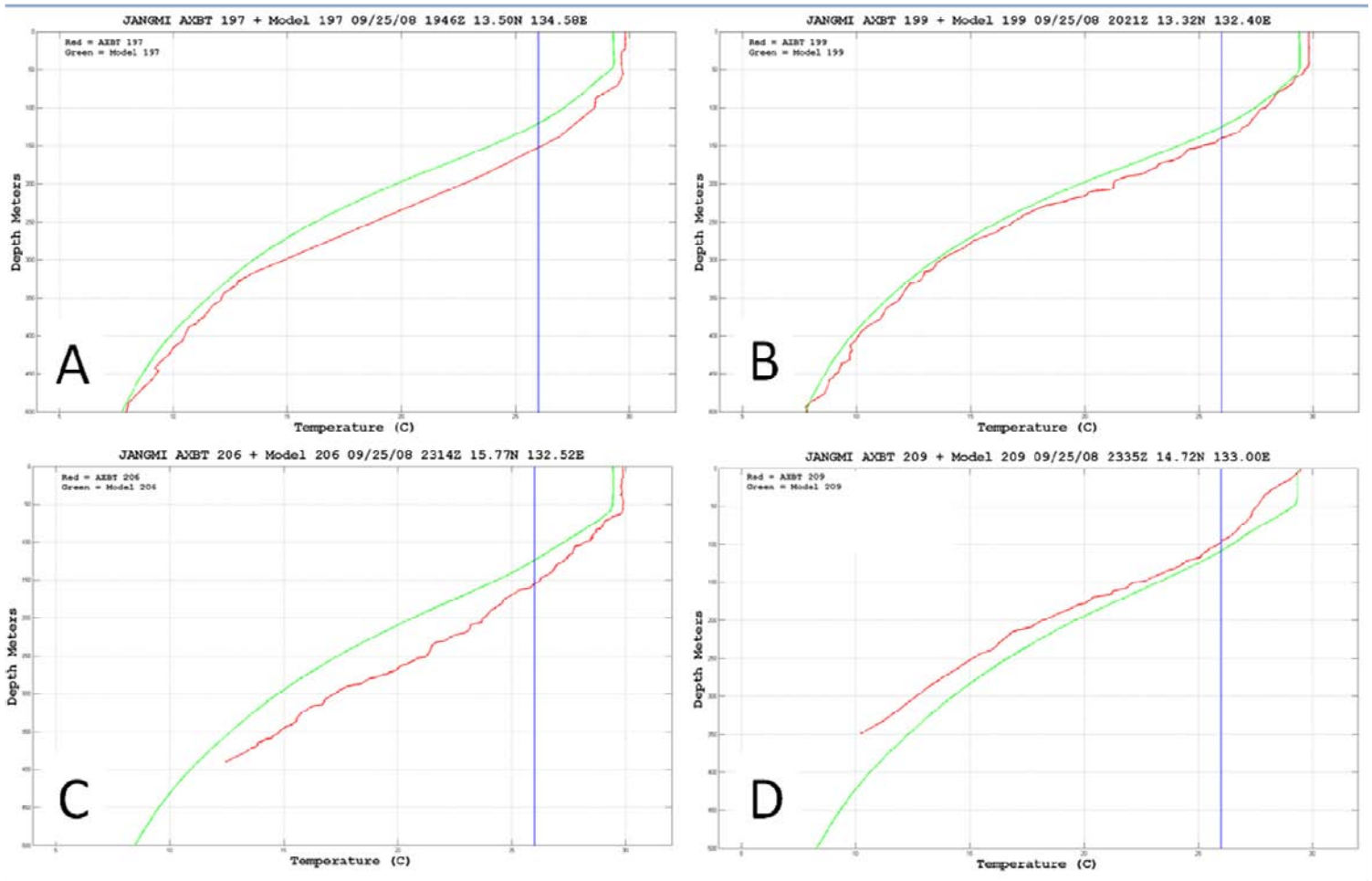

Figure 60. Comparisons of AXBT profiles (red) with EASNFS analysis profiles (green) for AXBTs (a) 197, (b) 199, (c) 206, and (d) 209 deployed during the flight on 25 September 2008. The depth interval is 50 m and the vertical line represents the 26^{o}C isotherm.

Data from the flight into STY Jangmi on 27 September 2008 were obtained over a variety of ocean regimes and were compared with the EASNFS analysis profiles (Table 16). The EASNFS average SST was 0.40°C higher than the AXBT average. The EASNFS average MLD was 18.74 m shallower than the AXBT average depth. Due once again to these compensating effects, the EASNFS average OHC was higher than the AXBT average by only 6.456 kJ cm^{-2}.

Table 16. Statistical comparison of EASNFS analyzed ocean parameters with AXBT data obtained during the flight into STY Jangmi on 27 September 2008.

Sept 27th	AXBT	EASNFS	Sample Size	Difference
Ave SST (°C)	28.269	28.669	19	0.400
Ave MLD (m)	57.105	38.368	19	-18.737
Ave OHC (kJ cm^{-2})	68.874	75.33	19	6.456

To examine possible EASNFS analysis biases in cold or warm eddies, EASNFS profiles were compared with AXBT observations obtained in three environments in STY Jangmi on 27 September 2008. The AXBTs 240, 241, 242, and 243 (Figure 61) were deployed in the cold eddy southeast of Taiwan. The AXBTs 231, 232, 248, and 249 (Figure 62) were deployed in the warm tongue southeast of the cold eddy, and the AXBTs 233, 234, 237 and 238 (Figure 63) were deployed in the vicinity of the weak cold eddy south of the warm tongue (Figure 45).

The EASNFS-AXBT profile comparisons in the cold eddy southeast of Taiwan (Figure 61) indicated that the EASNFS average SST of 27.82°C was exactly the same as the AXBT average SST. The EASNFS average MLD was 16 m shallower than the AXBT average depth. The EASNFS average OHC was 17.13 kJ cm^{-2} lower than the AXBT average, which may be attributed to the EASNFS Z26 average depth being 27.33 m more shallow than the AXBT average. While it is clear that the model represents the SST accurately, there are significant differences in EASNFS representations of the underwater structure of the cold feature, which significantly impacts the EASNFS OHC.

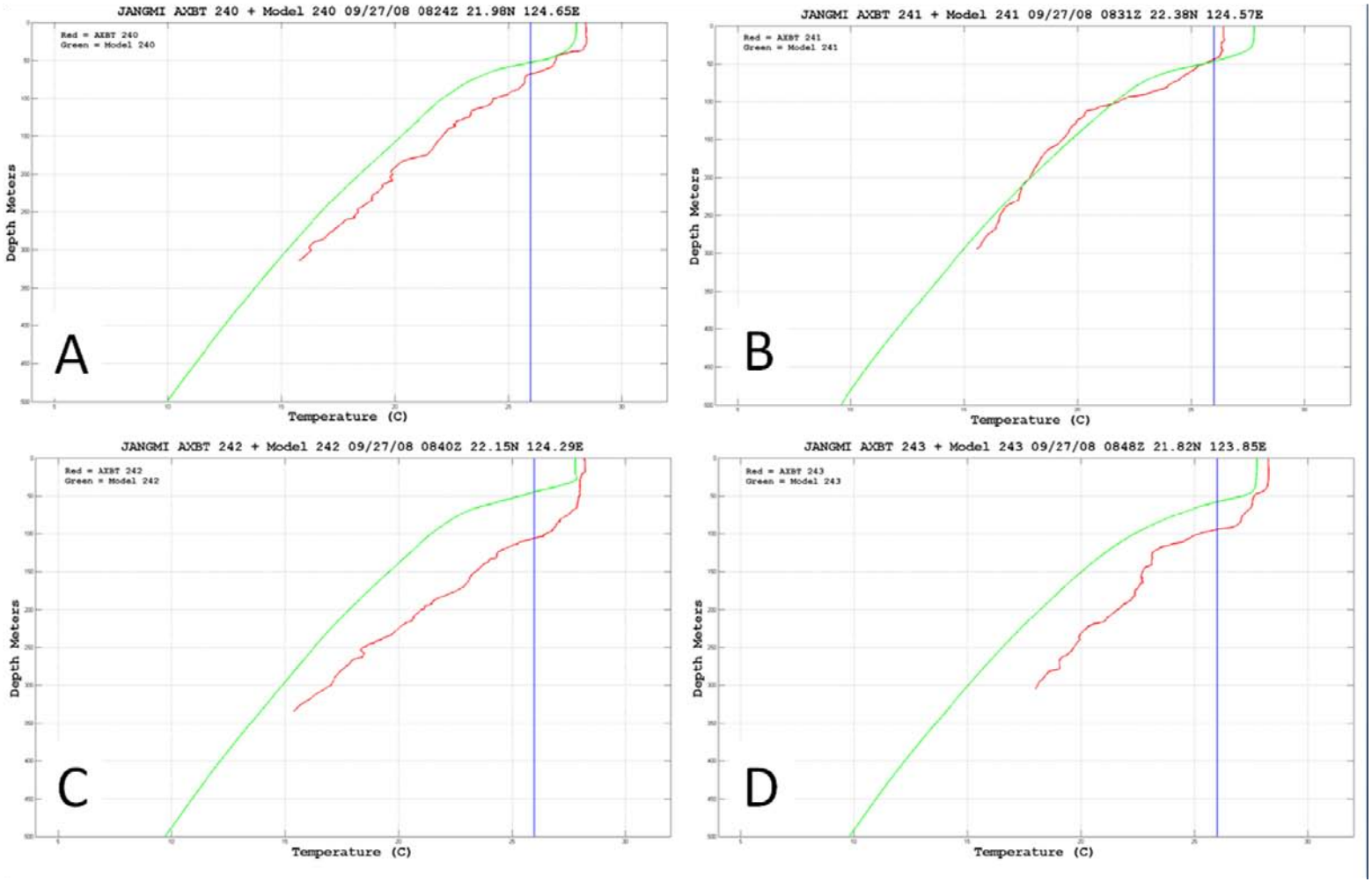

Figure 61. Comparisons of AXBT profiles (red) with EASNFS analysis profiles (green) as in Figure 60, except for AXBTs (a) 240, (b) 241, (c) 242, and (d) 243 deployed in the cold eddy southeast of Taiwan during the flight on 27 September 2008.

The AXBT 231 (Figure 62a) was deployed in the center of the warm feature (Figure 45) and had a temperature profile that was close to the EASNFS profile. The AXBTs 248 and 249 (Figures 62c and d) were also deployed close to the center of the warm feature and they measured a lower SST than in the EASNFS analysis, but the observed MLD was deeper. Therefore, the compensation between these errors resulted in the EASNFS and AXBT OHC values being similar. However, the EASNFS profile corresponding to AXBT 232 (Figure 62b) had characteristics much more representative of a warm feature than was observed. The AXBT 232 (Figure 62b) was actually on the edge of the warm feature adjacent to the cold eddy (Figure 45). However, the boundary between the warm and cold feature was not represented correctly in the EASNFS analysis, which may reflect the lack of proper representation of the mixing and cooling caused by TY Sinlaku when it passed through the area two weeks earlier.

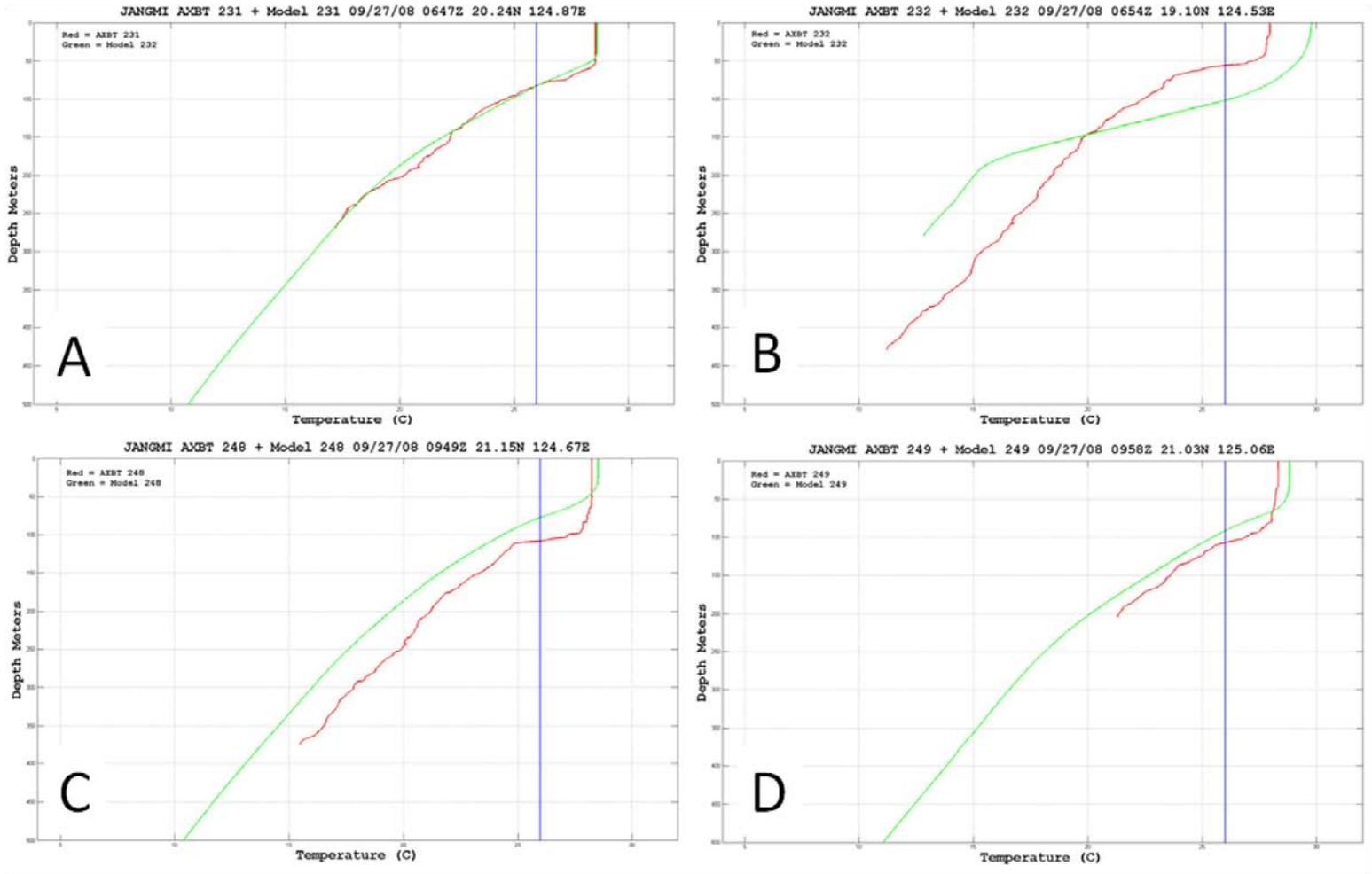

Figure 62. Comparisons of AXBT profiles (red) with EASNFS analysis profiles (green) as in Figure 60, except for AXBTs (a) 231, (b) 232, (c) 248, and (d) 249 deployed in the warm tongue southeast of the cold eddy during the flight on 27 September 2008.

The third subset of EASNFS-AXBT comparisons from the flight on 27 September 2008 was located behind the storm in the area of mixing that is the most difficult for the EASNFS analysis to resolve. This subset includes AXBTs 233, 234, 237, and 238 (Figure 63), and the EASNFS SSTs were higher than the observed AXBT SSTs and the average bias was 0.78^{o}C. Although these AXBTs were deployed behind the storm, they were deployed into the warm tongue (Figure 45). Therefore, the warm bias in the EASNFS analysis likely indicates the mixing caused by the storm was under-represented, which is consistent with the EASNFS average MLD being 19 m shallower than the AXBT average depth. The majority of this bias is due to the MLD in AXBT 237 (Figure 63c) being much deeper than the EASNFS MLD. The AXBT 237 was deployed near the boundary of the warm tongue and the large difference between the EASNFS and AXBT MLDs may have been due to an improper placement of the cold eddy in the EASNFS analysis. The EASNFS average OHC was 16.79 kJ cm^{-2} higher than the AXBT average, even though the EASNFS average Z26 depth was essentially identical (only 0.40 m deeper) to the AXBT average. The EASNFS OHC bias is consistent with the high SST bias coupled with shallow MLD bias, which again suggests the under-representation of the mixing and cooling by the storm.

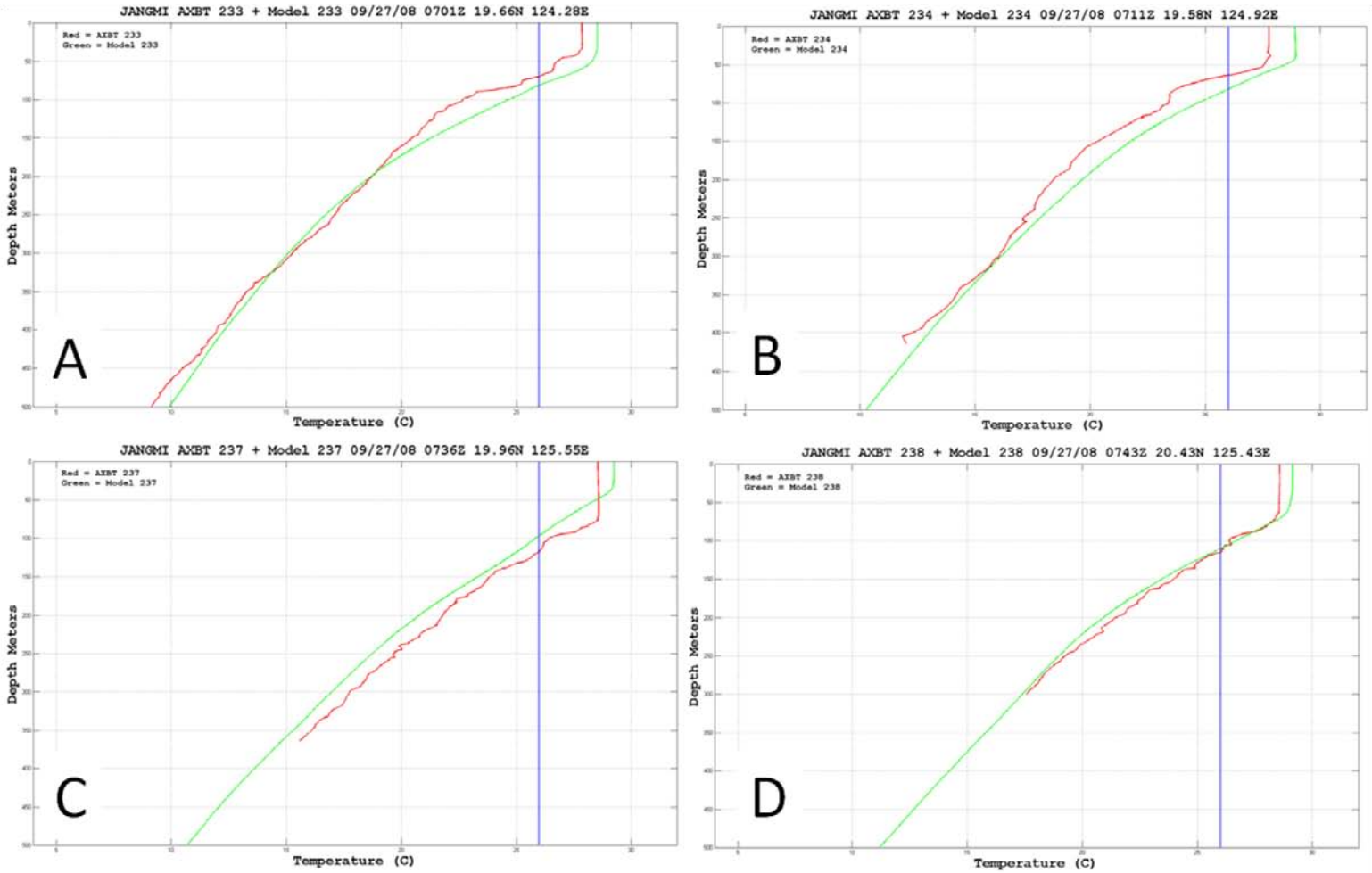

Figure 63. Comparisons of AXBT profiles (red) with EASNFS analysis profiles (green) as in Figure 60, except for AXBTs (a) 233, (b) 234, (c) 237, and (d) 238 deployed behind the typhoon during the flight on 27 September 2008.

Since TY Sinlaku had previously passed over the same cold eddy as it approached Taiwan, a subset of AXBTs 140, 144, 146, and 148 (Figure 64) from the 11 September 2008 flight into Sinlaku was also compared with EASNFS analysis profiles. The first two AXBTs were deployed near the center of the cold eddy and the second two AXBTs were along the edge of the eddy, but still on the colder side (Figure 17). In this subset, the EASNFS average SST was 0.62^{o}C higher than the AXBT average SST. The EASNFS MLD was consistently more shallow than the AXBT MLD with an average difference of 27.43 m. The EASNFS Z26 depth was also consistently more shallow than the AXBT depth, with the higher SST the EASNFS average OHC was only 10.19 kJ cm^{-2} lower than the AXBT average OHC. This subset of EASNFS-AXBT comparisons was very similar to the cold eddy subset during Jangmi in which the significantly smaller MLD and Z26 resulted in EASNFS OHC values that were less than the *in situ* AXBT OHC values.

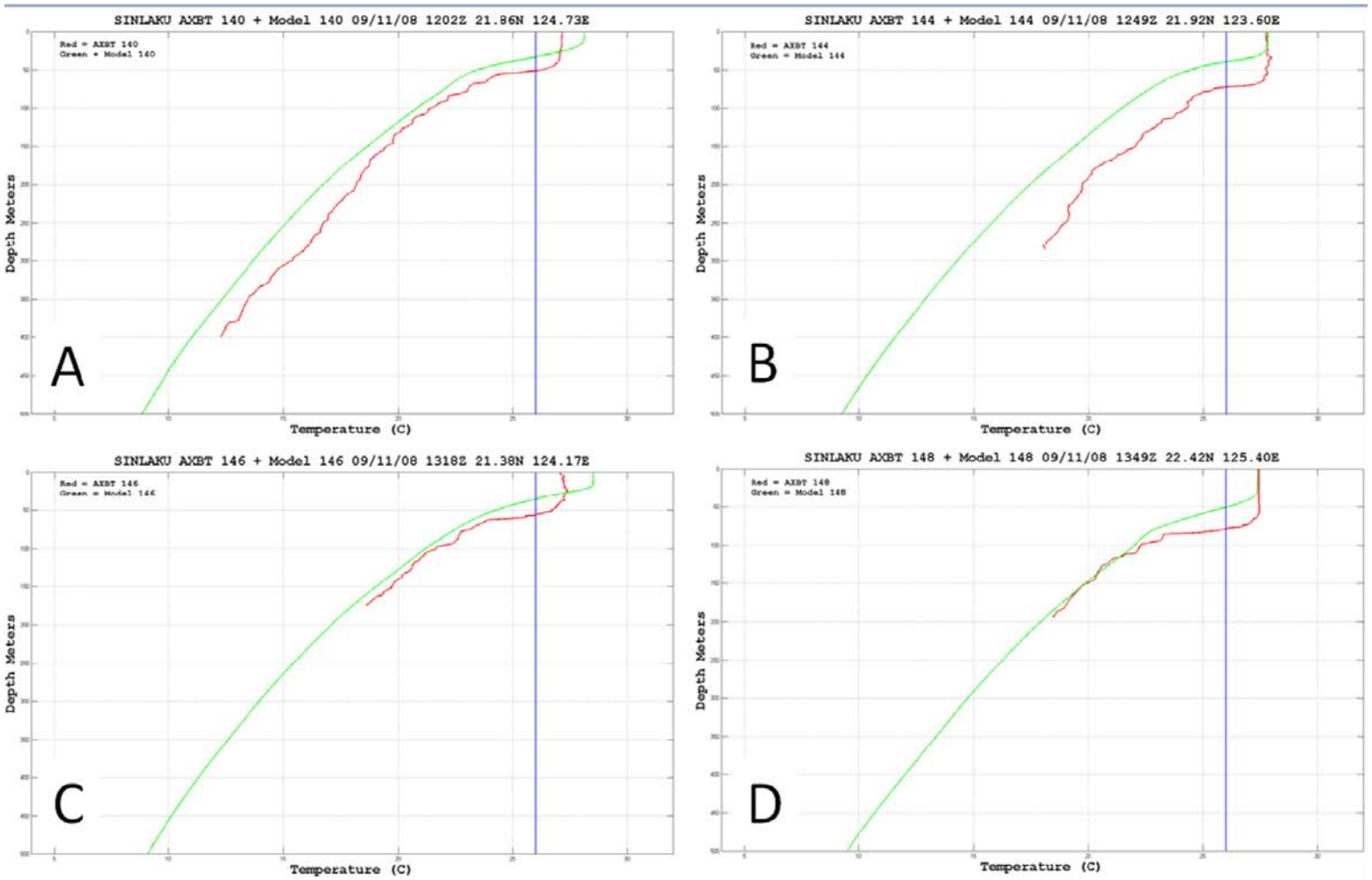

Figure 64. Comparisons of AXBT profiles (red) with EASNFS analysis profiles (green) as in Figure 60, except for AXBTs (a) 140, (b) 144, (c)146, and (d) 148 deployed in the cold eddy during the Sinlaku flight on 11 September 2008.

In the final subset, four AXBTs from flights into STY Jangmi that were deployed well outside the influence of the storm are compared with the EASNFS analysis. This subset consisted of AXBTs 200, 201, and 204 that were deployed on 25 September 2008 and 225 that was deployed on 26 September 2008 (Figure 65). In this subset, the EASNFS average SST was 0.07^{o}C lower than the AXBT average SST. The EASNFS average MLD was 15.50 m shallower than the AXBT average depth. Whereas three of the EASNFS and AXBT profiles matched closely, AXBT 204 (Figure 65c) had large differences. The EASNFS average OHC was 19.38 kJ cm^{-2} smaller than the AXBT average OHC, in part because the EASNFS Z26 depth was 14.37 m smaller than the AXBT average. Overall, the EASNFS and AXBT profiles outside the influence of the storm were better matched than those within the storm-influenced environment.

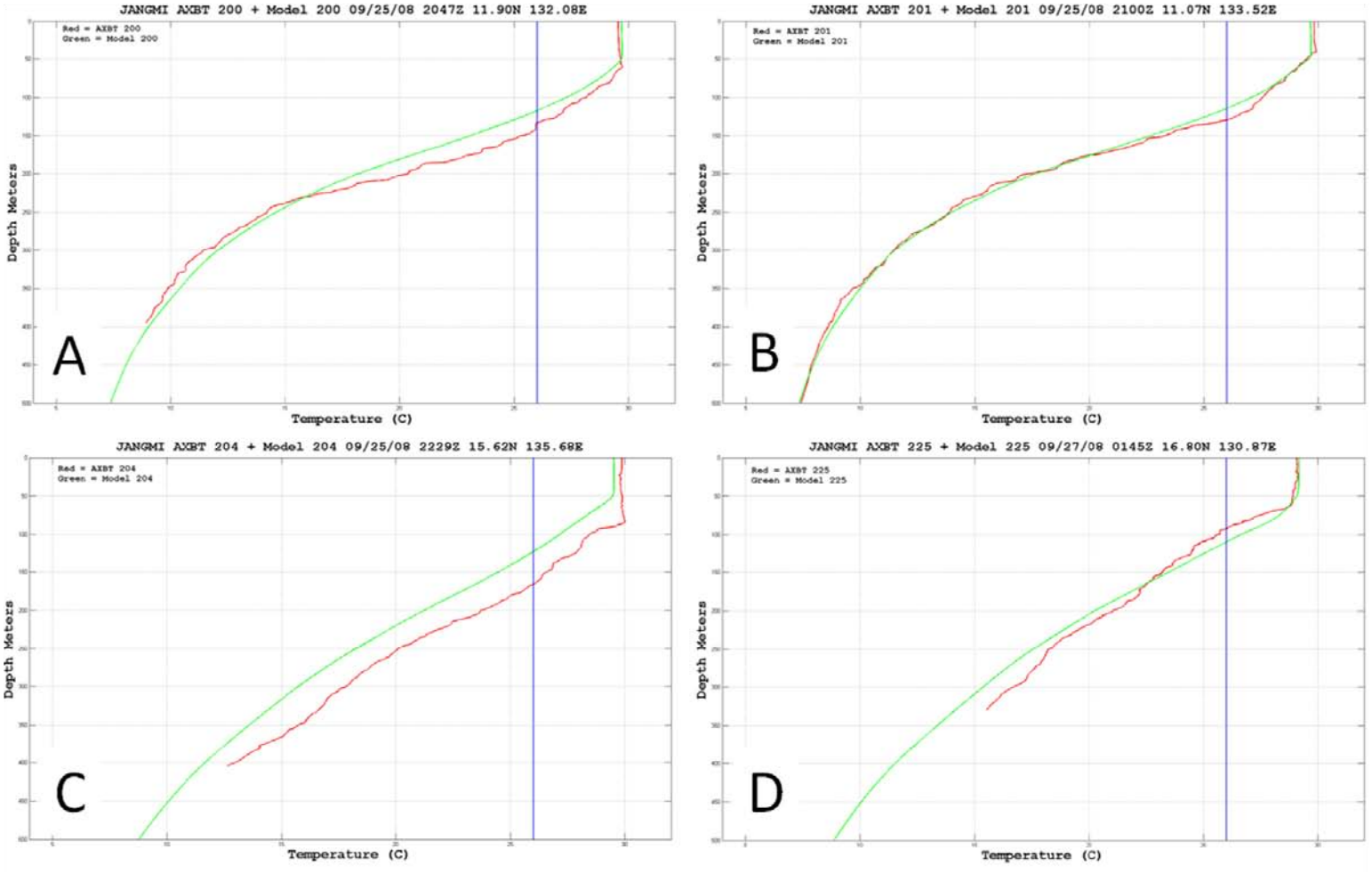

Figure 65. Comparisons of AXBT profiles (red) with EASNFS analysis profiles (green) as in Figure 60, except for AXBTs (a) 200, (b) 201, (c) 204, and (d) 225 deployed outside of Jangmi's 35 kt wind radius on 25 and 26 September 2008.

Comparisons between the *in situ* AXBT profiles and the EASNFS analysis profiles revealed that in over 75% of the cases the EASNFS profile had a smaller MLD and a steeper temperature decrease in the thermocline below the mixed layer. The effect of these biases was to reduce the overall OHC bias. In any cold ocean feature, this OHC bias tended to be larger. In warm ocean features, the OHC bias was often smaller or near zero because of the slight warm bias in SST for the EASNFS analysis. For the flights into Jangmi on 25 and 26 September 2008, the EASNFS SST, MLD, and OHC were all smaller than the observed values. For all of the AXBTs from both typhoons, the EASNFS SST was higher than the AXBT SST. However, a smaller EASNFS MLD resulted in a smaller EASNFS OHC.

In conclusion, some evidence exists that the EASNFS analyses are being overly influenced by climatological inputs, especially in the analysis of the MLD. A second possibility is that in close proximity to the storm the analysis is not representing well the mixing, wave action, and cooling by dynamic forcing associated with the storm that modify the ocean structure. The EASNFS seemed to be most accurate in analyzing the vertical temperature profiles outside and away from the storm environment.

THIS PAGE INTENTIONALLY LEFT BLANK

IV. CONCLUSION

A. SUMMARY

The ocean and atmospheric environments have important roles in the development and intensification of tropical cyclones. Some balance is required between these two factors. Enough OHC must be available to provide moisture and heat to the low-level flow into the storm center to allow formation and intensification. Vertical wind shear must be low enough to allow vertical development of deep convection such that a warm mid-troposphere remains centered above a low surface pressure center. Given a favorable atmospheric environment and not too large translation speed, OHC becomes an important factor that can impact the maximum allowable intensity of the TC (Emanuel et al. 2004)

Prior to formation, the pre-Sinlaku and pre-Jangmi disturbances moved across a near-uniformly warm tropical Pacific Ocean under the influence of moderate vertical wind shear. Neither disturbance formed a closed cyclonic circulation until the vertical wind shear was reduced to less than 8 kt. Once each became a Tropical Depression (TD), deep convection around the closed low seemed to shield the circulation center from vertical wind shear. At this time, each TD was over water with very high OHC and moderate vertical wind shear between 8–12 kt, under these conditions, each TC slowly intensified. At all times when vertical wind shear increased above 12 kt both storms quickly started to weaken.

This study has found noticeable impacts on storm intensity when the storms passed over a warm or cold ocean feature. Typhoon Sinlaku was steadily intensifying over a warm ocean until it passed over a weak cold ocean eddy on 9 September that resulted in a 12-hour pause in intensification. On 13 September, TY Sinlaku was weakening due to the influence of increased vertical wind shear. However, the storm then passed over a warm ocean feature at the same time shear weakened to 8 kt. In this 12-hour time period, the maximum winds increased from 85 to 100 kt. Super Typhoon

Jangmi was at peak intensity of greater than 140 kt over a warm eddy and when Jangmi passed from the warm eddy to over a cold eddy on 27 September it began to weaken even though vertical wind shear at that time was very weak.

Forward translation speed did play a role in the intensification of both storms. Super Typhoon Jangmi moved twice as fast (6 m s^{-1}) as TY Sinlaku (3 m s^{-1}). This is a likely factor in why Jangmi did not reach higher than 90 kt intensity when both storms approached the eddy zone around 18–19^{o}N. Jangmi was moving at the upper limit of the translation speed considered favorable for intensification according to Lin et al. (2009), which may have prevented it from fully coupling with and drawing heat and moisture from the ocean prior to 25 September.

The comparison of the AXBT profiles with the EASNFS analysis profiles consistently indicated that the EASNFS profiles had a too-small MLD bias. Additionally, the EASNFS profiles had a larger temperature decrease in the thermocline below the MLD than the observed profiles. This bias in the thermocline may be attributed to the use of climatological profiles in defining the deep ocean characteristics. In a majority of the comparisons, a warm SST bias was also present in the EASNFS profile. The combination of the warm SST bias and the shallow MLD bias resulted in compensating errors in the OHC calculations. The warm SST bias for the EASNFS seemed to be related to an under-representation of the influence of the storm mixing on the ocean environment. Overall, the EASNFS-AXBT differences were larger within the storm environment than in the environment farther away from the influence of the storm on the ocean.

The TCS-08/T-PARC program provided a unique opportunity to gather detailed observations of ocean structure in the environment of tropical cyclones over the western North Pacific. These measurements allowed identification of changes in storm intensity that were consistent with ocean conditions and atmospheric conditions. Therefore, routine analysis of ocean features in the storm environment should lead to improved analysis and forecasts of tropical cyclone intensity.

B. RECOMMENDATIONS FOR FUTURE RESEARCH

In this study, OHC and vertical wind shear were analyzed prior to storm recurvature and before each storm entered the much more dynamic midlatitudes. When TY Sinlaku tracked south of Japan, it was in a high vertical wind shear environment but moved over an area of high OHC. During a 6-h period, the storm translation speed slowed and the storm intensified into a minimal typhoon. A study of this event with OHC and atmospheric dynamic conditions coupled with the study by Sanabia (2010) is recommended.

In ITOP 2010, a particular flight on 8 September 2010 was devoted to studying the influence of the internal tides on the ocean column. Numerous AXBTs were dropped over the same points in the ocean over a period of 8 hours to monitor changes in Z26. Especially in the 100–200 m depth range, significant rises and falls of the warm layer of ocean were observed that are attributed to tidal effects. This effect should be studied in depth to determine what influences that tidal forces may have on OHC and TC forecasts.

The differences between *in situ* AXBT profiles and EASNFS analysis based profiles would make a good topic for further investigation. Since aircraft are only rarely available to sample the ocean, analyzing the differences found here and improving the analysis and forecasts of ocean profiles should lead to improved forecasts of TC intensification.

A study of the numerical forecast sensitivity to different ocean conditions identified between observed and EASNFS-based profiles should be undertaken. This type of study would identify magnitudes of intensity change that may be realized if ocean conditions were better represented.

THIS PAGE INTENTIONALLY LEFT BLANK

LIST OF REFERENCES

Black, P. G., E. A. D'Asaro, W. M. Drennan, J. R. French, P. P. Niiler, T. B. Sanford, E. J. Terrill, E. J. Walsh, and J. A. Zhang, 2007: Air-sea exchange in hurricanes. *Bulletin of the American Meteorological Society*, **88**, 357–373.

DeMaria, M., M. Mainelli, L. K. Shay, J. A. Knaff, and J. Kaplan, 2005: Further improvements to the Statistical Hurricane Intensity Prediction Scheme (SHIPS). *Weather and Forecasting*, **20**, 531–543.

Dunkerton, T.J., M. T. Montgomery, and Z. Wang, 2009: Tropical cyclogenesis in a tropical wave critical layer: Easterly waves. *Atmos. Chem. & Phys*., **9**, 5587–5646.

Elsberry, R. L., and P. A. Harr, 2008: Tropical Cyclone Structure (TCS-08) Field Experiment Science Basis, Observational Platforms, and Strategy, *Asia-Pacific Journal of Atmospheric Sciences*, **44**, 209–231.

Emanuel, K. E., 1999: Thermodynamic control of hurricane intensity. *Nature*, **401**, 665–669.

——, C. DesAutels, C. Holloway, and R. Korty, 2004: Environmental control of tropical intensity. *Bulletin of the American Meteorological Society*, **61,** 843–858.

Leipper, D. and D. Volgenau, 1972: Upper ocean heat content of the Gulf of Mexico. *Journal of Physical Oceanography*, **2**, 218–224.

Lin, I.-I., C.-C. Wu, K. A. Emanuel, I.-H. Lee, C.-R. Wu, and I.-F. Pun, 2005: The interaction of Supertyphoon Maemi (2003) with a warm ocean eddy. *Monthly Weather Review*, **133**, 2635–2649.

——, C.-C. Wu, I.-F. Pun, and D.-S. Ko, 2008: Upper-ocean thermal structure and the western North Pacific category 5 typhoons. Part I: Ocean features and the category 5 typhoons' intensification. *Monthly Weather Review*, **136**, 3288–3306.

——, I.-F. Pun, and C.-C. Wu, 2009: Upper-ocean thermal structure and the western North Pacific category 5 typhoons. Part II: Dependence on translation speed. *Monthly Weather Review*, **137**, 3744–3757.

Mainelli, M., 2000: On the role of the upper ocean in tropical cyclone intensity change. *Master's Thesis*. University of Miami, 73 pages.

——, M. DeMaria, L. K. Shay, and G. J. Goni, 2008: Application of oceanic heat content estimation to operational forecasting of recent Atlantic category 5 hurricanes. *Weather and Forecasting*, **23**, 3–16.

Marks, F. D., and L. K. Shay, 1997: Landfalling tropical cyclones: Forecast problems and associated research opportunities. *Bulletin of the American Meteorological Society,* Report of the Fifth Prospectus Development Team to the U.S. Weather Research Program,**79**, 305-323.

Melton, B. F. Jr., 2007: *Sea Cobra, Admiral Halsey's task force and the great Pacific typhoon*. Lyons Press, 247–274

Price, J. F., 2009: Metrics of hurricane-ocean interaction: Vertically–integrated or vertically-averaged ocean temperature? *Ocean Science*, **5**, 351–368.

Sanabia, E. R., 2010: The Re-intensification of Typhoon Sinlaku (2008). *PhD Dissertation,* Naval Postgraduate School, 233pp. Available at http://edocs.nps.edu/npspubs/scholarly/dissert/2010/Jun/

Wang, B., and J. C. L. Chan, 2002: How strong ENSO events affect tropical storm activity over the western North Pacific. *Journal of Climate*, **15**, 1643–1658.

Wu, C.-C., C.-Y. Lee, and I.-I. Lin, 2007: The effect of the ocean eddy on tropical cyclone intensity. *Journal of the Atmospheric Sciences*, **64**, 3562–3578.

INITIAL DISTRIBUTION LIST

1. Defense Technical Information Center
   Ft. Belvoir, Virginia

2. Dudley Knox Library
   Naval Postgraduate School
   Monterey, California

3. Professor Patrick Harr
   Naval Postgraduate School
   Monterey, California

4. Professor Russell Elsberry
   Naval Postgraduate School
   Monterey, California

5. Dr. Pete Black
   Naval Research Laboratory
   Monterey, California

6. Dr. D.-S. Ko
   Naval Research Laboratory
   Stennis Space Center, Mississippi

7. Superintendent
   Naval Research Laboratory
   Monterey, California

8. Director Joint Typhoon Warning Center
   Joint Typhoon Warning Center
   Pearl Harbor, Hawaii

9. Richard Jeffries
   Commander Naval Meteorology and Oceanography Command, N4/7
   Stennis Space Center, Mississippi